AD-A250 898

TION PAGE

Form Approved
OMB No. 0704-0188

Pub
gat
coll
Dav

erage 1 hour per response, including the time for reviewing instructions, searching existing data sources, the collection of information. Send comments regarding this burden estimate or any other aspect of this Washington Headquarters Services, Directorate for information Operations and Reports, 1215 Jefferson Management and Budget, Paperwork Reduction Project (0704-0188), Washington, DC 20503.

1.	TE	3. REPORT TYPE AND DATES COVERED
	Dec 1991	Final 1 Aug 89 - 31 Jul 91

4. TITLE AND SUBTITLE (U)

Feedback Stabilization of Hydrodynamic Instabilities

5. FUNDING NUMBERS

PE - 61102F
PR - 2307
SA - BS
C - AFOSR 89-0519

6. AUTHOR(S)

Professor M. Gaster

7. PERFORMING ORGANIZATION NAME(S) AND ADDRESS(ES)

University of Cambridge
Engineering Dept
Trumpington Street
Cambridge CB2 1PZ
UK

8. PERFORMING ORGANIZATION REPORT NUMBER

AFOSR-TR- 92 0364

DTIC
ELECTE
MAY 1 9 1992
S C D

9. SPONSORING/MONITORING AGENCY NAME(S) AND ADDRESS(ES)

AFOSR/NA
Bolling AFB DC 20332-6448

10. SPONSORING/MONITORING AGENCY REPORT NUMBER

AFOSR-89-0519

11. SUPPLEMENTARY NOTES

12a. DISTRIBUTION/AVAILABILITY STATEMENT

Approved for Public Release;
Distribution unlimited

12b. DISTRIBUTION CODE

13. ABSTRACT *(Maximum 200 words)*

The stabilization of boundary layers via control compared to passive boundary layer control techniques. To date, all experimental disturbances in the laminar boundary layer. To further improve the level of disturbance attenuation in the boundary layer requires an inherently three dimensional approach. The goal of this study was to control the boundary layer response to random three dimensional disturbances introduced near the leading edge of a flat plate. This goal was not fully achieved in the shortened time frame of this investigation.

The basic flow structure to be controlled is the three-dimensional wave packet, i.e. the boundary later response to localized pulse excitation. Since the control is to take place in the linear region of the transition zone, any conceivable flow disturbance can be synthesized and hence cancelled by appropriate wave packet superposition.

14. SUBJECT TERMS

boundary layer, turbulent flow, transition

15. NUMBER OF PAGES

114

16. PRICE CODE

17. SECURITY CLASSIFICATION OF REPORT	18. SECURITY CLASSIFICATION OF THIS PAGE	19. SECURITY CLASSIFICATION OF ABSTRACT	20. LIMITATION OF ABSTRACT
Unclassified	Unclassified	Unclassified	

NSN 7540-01-280-5500

Standard Form 298 (Rev. 2-89)

AFOSR - 89 - 0519

Feedback Stabilization of Hydrodynamic Instabilities

Roland A.E. Heinrich and Mike Gaster F.R.S.

Final Report
August 1, 1989 to July 31, 1991

A-1

Summary

The stabilization of boundary layers via active control promises drag reduction with relatively small power requirements compared to passive boundary layer control techniques. To date, all experimental active control investigations have concentrated on two-dimensional disturbances in the laminar boundary layer. To further improve the level of disturbance attenuation in the boundary layer requires an inherently three-dimensional approach. The goal of this study was to control the boundary layer response to random three-dimensional disturbances introduced near the leading edge of a flat plate. This goal was not fully achieved in the shortened time frame of this investigation.

The basic flow structure to be controlled is the three-dimensional wave packet, i.e. the boundary layer response to localized pulse excitation. Since the control is to take place in the linear region of the transition zone, any conceivable flow disturbance can be synthesized and hence cancelled by appropriate wave packet superposition.

The project was divided into two main parts, (i) numerical modelling of the control process, and (ii) experimental investigation of the most promising control arrangement identified in (i). The numerical modelling was an integral part of our approach and allowed us to a priori assess the best possible control performance achievable with a given design. The numerical model allows rapid testing of different spanwise and streamwise distributed detector and actuator arrays. Using this model, a promising control configuration was identified, implemented in the Cambridge University low turbulence wind tunnel facility and tested in part (ii) of this work.

The experimental investigation achieved significant control of single mode disturbances. In fact, control to about twice the natural background level was possible for frequencies within the unstable T-S band (attenuation up to 32dB). The disturbance detection was based on a difference microphone arrangement in order to reject acoustic disturbances in the facility. This microphone arrangement proved to be ideally suited for the current purpose. The actuators, embedded miniature loudspeakers, proved capable of controlling moderate sized instability waves.

Wave packet control was attempted but failed due to inadequate real time behaviour of the electronic filtering circuit. This was traced to exceedingly large rise and settling times of the electronic circuit.

AFOSR - 89 - 0519

Feedback Stabilization of Hydrodynamic Instabilities

Roland A.E. Heinrich and Mike Gaster F.R.S.

Final Report

August 1, 1989 to July 31, 1991

1. Introduction

The possibility of "active" control of instability waves in boundary layers has attracted the renewed attention of scientists since the early 80s. Active control denotes a concept in which the manifestations of flow instability, i.e. the Tollmien-Schlichting (T-S) waves are influenced by direct means using wave superposition principles. It is inherently different from "passive" methods of control which modify mean flow features to achieve stability with regard to small disturbances.

The potential benefit of active rather than passive control of external fluid flows (i.e. boundary layers) lies in the reduced power requirement of the former. Even though passive means of flow control have been successful in flight experiments in delaying transition by, say, boundary layer suction or wall cooling (air), the undeniable benefit in drag reduction for practical applications is partly negated by the power requirement for the specific

technique employed (Antonatos, 1966; Whites, Sudderth, and Wheldon, 1966; Pfenninger and Reed, 1966; Nenni and Gluyas, 1966; Wagner and Fischer, 1983).

The power requirement for an active control configuration is proportional to the energy content of the flow disturbances and thus is small compared to a passive control implementation. Nossenchuck (1982) increased the transition length in a flat plate boundary layer in water by 25% using an active controller with 1 Watt power input. The same delay using passive control (wall heating) required 1900 Watts!

Though not as widely known as the passive flow control methods mentioned above, active flow control has been explored since the mid 60s (Wehrmann, 1965; Schilz, 1965/66) and re-emerged in the early 80s (Milling, 1981; Liepmann, Brown and Nosenchuck, 1982; Thomas, 1983; Strykowski and Sreenivasan, 1985; Maestrello, 1985; Ladd and Hendricks, 1988; Ladd, 1990). Improved data-acquisition techniques and advances in micro-electronics are at least partially responsible for the renewed focus on these techniques.

The early experiments by Wehrmann (1965) and Schilz (1965/66) demonstrated the experimental viability of active control by cancelling two-dimensional instability waves via a downstream out-of-phase controller input (through flexible wall or sound excitation). Milling (1981) used the vibrating ribbon technique to excite T-S waves in his water channel experiment. A second wire

downstream introduced an "anti-wave", i.e. a wave with phase and amplitude adjusted to cancel the downstream propagating T-S wave. Liepmann, Brown and Nosenchuk (1982) used a novel technique to excite T-S waves in their water tunnel experiment. Here, flush mounted surface heaters were activated to excite the T-S waves in a zero pressure gradient flat plate boundary layer. Downstream cancellation was attempted via a second set of heater strips driven with the appropriate anti-wave. A reduction in disturbance amplitude and a delay of transition was achieved. Liepmann and Nosenchuck (1982) extended the technique to the control of natural transition, i.e. the T-S waves were not artificially introduced as in the above mentioned experimental studies but were generated naturally by the background free-stream disturbance. A hot-film probe was used as a sensor downstream of the heater strip which served as the control actuator. The sensor output was analyzed and a signal was synthesized to drive the actuator. This feedback control system showed T-S wave attenuation or reinforcement depending on the relative phase of sensor and actuator signal. Thomas (1983) studied the influence of vibrating ribbon control (two-dimensional) on the evolution of the three-dimensional structures in the transition region. He showed that even though transition could be delayed with two-dimensional active control, the weak three-dimensional background disturbance field interacted with the remainder of the two-dimensional primary field to restart the transition process. A modified vibrating ribbon technique was used in a wind tunnel experiment by Strykowski and Sreenivasan (1985) to excite and then cancel the T-S wave. In this experiment,

the ribbons where supported in slots in the surface of the plate and hence created disturbances more like localized suction and blowing. The experiment was successful in controlling the TS-wave. They also tried to use the heater strip technique of Liepmann et al. to generate and cancel T-S waves in air. However, they were unable to observe any flow perturbations using this technique. This suggests that the heater strip technique might not be suitable for active control actuation in zero pressure gradient airflow applications. In boundary layers with streamwise pressure gradients, however, this might be different. In fact, Maestrello (1985) has used heating strips to generate instability waves in boundary layers with favorable (!) pressure gradients. He also used an external sound field to generate an out-of-phase control signal which led to T-S wave reduction. The recent experimental investigations by Ladd and Hendricks (1988) and Ladd (1990) are concerned with the active control of artificially excited and natural occuring instability waves on an axissymetric body. The experiments were carried out in a water tunnel using hot-film detector and exciter arrays. A feedback loop using an adaptive control algorithm was used to successfully control two-dimensional disturbances. The authors discuss the strong three-dimensional (azimuthal) disturbance components and envision improved results if a three-dimensional control scheme were implemented.

Numerical simulations of active boundary layer control have been performed by various investigators. Most of them integrate the Navier-Stokes equations numerically in one form or another. A

review [see Kral (1988)] of these is outside the scope of this work, it suffices to mention that until recently the majority dealt only with two-dimensional disturbances and essentially modelled vibrating ribbon experiments [but see three-dimensional numerical simulations of active control in boundary layers by Laurien and Kleiser (1985), Laurien (1985) and Zang and Hussaini (1985a, 1985b)]. All studies confirm the feasibility of active control transition delay or enhancement.

2. Scope of Investigation

The above survey highligths the achievements and limitations of current active control boundary layer research. One serious limitation of all the reported experimental investigations is their restriction to two-dimensional active control. This limitation is a heritage of Schubauer and Skramstad's (1947) experimental verification of the nearly two-dimensional nature of T-S waves in the early stage of the transition process. By now, however, it is well established that the transition process is inherently three-dimensional and the concentration on two-dimensional waves seems unjustified. In fact the above cited studies by Thomas (1983) and Ladd (1990) discuss the need of controlling the three-dimensional structures in order to advance the active control concept. The classical vibrating ribbon cannot generate a three-dimensional control input and hence a different configuration is required. The technique of flush mounted surface heaters used by Liepmann et al.

is in principle suited to three-dimensional control actuation, however, the relative large size of the surface heaters and the rather limited power input possible might preclude their successful use in air flow applications.

The current investigation is based on analytical and experimental work on three-dimensional wave packets in the laminar boundary layer by Gaster (1968, 1975, 1981, 1985). Starting conceptually from a local three-dimensional disturbance in the boundary layer produces an approach more suited to the control problem at hand. Since it is possible (in linear theory) to superpose point sources to synthesize arbitrary forcing fields, the pulse response can be viewed as a generic flow disturbance. A localized pulse generates a wave packet which propagates downstream in the boundary layer and may form into a turbulent spot. Isolated turbulent spots grow and merge to form a fully developed turbulent boundary layer. Gaster (1975) has shown that the wave packet development in its early stage can be modelled accurately by linear mode superposition. Hence, extending the ideas of T-S wave cancellation via an anti-wave, the cancellation of the evolving wave packet by superposition with an "anti-packet" should be possible. Viewing the linear wave packet as fundamental building block of the transition process we propose the use of wave packet superposition to delay boundary layer transition due to artificially excited and - ultimately - randomly excited disturbances.

In order to establish the feasibility of three-dimensional random

disturbance control, the following issues were investigated in the course of this project: (a) sensor/actuator selection for control problem, (b) sensor/actuator arrangement based on numerical model of control system including boundary layer response, (c) disturbance detection in a "noisy" environment. Finally, a wind tunnel experiment was carried out in order to evaluate the selected control arrangement.

This report is divided into three sections. In Section 3 below the computer model of the linear three-dimensional control process it described. Once a promising control configuration was identified through the modelling process, the required hardware was built and an experimental investigation was launched. In Section 4 this experimental investigation is described in detail. Final, in Section 5 conclusions are drawn from the experience gained during this investigation and a course of future research is suggested.

3. Computer Model of Active Control Process

In order to minimize the amount of experimental "trial and error" necessary to find a viable arrangement of local surface detectors and control actuators, full use was made of computer simulation to test ideas and optimize (up to a certain point) the setup before the active control experiment was performed. In Subsection 3.1, the specific flow control configuration will be presented. The control task will be discussed. Subsection 3.2 deals with the model of the

flow field response based on the three-dimensional Orr-Sommerfeld stability equation. In Subsection 3.3 we digress and compare our numerical flow field response with the experimental flow field response obtained in a preliminary wind tunnel investigation. In Subsection 3.4 we use the model of our flow field response to tackle the boundary layer control problem by modelling various spanwise detector and actuator arrangements. This modelling leads to the definition of the most "suitable" control arrangement for the control experiment described in Section 4. (Listings of the computer programmes developed in the course of this project can be found in Appendix E.)

3.1 Control Task Definition

At the outset it is necessary to specify the system to be modelled and controlled. As stated above, the unstable T-S disturbances propagating in a flat plate Blasius boundary layer are to be controlled. Figure 1 shows a schematic of the flat plate boundary layer and introduces the control problem.

In typical flow situations, disturbances which are naturally present in the flow environment will enter the boundary layer and generate T-S instability waves. The processes by which these external disturbances enter the boundary layer - the "receptivity" problem - are still not fully understood and urgently require further research. Our current understanding suggests, however,

that - in the absence of any wall roughness or wall humps - the external disturbances enter the boundary layer predominantly in the leading edge region. In order to model this process properly, a distributed disturbance generation in the region downstream of the leading edge would be necessary. For the current investigation, however, the disturbance generation process is assumed to take place at a certain fixed distance downstream of the leading edge. It is important to emphazise that the artificial disturbance generation downstream of the leading edge is an aid in the modelling and experimental phase of the current investigation. Ultimately the flow disturbances should be generated by "natural" means, i.e. turbulence grids upstream of the plate.

Once the disturbances have entered the boundary layer, they will be damped or amplified as they propagate downstream (see Subsection 3.2) and will reach the detector location in the flow. Here a spanwise array of detectors will measure the disturbances present in the flow. In essence, the continuous time-dependent and spanwise varying flow field will be "discretized" with a finite number of spanwise detectors. (Since an analogue control circuit will be used no time discretization takes place.) After detection of the signal it will be analyzed and filtered appropriately. A control signal will be synthesized and injected into the flow at discrete spanwise actuator locations.

The controlled flow field will be filtered by the boundary layer and the control performance will be monitored downstream of the

control location in the "target" zone. It is conceivable that a separate row of detectors in this target zone provides the necessary information for true closed loop feedback. In the present study, however, signals obtained at the target location are only used to monitor the control performance and are not fed back into the control circuit.

The equivalent of the just described physical system is represented in block diagram form in Fig. 2a. Script H denotes a system transfer function and round and square brackets identify continuous and discrete representations respectively. $H1(k,\omega)$ and $H2(k,\omega)$ denote the boundary layer response to the external forcing upstream and downstream of the control location. $H12(k,\omega)$ is the boundary layer response in between the physical location of control detection and actuation. The bottom branch of the loop in the block diagram includes detector, controller and actuator transfer functions. Detector and actuator transfer functions are each split into two distinct parts, the first (1) taking into account the discrete spanwise nature of the detection and actuation, the second part (2) dealing with the finite frequency response of the physical components. Included in the figure are some possible control strategies, namely gain scheduling or adaptive control. None of those however will be considered in this report.

A simplified block diagram is presented in Fig. 2b. Here, the loop's complexity is reduced by neglecting the disturbance modification due to the flow field inbetween detector and actuator.

This simplification is justified if detector and actuator are physically close together as will be the case in the configuration chosen for our study. Furthermore, in this simplified case, the finite frequency response of the detectors and control actuators is neglected, i.e. these components are presumend to have an infinite bandwidth flat frequency response characteristic. This assumption is justified for the current investigation since embedded microphones and loudspeakers were choosen for detection and actuation respectively and these respond essentially flat in the relevant T-S frequency band [150 Hz to 400 Hz].

3.2 Boundary Layer Impulse response

The modelling of the control circuit described in the previous subsection requires knowledge of the boundary layer response, i.e. the system transfer functions H1, H12 and H2 (Fig. 2). Since the early stage of the boundary layer transition process is described by linear theory, the impulse response of the boundary layer provides the required information. Linear systems theory allows to construct the flow response to any arbitrary input by simple convolution of this input with the impulse response function.

Since an impulsive input is modelled as a Dirac spike, the initial condition for the numerical model of the boundary layer impulse response consists of a flat spectrum of unit amplitude. The downstream development of each individual Fourier component can be

determined from classical linear stability theory. The pulse response at a certain downstream location is obtained by superposing the contribution of all Fourier components at this point. The linear theory describing the three-dimensional disturbance development in a flat plate boundary layer is based on the Orr-Sommerfeld equation invoking Squire's transformation to reduce the three-dimensional problem to an equivalent two-dimensional one (Mack, 1969). Solving the resulting eigenvalue problem provides the complex wavenumber "a" as a function of local Reynoldsnumber and forcing frequency ω. The impulse response at a certain downstream location "x_m" as a function of spanwise position is thus described by

$$u'(\text{time},z\text{-span}) = \sum_i \sum_j \exp\left[i\left(\int_{x_0}^{x_m} a(x)\,dx + b_j z - \omega_i t\right)\right] .$$

Here u' denotes the disturbance velocity component parallel to the wall in mean flow direction. Approximately 10000 eigenvalues "a" need to be calculated in order to represent the temporal and spanwise development properly. The integral in the exponent is evaluated using a Romberg integration procedure. In order to rapidly calculate the large number of required eigenvalues, an efficient algorithm (Gaster, 1978) was used which expresses the eigenvalue dispersion relationship in a complex double series,

$$\frac{\omega}{a_{3D}} = \sum_n \sum_m A_{nm}\left(aR - |\tilde{\alpha}R|_0\right)^n \left(a^2 + b^2 - \tilde{\alpha}_0^2\right)^m$$

$$\tilde{\alpha}_{2D}^2 = a_{3D}^2 + b_{3D}^2$$

$$\tilde{\alpha}R_{2D} = aR_{3D} \quad .$$

The spatial eigenvalue evaluation required Newton-Raphson iteration. Using the Gaster double series, the 10000 eigenvalues were obtained in about 15 minutes on a SUN-Sparc station. It should be noted that only eigenvalues falling within a certain area surrounding (and of course inside) the neutral stability curve were considered since the other highly damped modes do not contribute significantly to the impulse response far away from the source.

Using the described procedure, the required boundary layer impulse response functions H1 and H2 were calculated. Figure 3 shows contour plots of the spanwise distribution of the disturbance u-velocity. Also shown is the convolution H1*H2, corresponding to the flow response at the target location (see Fig. 1) due to pulse forcing at the exciter location. The modelled boundary layer impulse response produces the expected wave packet shape (Gaster and Grant, 1975; Gaster; 1975). In the following subsection, this predicted wave packet shape will be compared more closely with the one obtained from experiment.

3.3 Comparison of Model and Experiment

The above described boundary layer response calculation forms the building block for the modelling of the control arrangement. Hence, before starting extensiv simulations based on this model it is sensitive to compare the predicted impulse response of the

boundary layer flow with suitable experiments. To this end a test plate was built and experiments were performed in the Cambridge University low turbulence research wind tunnel. Details of the hardware are described in Appendix C and the experiment itself is presented in Appendix D. The experiment was set up to model the parameters of our numerical model, i.e. disturbance generation at $Re_{\delta^*} = 870$, and measuring position at $Re_{\delta^*} = 1235$, corresponding roughly to the fictitious "control" location of $Re_{\delta^*} = 1260$. Measurements of the fluctuating u-velocity component where obtained with a constant temperature hot-wire positioned just outside the boundary layer where the T-S eigenfunctions exhibit an outer (flat) maxima. In the experiment, the flow was excited by a short duration (0.5ms) computer generated pulse via an embedded loudspeaker. The results are presented as isometric views and contour plots for the u-velocity fluctuation.

Figure 4 shows the experimental wave packet results from ensemble averaged records. The equivalent flow field calculation based on our numerical model is shown in Fig. 5. Since the model based on the Orr-Sommerfeld eigenvalue problem does not provide absolute amplitude levels, the amplitude level in the simulation was adjusted to the experimental maximum. Comparing experimental and numerical result shows remarkable agreement. In particular the location of the wave packet within the time record is very well reproduced by the model. This can be seen even more clearly in Fig. 6 which shows a comparison of experimental result and numerical result on the packet centre line. Considering that the model is

based on a locally parallel boundary layer approximation, the agreement is excellent.

3.4 Control Simulation

Having established that the numerical model of the flow response and the actual flow response obtained by wind tunnel experiment are nearly identical, the simulation of the control arrangement introduced in Subsection 3.1 can be performed.

3.4.1 General Performance Considerations

Conceptually, the control circuit (Fig. 1) consists of the following components (in flow direction): (i) event detectors, (ii) control actuators, and (iii) residue disturbance detectors which are located in the "target" zone downstream of the actuators. The event detectors upstream of the actuators are required since the disturbance wave packets (events) appear at random times. We are searching for viable control geometries, i.e., we use the numerical model to rapidly explore the advantages and disadvantages of different streamwise and spanwise detector/actuator arrangements. The numerical "control" process proceeds as follows: the flow response at the detector location ($Re_{\delta^*} = 1235$) due to any time dependent input disturbance f(t) is obtained by convoluting f(t) with the apropriate system transfer function (H1). As canonical

case, we choose the pulse as input disturbance, i.e. $f(t) = \delta(t)$. At the control location we "detect" the disturbance and can "control" by arbitrarily modifying the numerical signal at different spanwise locations. This "controlled" disturbance is then convoluted with the sytem transfer function H2 in order to provide the disturbance flow in the target zone at $Re_\delta = 1780$ (Fig. 1). In this first attempt to establish a viable control geometry the individual detector and actuator dynamics is not taken into account. Hence, "ideal" control is simulated, i.e. the components of the control circuit are assumed to have an undistorted, infinitely wide frequency response with zero response delay (see Fig. 2b). Three different open-loop control configurations are explored:

- Case 1, the ideal controller is located at the centre-line,
- Case 2, in addition to the controller at the centre-line, two controllers are placed symmetrically 12mm to each side of the centre-line, and
- Case 3, a total of four controllers are used which are placed symmetrically at 6mm and 21mm above and below the centre-line. In order to assess the control performance, the pseudo-energy (u') in the target zone is integrated over the whole disturbance flow field. The cost function in the target zone is minimized by "optimal" choice of controller gain and phase. Without any control, Fig. 7a shows the modelled flow response at the target location. The pseudo disturbance energy in the field is 15.6. This serves as the reference case to assess the control performance. Figure 7b shows the best possible control for case 1, a single controller on the centre-line. Even though the fringes of the packet can not be

controlled, the disturbance energy is reduced by a factor of 3 to 5.0. Figures 8a, b show the best control possible for the three controllers and four controllers configuration respectively. With four controllers, the residual disturbance energy is reduced to 0.6 which is just 4% of the uncontrolled level. The sensitivity of our open loop control to variation in amplifier gain and controller phase is shown in Fig. 9. As expected, proper phase control is crucial for a successful active control implementation. It is interesting to note that the minimum in the amplifier gain curve (Fig. 9a) is rather shallow indicating a moderate cost penalty for a controller gain mismatch. For comparison, the dotted line in Fig. 9a, b indicates the control sensitivity for the case of a purely two-dimensional single mode wave controlled with an ideal two-dimensional control arrangement. Obviously, a control amplifier gain of unity allows complete cancellation for this hypothetical case. A properly matched amplifier gain is more critical for this case than for the three-dimensional wave packet cases presented above, while the phase sensitivity is about equal.

From the simulations described in this subsection, it was decided that a spanwise spacing of about 10mm would provide an acceptable balance of achievable control performance and hardware complexity.

3.4.2 Performance of chosen Configuration

The "ideal" control circuit used above did not take into account the physical spacing of detectors and actuators. It was based on the simplified block diagram in Fig. 2b. The streamwise spacing of detector and actuator array can be included into our numerical model. Furthermore, the detection was modelled as an ideal point detection. Embedded microphones were choosen to provide disturbance pressure detection. Experience from previous own experiments and the work by Kendall (1990) shows, that acoustic disturbances present in the wind tunnel environment produce wall pressure fluctuations an order of magnitude larger than those associated with the instability waves. These acoustic pressure fluctuations have to be eliminated from our signal in order to allow detection of the relevant disturbances, the instability waves. This was done using two microphones spaced a "small" (on an acoustic scale) distance apart in streamwise direction and switched such that the signals are substracted from each other. The streamwise distance was in effect chosen to be roughly (0.5*lambda), "lambda" being the wavelength of the most amplified instability wave component at the detector location. Hence this double microphone arrangement will effectively reject the long acoustic wavelength but will enhance the detectability of disturbances with wavelengths in the relevant instability wave range. The behaviour to be expected for this arrangement is shown in a Bode plot in Fig. 10. The frequency for which the difference microphone arrangement is tuned is denoted by F_o and a 6dB

amplification is achieved for this particular frequency. For lower frequencies corresponding to longer wavelengths, the amplitude response is lower, asymptotically approaching a typical first order attenuation of 20dB per frequency decade. It is conceptually helpfull to view the double microphone arrangement from a finite difference standpoint. Essentially the difference microphone approximates the derivative of the passing signal at the midpoint between the microphone location. Integrating the difference microphone signal electronically should recover the exact signal at the midpoint (without the constant contribution from the acoustic contamination) providing the "ideal" response indicated in the graph. The actual combined response of difference microphones and integrator is constructed by simple addition of the appropriate curves in the Bode plot. It should be noted that in principle the signal detected with the difference microphone arrangement is distorted by folding (aliasing) due to higher disturbance frequencies with shorter wavelength than can be resolved with the selected streamwise separation of the microphones. However, since the unstable frequency band is rather narrow and frequencies which exceed F_o by a factor of 2 or higher are strongly damped, this spatial aliasing is insignificant.

In order to minimize interference between actuator loudspeaker and detector microphone, it was decided to place the actuator loudspeakers staggered in the spanwise direction with respect to the microphone array (Fig. 10). It is then sensible to synthesize the control actuator input by a weigthed average of the nearest

difference microphone detectors.

Including the difference microphone with integrator and the spanwise staggering of the detector/actuator arrangement in our numerical model and taking furthermore the boundary layer flow development in the controller region (impulse response function H12 in Fig. 2a) into account, the performance of the full control system was analyzed. Figure 11a shows the uncontrolled model flow field at the target location due to excitation at the exciter location near the leading edge. The input at the exciter location was chosen as a random function in time and spanwise distribution in order to present a more realistic flow picture. (Of course, testing the control performance with a single pulsed point source exciter reveals exactly the same information since the system is modelled linearly.) As before, Fig. 11a shows a contour plot of the disturbance u-velocity distribution as a function of time and spanwise position. For the sake of clarity, the center time trace and the spanwise distribution at a particular point in time are extracted and plotted separately below and to the right of the contour plot respectively. Considering the temporal structure first, the signal looks plausible in comparison to typical oscilloscope traces of natural (i.e. random) transition experiments. Concentrating on the spanwise distribution it is apparent that the structure is predominantly two-dimensional in nature, i.e. the wave fronts are aligned almost perpendicular to the mean flow direction. This again is expected from linear stability theory since two-dimensional disturbances are in

principle the most amplified ones. However, the structure shows sufficient spanwise modulation to ruin any control attempt based solely on a disturbance detection at one spanwise location. In other words, this plot confirms the necessity of the distributed control approach chosen in the current investigation if cancellation of the disturbance structure over a significant surface area is to be successful.

The same flowfield at the target location with the control active is shown if Fig. 11b. Obviously no total cancellation is achievable with the choosen detector/actuator arrangement. However, the maximum amplitude in the whole flow field was reduced to 18% of its uncontrolled value and the overall pseudo disturbance energy was reduced to about 4% of the uncontrolled result. The achieved control has to be viewed as the best possible control in an ideal setting and it is to be expected that the implementation in a wind tunnel experiment will degrade the performance. Nevertheless, the predicted amplitude reduction to about one-fifth of its uncontrolled value justifies the implementation of the control system in a wind tunnel experiemnt.

4. Active Control Experiment

An insert for the test plate was designed and built which incorporated the detector and actuator arrangement arrived at by numerical modelling as described above. The mechanical and electronic hardware used is described in more detail in Appendix C. The experimental investigation was divided into three different stages described below. In Subsection 4.1, the suitability of the embedded miniature loudspeakers for the control of instability waves was tested. Subsection 4.2 deals with the important issue of disturbance detection and noise rejection. Implementation of the full control arrangement including both microphone detectors and loudspeaker actuators is described in Subsection 4.3.

4.1 External Control

As a first step to a successful control of boundary layer instability waves, it is important to ascertain that the control actuators, i.e. the miniature loudspeakers embedded in the plate can indeed produce the disturbance level required for cancellation at the actuator location. In order to do so, an "external" control experiment was devised, bypasssing disturbance detection entirely. A continuous single mode disturbance of known fixed frequency was introduced at the exciter location. At the control location, the detectors were uncoupled from the circuit. The control signal driving the control loudspeakers was generated externally with a

frequency generator set to the same frequency as the exciter frequency. Finally the phase and amplitude of this external "controller" was manually adjusted until disturbance cancellation was achieved as monitored by a hot-wire on the centre-line at the target location. This procedure was repeated for different frequencies and exciter amplitudes in order to establish the maximum disturbance amplitude which could be cancelled using the chosen actuator arrangement. It transpired that the chosen actuators could control disturbances of moderate amplitude. This moderate amplitude disturbances were generated by driving the exciter speaker near the leading edge with roughly 40% of the maximal voltage allowable for linear disturbance generation. In other words, driving the exciter speaker 2.5 times as hard produces a disturbance 2.5 times as big (hence the system response linearly) but the control actuators were not able to cancel it at the controller location downstream.

Figure 12a shows a hot-wire trace of an uncontrolled disturbance generated by simultaneously feeding three discrete frequencies into the exciter speaker. Prior to this superposition, each of these three frequencies had been controlled individually by external control as described above. If the system is linear, switching on the externally tuned controllers of all three frequencies simultaneously should eliminate the signal. Figure 12b shows the hot-wire trace of the controlled result and comparison with the unforced reference case (not shown) reveals that the residual disturbance in the controlled case is twice the size of

the natural background noise. Hence from this experiment we could conclude:

(a) the control actuators are suitable for control of moderatly sized instability waves, and

(b) the system behaves linearly as expected, i.e. linear superposition holds.

As a next step, the spanwise distribution of the control "wedge" generated by a finite number of spanwise actuators was examined in an external control setting. In Fig. 13, the spanwise distribution of the hot-wire rms integrated over the relevant T-S band is shown. The particular case represents superposed forcing and control of two distinct frequencies. The external controller was driving four control actuators simultaneaously (indicated by black triangles on the abcissa), only half of the flow field is shown in the graph. In the uncontrolled case we see the expected roll-off in the spanwise direction. In the controlled configuration, the very local nature of the control near the centre-line is apparent. It is interesting to note that there is no performance penalty at the fringes of the controlled region due to possible in-phase amplification of the flow disturbance.

4.2 Disturbance Detection

The quality of the sensor signal is of crucial importance for good control performance. This requires proper sensing of disturbance

amplitude and phase as well as adequate noise rejection. The later point is particularly important due to the dominant acoustic disturbance field present in the wind tunnel environment. As described above, a double microphone arrangement was chosen as sensor, the small (acoustic scale) st.eamwise spacing of the microphones allowing rejection of acoustic disturbances. In order to ascertain the "coherence" of the relevant flow disturbance, i.e. T-S instability wave, and detector signal, a hot-wire was placed at the centre of the double microphone in streamwise position but displaced sideways in spa:i by 8mm. This spanwise displacement was chosen in order to avoid any influence of the local flow field generated by the hot-wire support structure on the microphone signal. A pulse disturbance was generated at the exciter location near the leading edge and three channels were recorded simultaneously providing (i) the hot-wire signal, (ii) the upstream microphone signal of the double microphone arrangement, and (iii) the downstream microphone signal of the same arrangement.

Figures 14a and 14b show a single realization of the hot-wire trace and the ensemble average of 64 realizations of the hot-wire signal respectively. The hot-wire trace shows a wave packet riding on a strong background disturbance field of comparable magnitude. The generated wave packet is clearly discernible after ensemble averaging the signal. However, a single hot-wire at the detector location would not be suitable for disturbance detection due to insufficient signal to noise ratio. Figures 15a and 15b show a single realization of a single microphone and of the double

microphone arrangement respectively. This data were taken simultaneously with the single shot hot-wire trace shown in Fig. 14a. No wave packet can be detected in the single microphone signal, rendering a single microphone totally unsuitable for our purpose of instability wave detection. However, using the microphone in conjunction with the second microphone placed downstream such that the difference signal is recorded, a spatial filter of excellent quality is obtained. In the single realization double microphone trace shown in Fig. 15b, the instability wave packet clearly rises above the background noise level. The signal to noise ratio is similar to the one obtained by ensemble averaging the hot-wire with 64(!) realizations.

4.3 Open Loop Control Performance

Given the control actuator performance discussed in Subsection 4.1 and the signal quality of a single shot difference microphone arrangement discribed in the previous subsection, the active control of instability waves in the boundary layer should be achievable with the present hardware configuration. In this subsection, we describe the control performance achieved using the described arrangement. We concentrate on the control performance at the centre-line. Due to time constraints, no spanwise traverses were recorded. The whole system thus looks as follows (see Fig. 1). Excitation takes place with a single "point source" exciter on the plate centre-line. At the control location detection via one set of

embedded double microphones on the centre-line takes place. This signal is then filtered (see Appendix C for hardware details) and fed to four control actuators simultaneously which are symmetrically distributed across the centre-line and are 10mm apart. The control performance is assessed in the target zone downstream of the control location with a hot-wire placed above the plate centre-line at the outer edge of the boundary layer.

In the first set of experiments single mode control was attempted using the full control arrangement. Figure 16a and b show the hot-wire trace at the target location with control off and on respectively. The almost complete cancellation of the disturbance signal is apparent. In fact, taking the Fourier transform of the controlled signal and comparing the integrated rms-value over the T-S frequency band of the controlled and the uncontrolled case reveals a reduction of about a factor of 10 in disturbance amplitude, i.e., a factor of 100 in disturbance energy. Comparing the controlled case with a reference case without any disturbance excitation (not shown) reveals that the control achieves attenuation of the disturbance amplitude to about twice the natural background level. It is thus apparent that our control arrangement is as good as the external control arrangement described in Subsection 4.1 in eliminating the instability wave. It should be pointed out, that in order to achieve this good control performance, a phase shifter within the control circuit (see Appendix C) had to be adjusted quite carefully. The control circuit was tested for different exciter frequencies and amplitudes and

control to twice the background level was consistently possible if the internal phase shifter was adjusted to a slightly different phase lag for each frequency. However, even if the phase shifter was not precisely tuned, i.e., it was set to a constant average value, the control of single mode frequencies over the whole unstable T-S band was still significant, i.e., a factor of 4 in u-disturbance amplitude for each frequency.

In carrying out these experiments, it became apparent that the proximity of disturbance detector and actuator leads to undesirable crosstalk, i.e., the two control actuators nearest the detector location influence the detector reading. The extent of interference is shown in Fig. 17. Detector output as a function of control actuator driving voltage is shown. In the absence of any cross-talk, the detector output should be independent of the actuator driving level. In Fig. 17a the interaction is apparent. Using, however, two control actuators further apart from the detector microphones, Fig. 17b shows that the interference problem is eliminated. Since the control performance using the arrangement of Fig. 17a did not deteriorate profoundly, no attempt was made to eliminate this interference problem by further filtering. The second problem which was unexpected was the varying phase lag requirement in the control circuit for different frequency components. From the beginning it was expected that a phase shift would be required to take account of the local receptivity behaviour at the actuator location. In other words, since it is not known what the (complex) "transmission" coefficient is between a

pressure disturbance generated at the wall and the downstream disturbance u-velocity component if would be fortuitous if it were identically zero. It was unexpected that this transmission coefficient is a function of frequency. Careful measurements of this transmission coefficient were performed such that a proper phase shifting all-pass filter can be designed at a later stage.

As the last experiment in this investigation full wave packet control was attempted. The difference between controlling single mode disturbances and a full wave packet is the appearance of the latter at a certain a priori unknown point in time. Hence, the time constant of the electronic control circuit plays a significant role. The influence of this time constant was underestimated in our control arrangement and led to the failure in controlling the wave packet. It was however not only the larger than expected rise time of our electronics which caused this failure. In addition, the settling time was exceeding the passing time of the wave packet thus causing a ringing of the control actuator which introduced additional disturbances into the boundary layer flow. The severity of this problem can be seen from Fig. 18. The top trace shows the detector signal and the wave packet can be identified in the trace. The spikes seen in this trace are due to a ground connection which was left floating by mistake. This was corrected in later attempts and should be ignored for the current argument. The bottom trace shows the control actuator signal driving the embedded control speakers. The delayed start of the control signal and the long settling time after the signal has passed are apparent. This long

settling time was traced to the narrow band filtering associated with the employed phase shifting device and could not be corrected in the time available for this experiment. The time delay due to the Bessel filters was found to be in the order of 1msec which is too large for the system to be able to control frequencies in the neighbourhood of 300Hz (period 3msecs) effectively. It is important to note, that the failure of the attempted wave packet control is not based on any unexpected flow behaviour but purely due to the inadequate electronic circuit. Fortunately, having concluded this experiment and having specified the circuit requirements it is feasible to construct an improved electronic control circuit taking into account the lessons learned.

5. Conclusions and Outlook

The stabilization of boundary layers via active control promises drag reduction with relatively small power requirements compared to passive boundary layer control techniques. To date, all experimental active control investigations have concentrated on two-dimensional disturbances in the laminar boundary layer. However, to further improve the level of disturbance attenuation in the boundary layer requires an inherently three-dimensional approach. The work presented in this report addresses this issue. The goal of this study was to control the boundary layer response to random three-dimensional disturbances introduced near the leading edge of a flat plate. This goal was not fully achieved in

the shortened time frame of this investigation. (The original proposal set out a three year programme, however, two years were funded.)

The basic flow structure to be controlled is the three-dimensional wave packet, i.e. the boundary layer response to localized pulse excitation. Since the control is to take place in the linear region of the transition zone, any conceivable flow disturbance can be synthesized and hence cancelled by appropriate wave packet superposition.

The project was divided into two main parts, (i) numerical modelling of the control process, and (ii) experimental investigation of the most promising control arrangement identified in (i). The numerical modelling was an integral part of our approach and allowed us to a priori assess the best possible control performance achievable with a given design. The numerical model allows rapid testing of different spanwise and streamwise distributed detector and actuator arrays. Using this model, a promising control configuration was identified, implemented in the Cambridge University low turbulence wind tunnel facility and tested in part (ii) of this work.

The experimental investigation achieved significant control of single mode disturbances. In fact, control to about twice the natural background level was possible for frequencies within the unstable T-S band. The disturbance detection was based on a

difference microphone arrangement in order to reject acoustic disturbances in the facility. This microphone arrangement proved to be ideally suited for the current purpose. The actuators, embedded miniature loudspeakers, proved capable of controling moderate sized instability waves. Slight cross talk between actuator and detector arrangement was observed but was not so severe as to adversely affect the control performance.

Wave packet control was attempted but failed due to inadequate real time behaviour of the electronic filtering circuit which could not be rectified in the experimental time remaining. This failure was due to exceedingly large rise and settling times of the electronic circuit. The former caused the control to "kick in" after about half the wave packet had passed the actuator location, while the latter caused excessive "ringing" of the actuator after the wave packet had passed thus in itself creating a disturbance in the flow field.

It should be emphasized that the failure to control the wave packet is not due to any unforseen flow behaviour but solely due to inadequate electronic circuitry. Redesigning the electronic filters is therefore the necessary first step in achieving wave packet control locally at the plate centre-line. Increasing the physical distance between control detectors and actuators is advisable in view of (a) eliminating cross talk and (b) allowing for more processing time in the control loop. After control at the centre-line is achieved, it is suggested to carefully explore the

spanwise distribution and compare this with the numerical model developed in the course of this project. Afterwards, several spanwise detector/actuator blocks can be combined to provide complete spanwise control of distributed random disturbance fields.

Appendix A: Figures

List of Figures

Fig. 1 Schematic of boundary layer control arrangement.

Fig. 2 Block diagram representation of boundary layer control system.
(a) full system
(b) simplified basic system

Fig. 3 Simulation of flow response due to point source excitation at $Re_{\delta^*} = 870$. Dashed lines correspond to negative values.
ST1 - System transfer function from $Re_{\delta^*} = 870$ to 1235.
ST2 - System transfer function from $Re_{\delta^*} = 1235$ to 1780.
ST1*ST2 - Disturbance flow response at $Re_{\delta^*} = 1780$ due to point source excitation at $Re_{\delta^*} = 870$ (STI convoluted with STII).

Fig. 4 Streamwise velocity fluctuations (u') measured at outer edge of boundary layer ($Re_{\delta^*} = 1235$). Single Pulse excitation at $Re_{\delta^*} = 870$.

Fig. 5 Numerical modelling of streamwise velocity fluctuation ($Re_{\delta^*} = 1235$). Single Pulse excitation at $Re_{\delta^*} = 870$.

Fig. 6 Comparison of disturbance u-velocity fluctuation along wave packet centre-line.

Fig. 7 Simulated flow response (u') in target zone ($Re_{\delta^*} = 1780$), dashed lines correspond to negative values.
(a) no control (dash-boxed insert of Fig. 3 rescaled)
(b) case (1): single controller on centre-line, contour levels as in (a)

Fig. 8 Simulated flow response (u') in target zone ($Re_{\delta^*} = 1780$), dashed lines correspond to negative values. Contour levels as in Fig. 10a. Relative size of wave packet at control location $Re_{\delta^*} = 1235$ and spanwise controller positioning is indicated in the left part of plot area.
(a) case (2): three controllers configuration
(b) case (3): four controllers configuration.

Fig. 9 Performance sensitivity to controller gain and phase mismatch for different control arrangements.
(a) gain mismatch
(b) phase mismatch

Fig. 10 Bode plot of amplitude and phase behaviour of difference microphone arrangement including ideal integrator.
(a) amplification vs. normalized frequency
(b) phase shift vs. normalized frequency

Fig. 11 Simulated flow response (u') in target zone (Re_{δ^*} = 1780), due to random disturbance excitation in spanwise position and time. Dashed lines correspond to negative values. Time trace along centre-line and spanwise distribution at intermediate time extracted to bottom and right of plot respectively.
(a) uncontrolled reference case
(b) controlled case

Fig. 12 Centre-line hot-wire trace at target location. Excitation with three discrete frequencies.
(a) uncontrolled case
(b) "external" control on

Fig. 13 Integrated hot-wire rms in T-S frequency band at target location versus spanwise probe position. "External" control of two superposed frequencies. Actuator location at control location indicated by full triangles on abcissa.

Fig. 14 Hot-wire trace at detector location (centred in streamwise position between double microphone but displaced sideways by 8mm to avoid interference). Pulse excitation near leading edge.
(a) single realization hot-wire record
(b) ensemble average of 64 realizations

Fig. 15 Microphone trace at detector location on centre-line. Pulse excitation near leading edge. Simultaneously recorded with hot-wire trace in Fig. 14a.
(a) Single realization of single microphone
(b) Single realization of difference microphone

Fig. 16 Centre-line hot-wire trace at target location. Single mode excitation near leading edge.
(a) uncontrolled signal
(b) controlled signal using control loop.

Fig. 17 Actuator/detector cross-talk. Detector output as a function of externally driven actuator forcing level.
(a) two actuators symmetrical to detector microphones, spanwise displaced by 5mm.
(b) two actuators symmetrical to detector microphones, spanwise displaced by 15mm.

Fig. 18 Settling time of control circuit.
(a) Detector trace showing passing of wave packet. [Spurious spikes in signal are due to floating ground connection in this particular case and should be ignored.]
(b) Synthesized control actuator driving signal showing long settling time.

Fig. C1 Aluminium test plate for active control experiments.

Fig. C2 Cambridge University Low Turbulence Research Tunnel.

Fig. C3 Electronic hardware for active control experiment.

Fig. D1 Boundary layer response in packet centre-line at Re = 1380. Data analogoue filtered between 20Hz and 2000Hz.
(a) single realization
(b) ensemble average of 189 realizations

Fig. D2 Power spectral density versus frequency plot of ensemble averaged data shown in Fig. D1b.

Fig. D3 Measured u-fluctuations at outer boundary layer edge at Re_δ= 1380. Ensemble averaged (189) and digitally filtered between 80Hz and 500Hz.
(a) perspective view
(b) contour plot, negative contours dashed

Fig. D4 Measured u-fluctuations in the boundary layer at Re = 1235 for twin pulse interaction experiment. Two pulses of same strength buth opposite sign excite flow at Re_δ= 880. Ensemble averaged data digitally filtered between 80Hz and 500Hz.
(a) perspective view
(b) contour plot, negative contours dashed

Fig. D5 Measured u-fluctuations in the boundary layer at Re_δ= 1235 for triple pulse interaction experiment. Three pulses of same strength (3cm apart spanwise) excite flow at Re_δ= 880. Middle pulse of opposite sign. Ensemble averaged data digitally filtered between 80Hz and 500Hz.
(a) perspective view
(b) contour plot, negative contours dashed

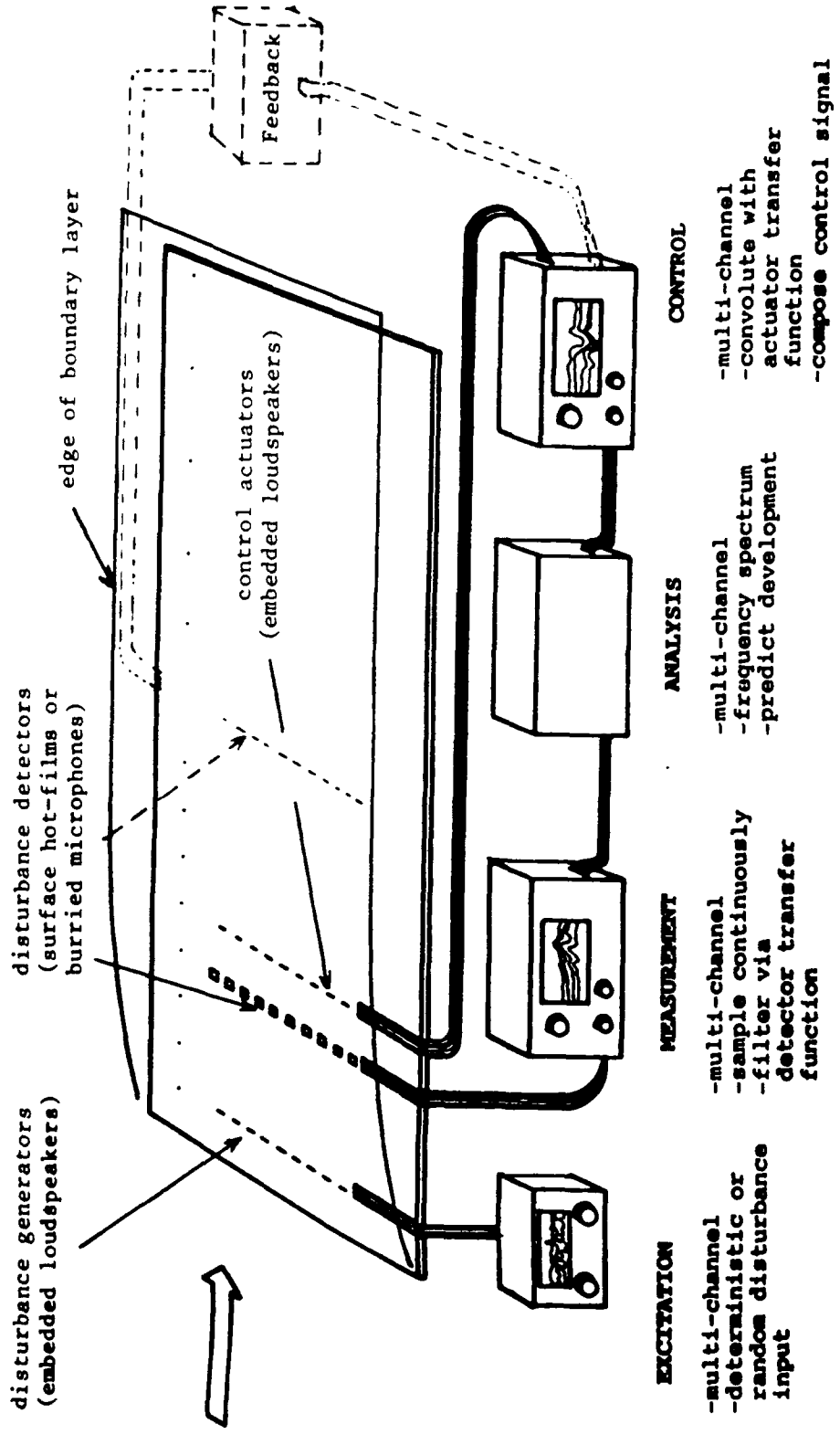

Fig. 1 Schematic of boundary layer control arrangement.

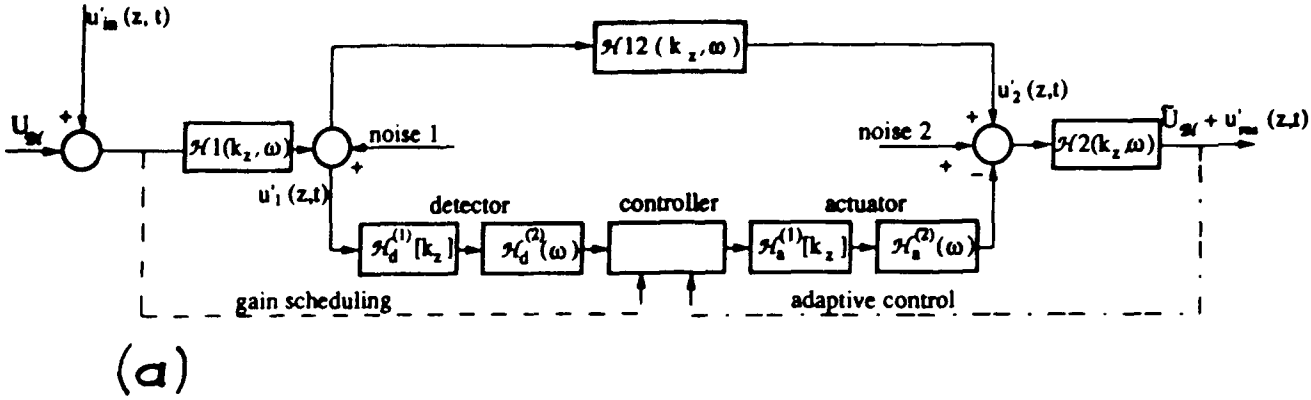

(a)

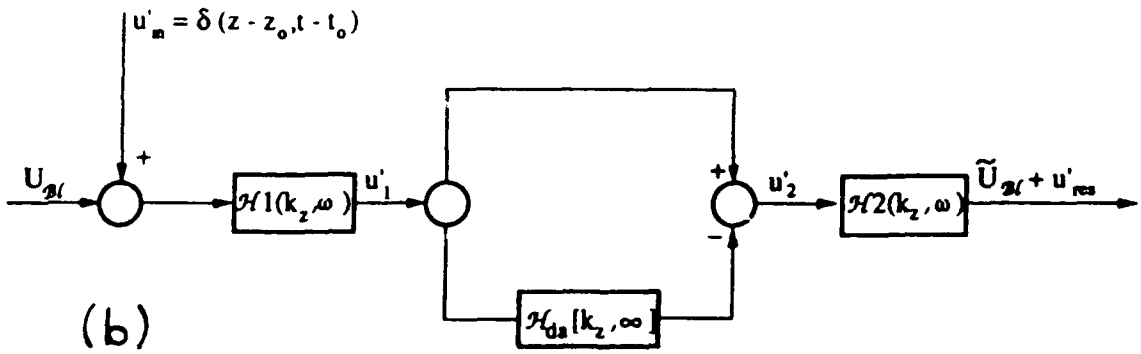

(b)

Fig. 2 Block diagram representation of boundary layer control system.
(a) full system
(b) simplified basic system

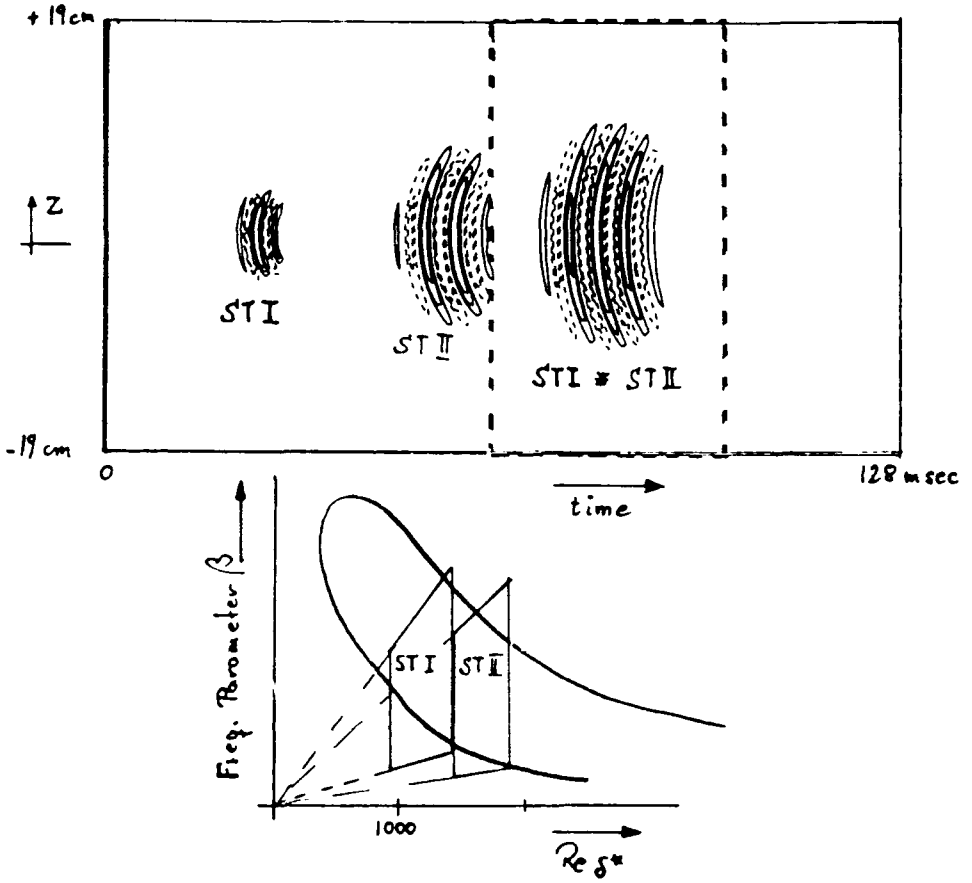

Fig. 3 Simulation of flow response due to point source excitation at Re_{δ^*}= 870. Dashed lines correspond to negative values.
ST1 - System transfer function from Re_{δ^*}= 870 to 1235.
ST2 - System transfer function from Re_{δ^*}= 1235 to 1780.
ST1*ST2 - Disturbance flow response at Re_{δ^*}= 1780 due to point source excitation at Re_{δ^*}= 870 (STI convoluted with STII).

EXPERIMENTAL RESULTS - SINGLE SOURCE

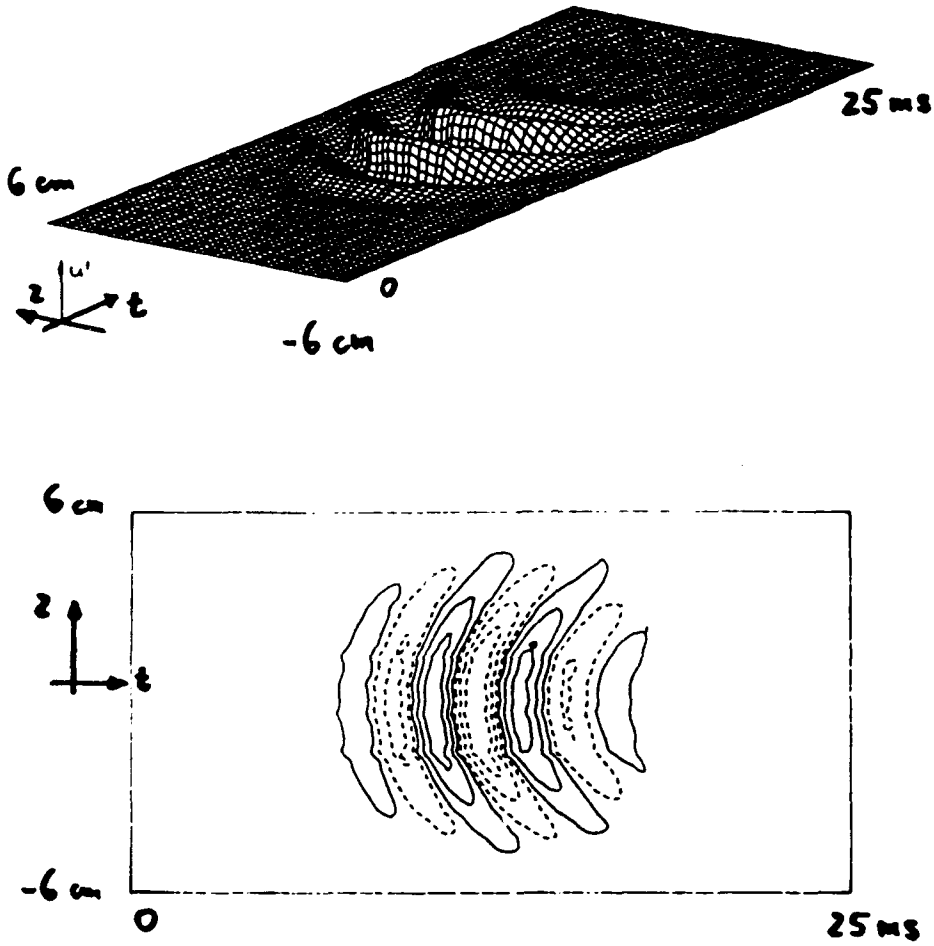

Fig. 4 Streamwise velocity fluctuations (u') measured at outer edge of boundary layer ($Re_{\delta'}$ = 1235). Single Pulse excitation at $Re_{\delta'}$ = 870.

SIMULATION RESULTS - SINGLE SOURCE

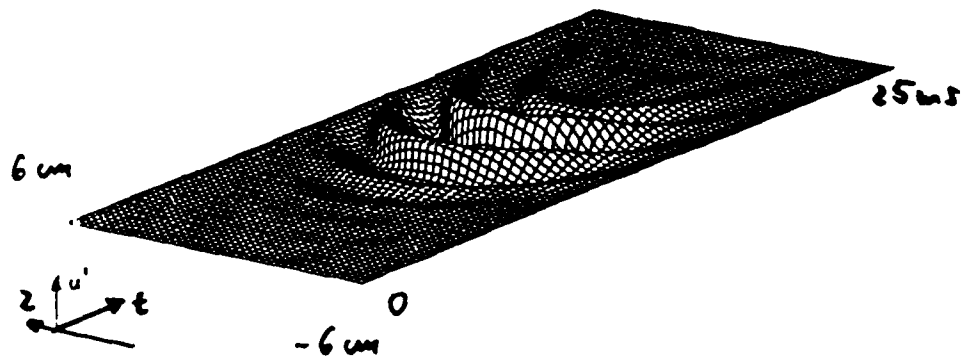

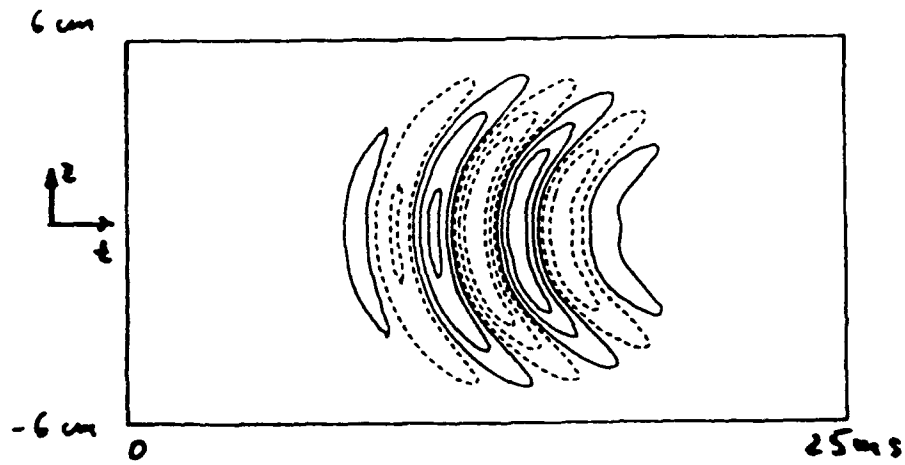

Fig. 5 Numerical modelling of streamwise velocity fluctuation (Re_{δ^*} = 1235). Single Pulse excitation at Re_{δ^*} = 870.

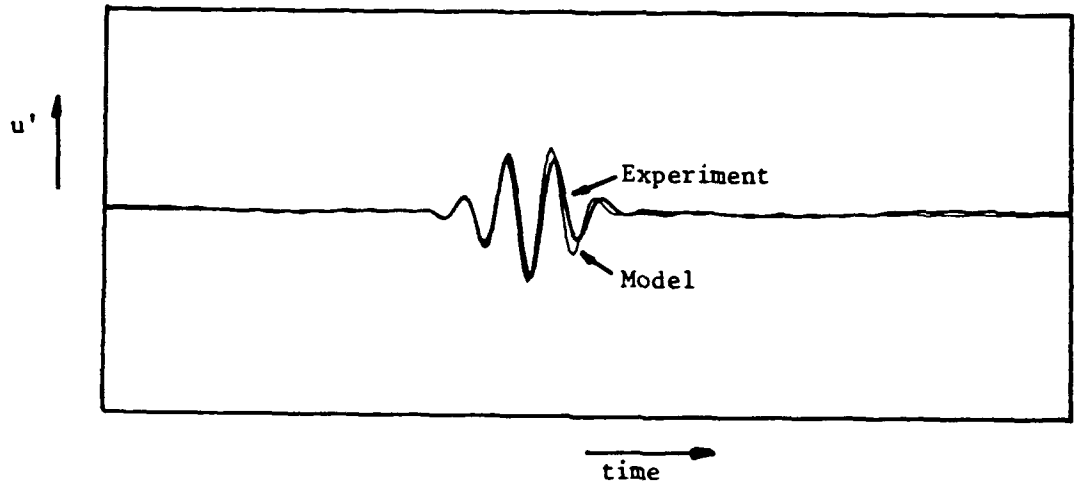

Fig. 6 Comparison of disturbance u-velocity fluctuation along wave packet centre-line.

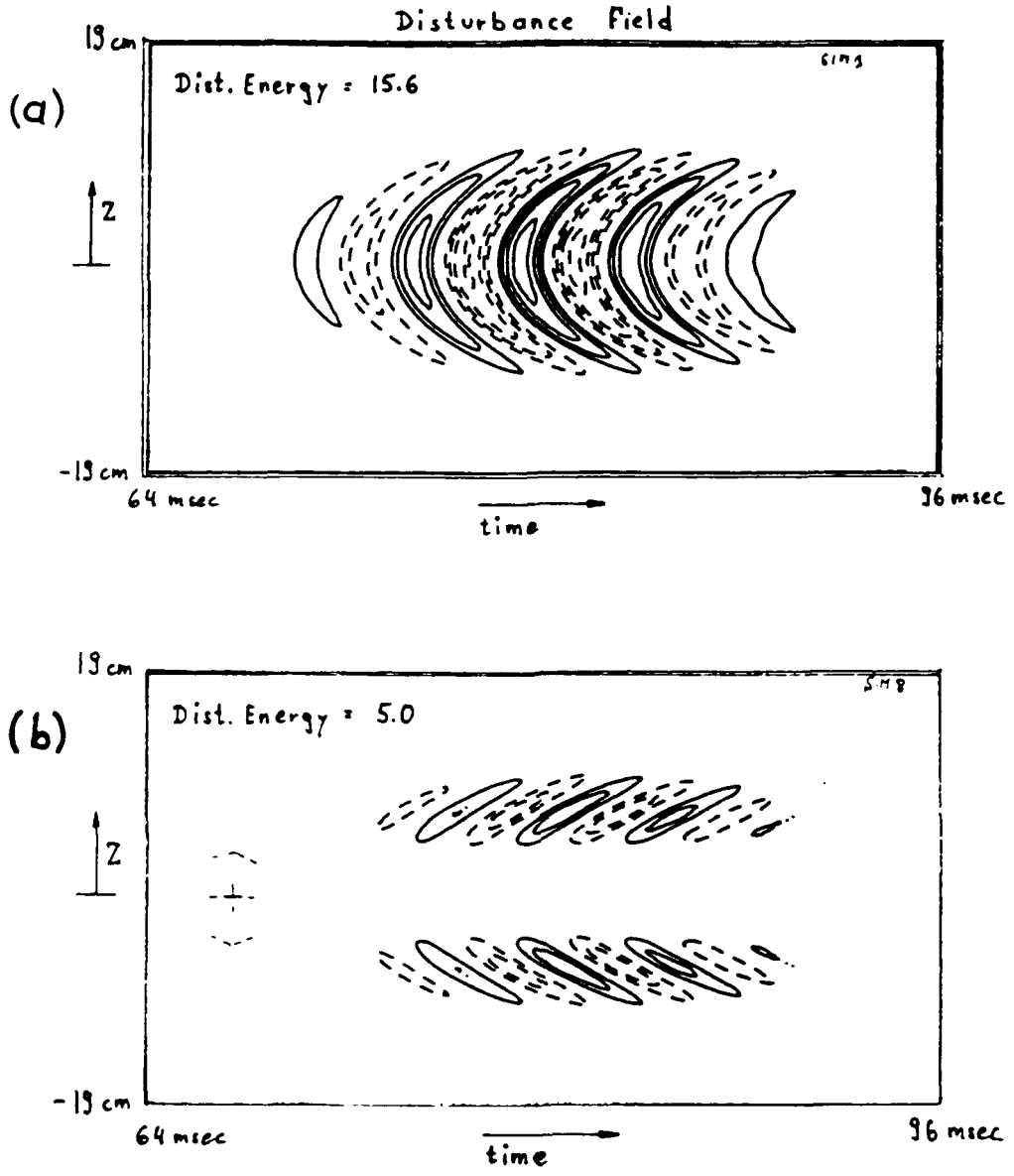

Fig. 7 Simulated flow response (u') in target zone (Re_{δ^*}= 1780), dashed lines correspond to negative values.
(a) no control (dash-boxed insert of Fig. 3 rescaled)
(b) case (1): single controller on centre-line, contour levels as in (a)

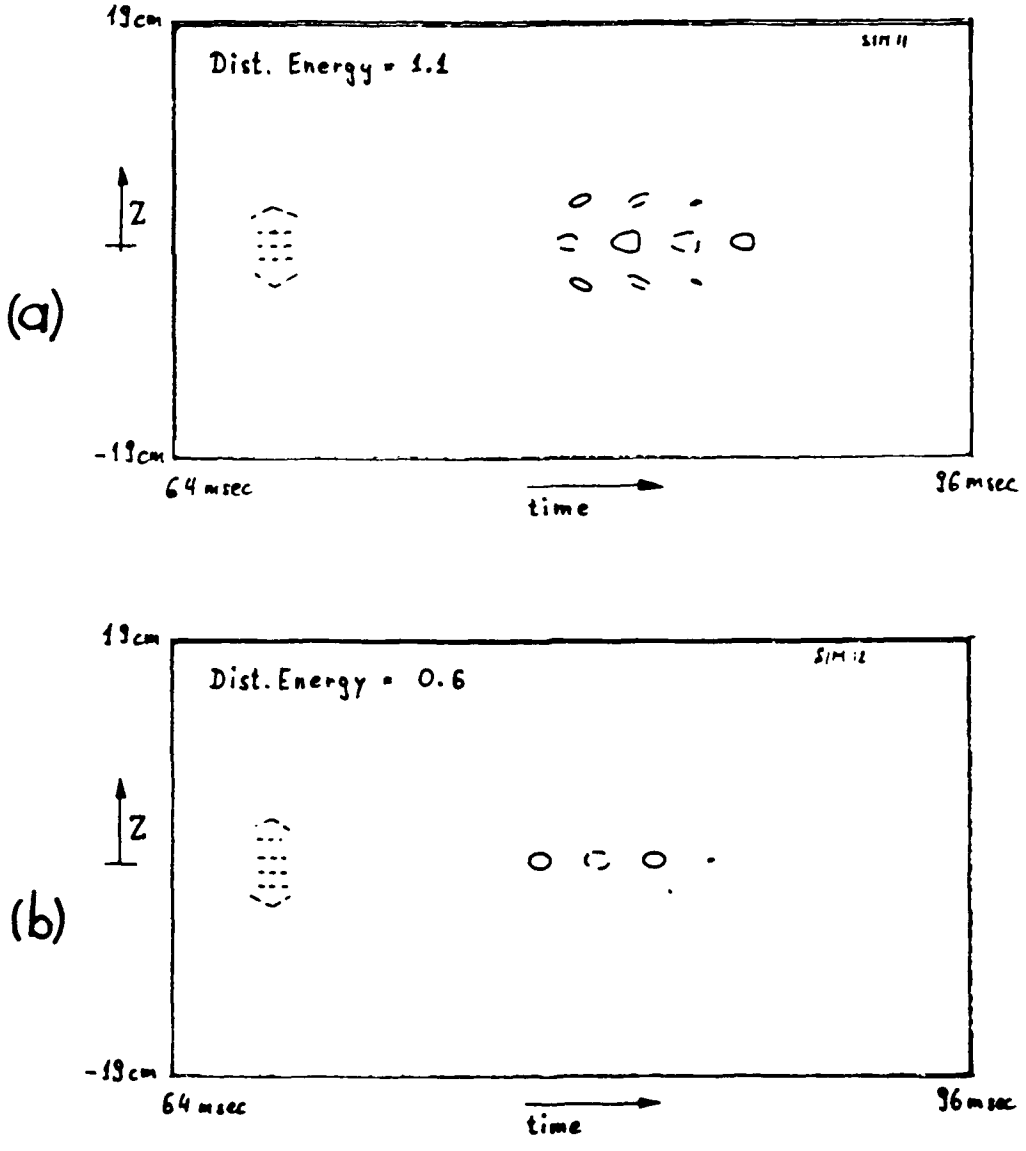

Fig. 8 Simulated flow response (u') in target zone (Re_{δ^*}= 1780), dashed lines correspond to negative values. Contour levels as in Fig. 10a. Relative size of wave packet at control location Re_{δ^*}= 1235 and spanwise controller positioning is indicated in the left part of plot area.
(a) case (2): three controllers configuration
(b) case (3): four controllers configuration.

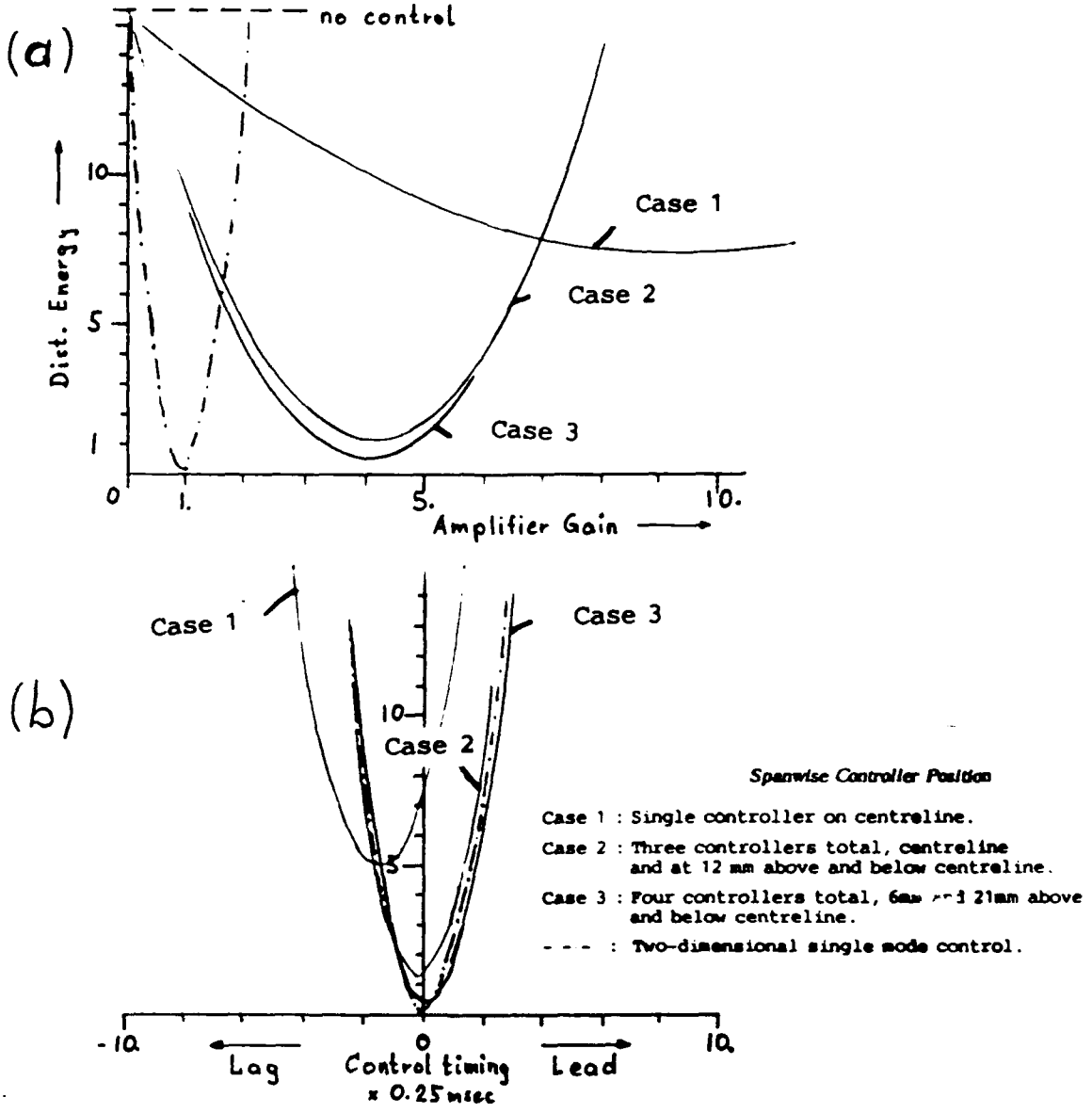

Fig. 9 Performance sensitivity to controller gain and phase mismatch for different control arrangements.
(a) gain mismatch
(b) phase mismatch

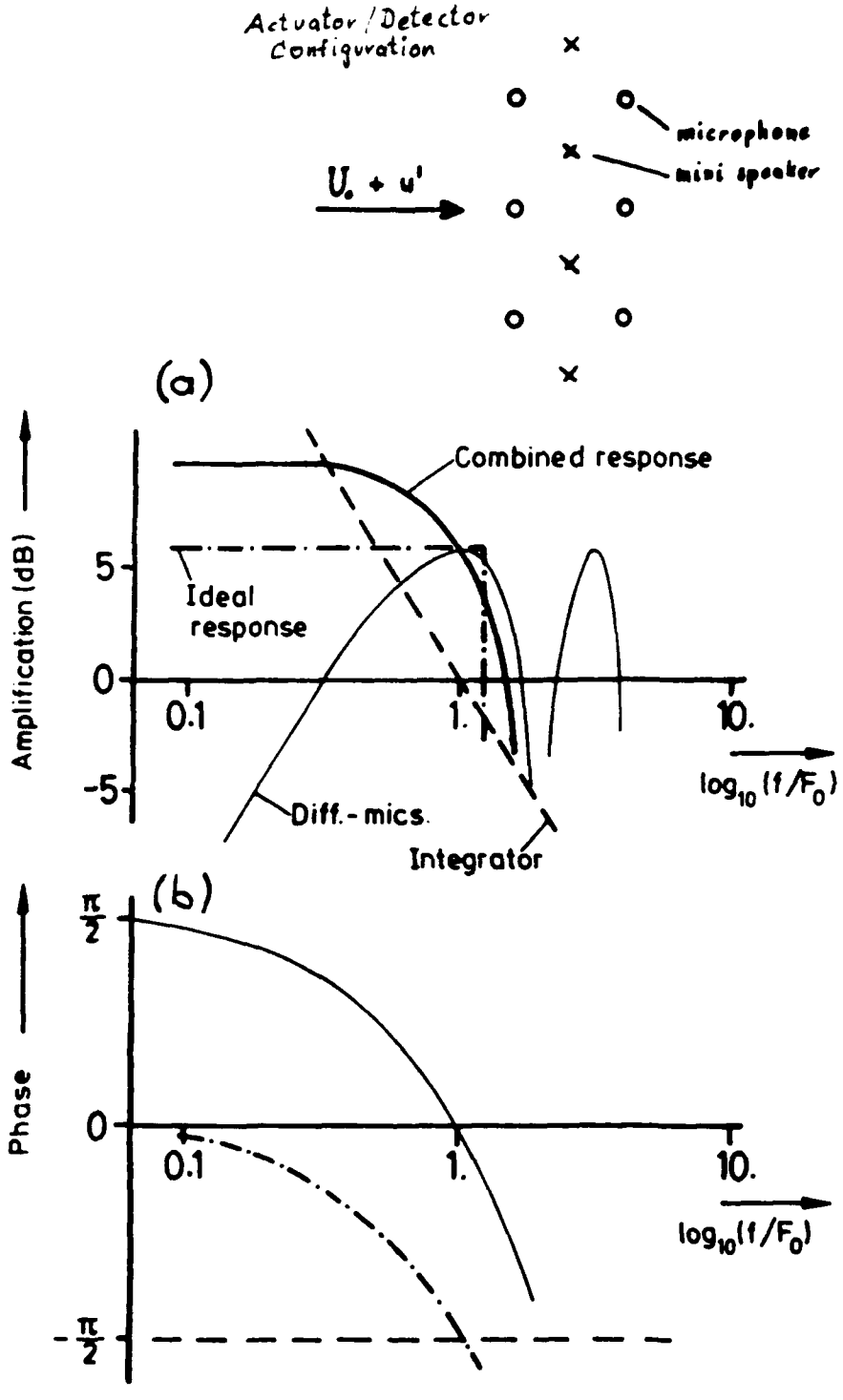

Fig. 10 Bode plot of amplitude and phase behaviour of difference microphone arrangement including ideal integrator.
(a) amplification vs. normalized frequency
(b) phase shift vs. normalized frequency

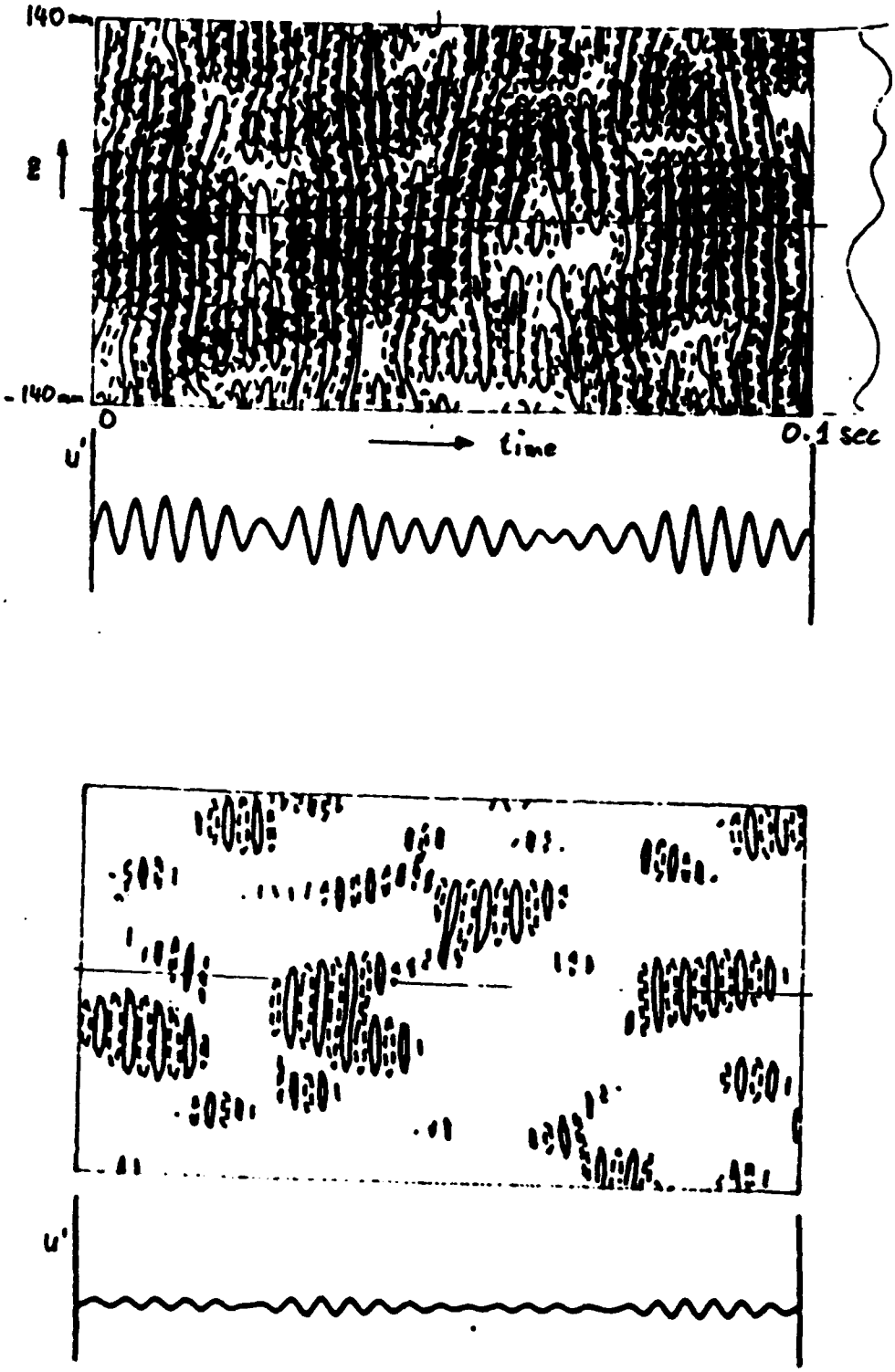

Fig. 11 Simulated flow response (u') in target zone (Re_{δ^*}= 1780), due to random disturbance excitation in spanwise position and time. Dashed lines correspond to negative values. Time trace along centre-line and spanwise distribution at intermediate time extracted to bottom and right of plot respectively.
(a) uncontrolled reference case
(b) controlled case

EXTERNAL CONTROL - THREE FREQUENCIES

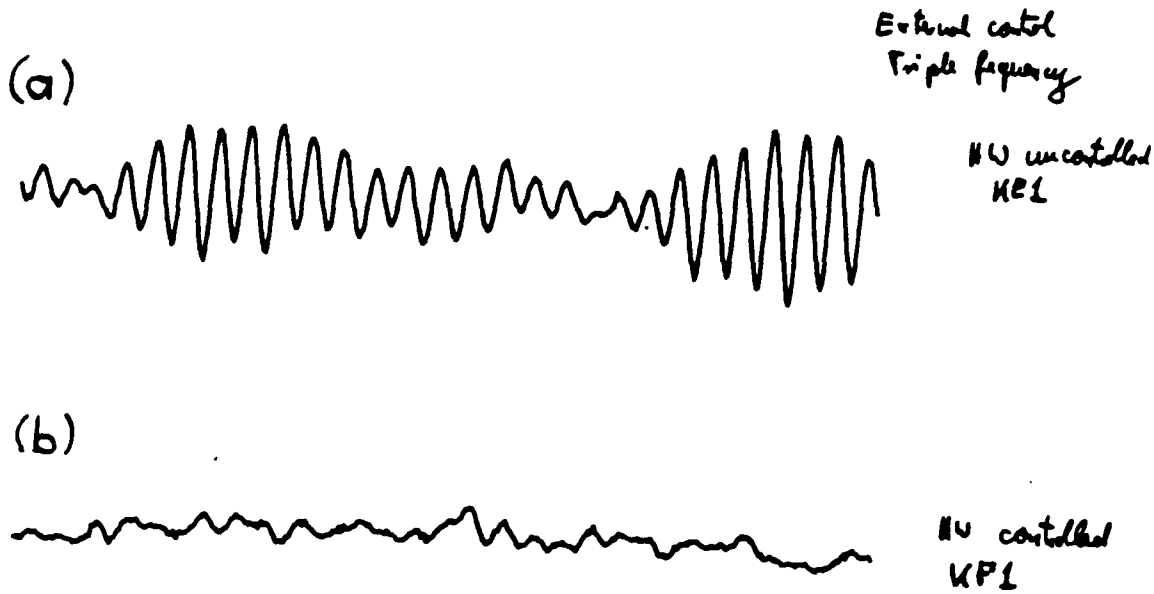

Fig. 12 Centre-line hot-wire trace at target location.
Excitation with three discrete frequencies.
(a) uncontrolled case
(b) "external" control on

SPANWISE DISTRIBUTION

* Forcing at Re_{δ^*} = 870, control at Re_{δ_1} = 1260, target zone at Re_{δ_1} = 1780

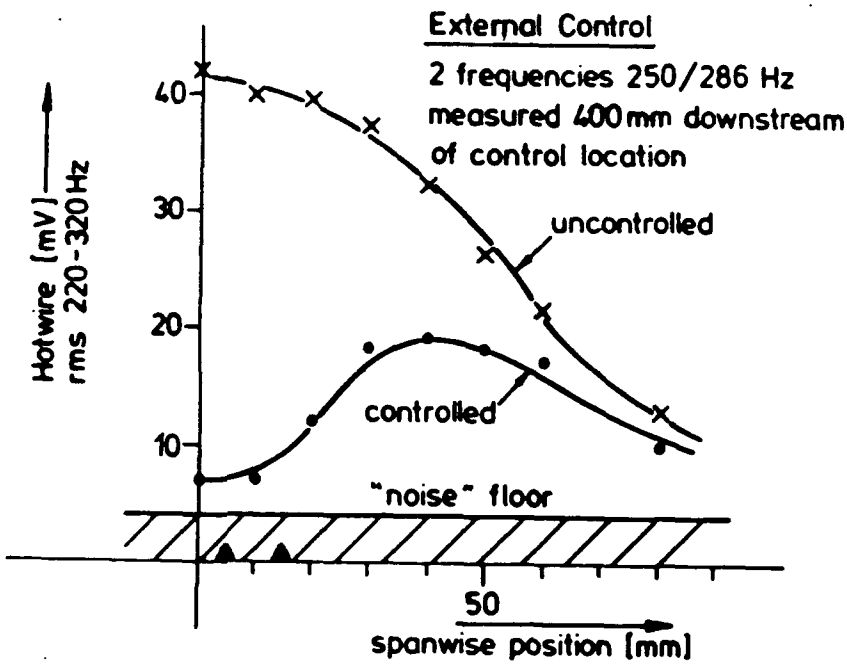

Fig. 13 Integrated hot-wire rms in T-S frequency band at target location versus spanwise probe position.
"External" control of two superposed frequencies.
Actuator location at control location indicated by full triangles on abcissa.

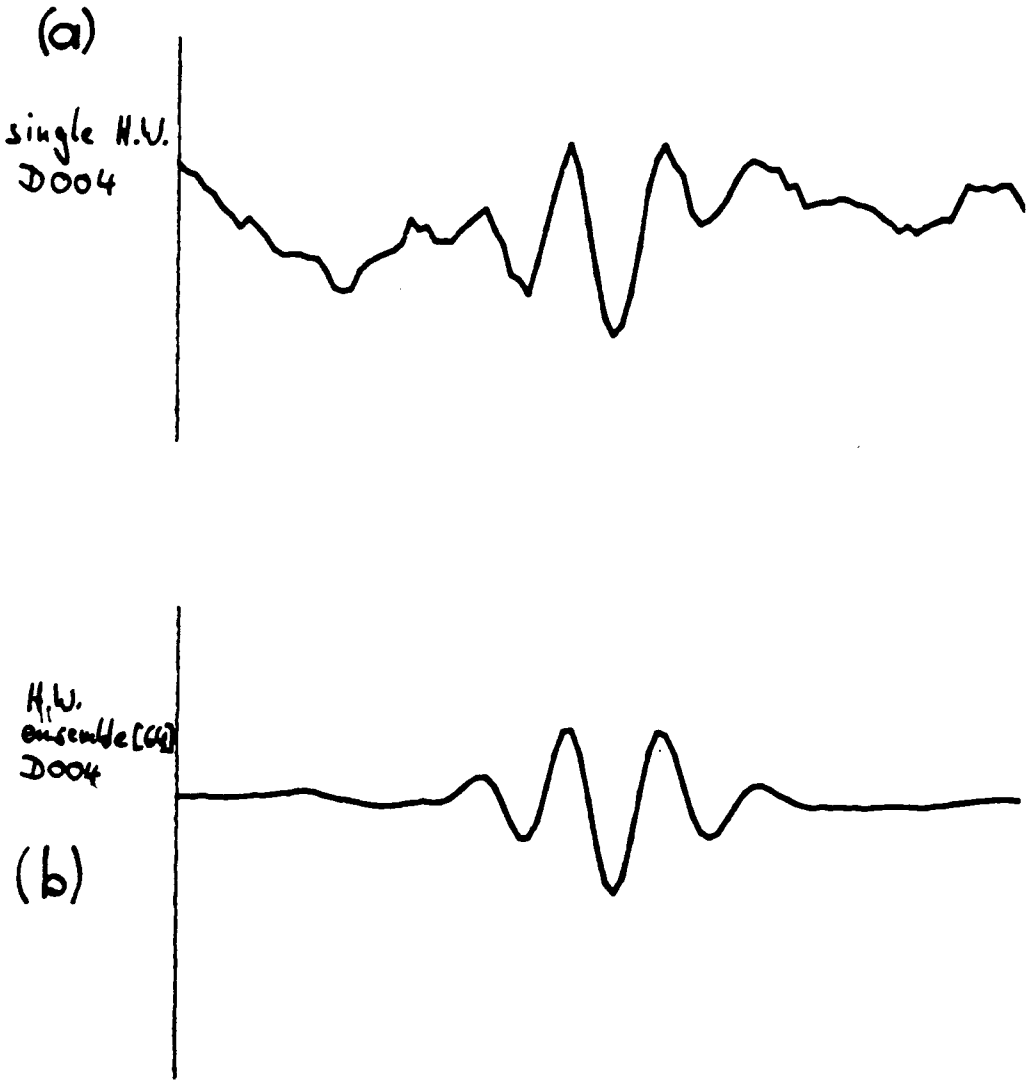

Fig. 14 Hot-wire trace at detector location (centred in streamwise position between double microphone but displaced sideways by 8mm to avoid interference). Pulse excitation near leading edge.
(a) single realization hot-wire record
(b) ensemble average of 64 realizations

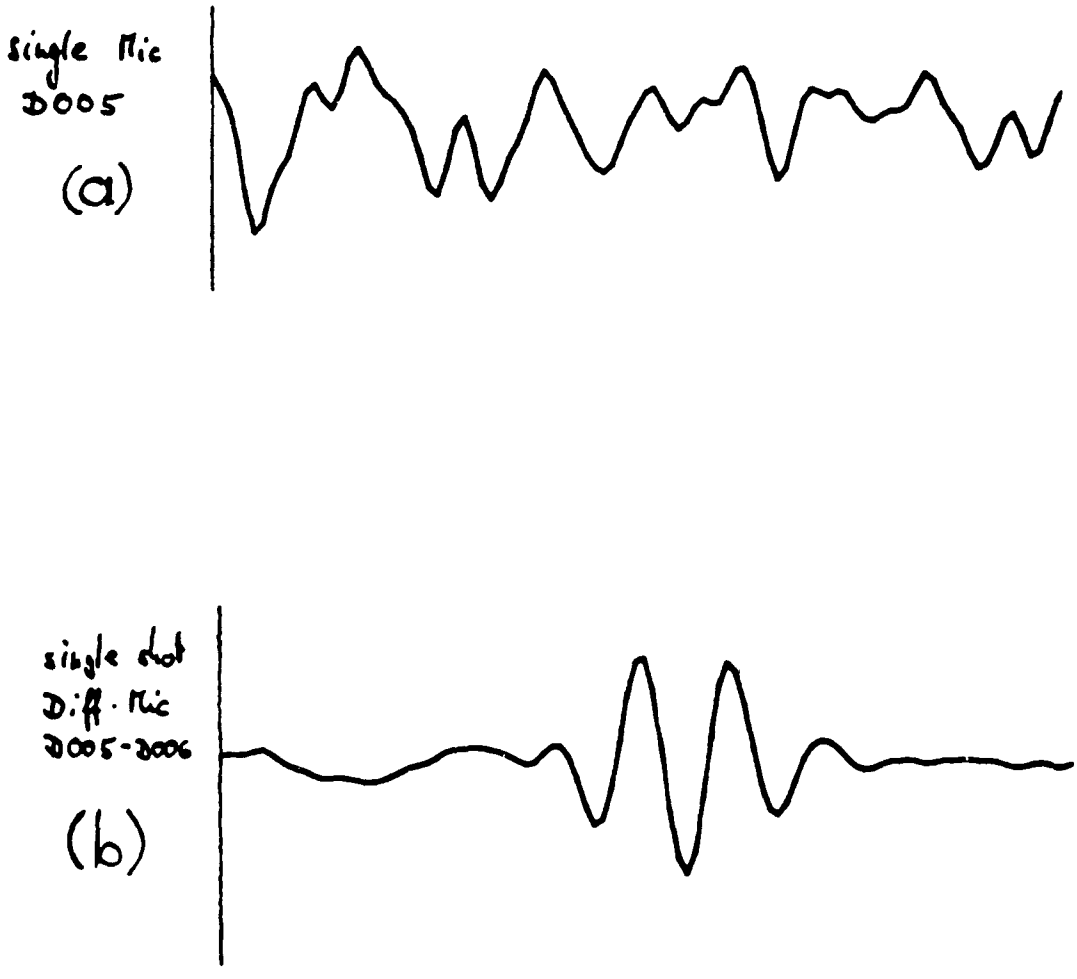

Fig. 15 Microphone trace at detector location on centre-line. Pulse excitation near leading edge. Simultaneously recorded with hot-wire trace in Fig. 14a.
(a) Single realization of single microphone
(b) Single realization of difference microphone

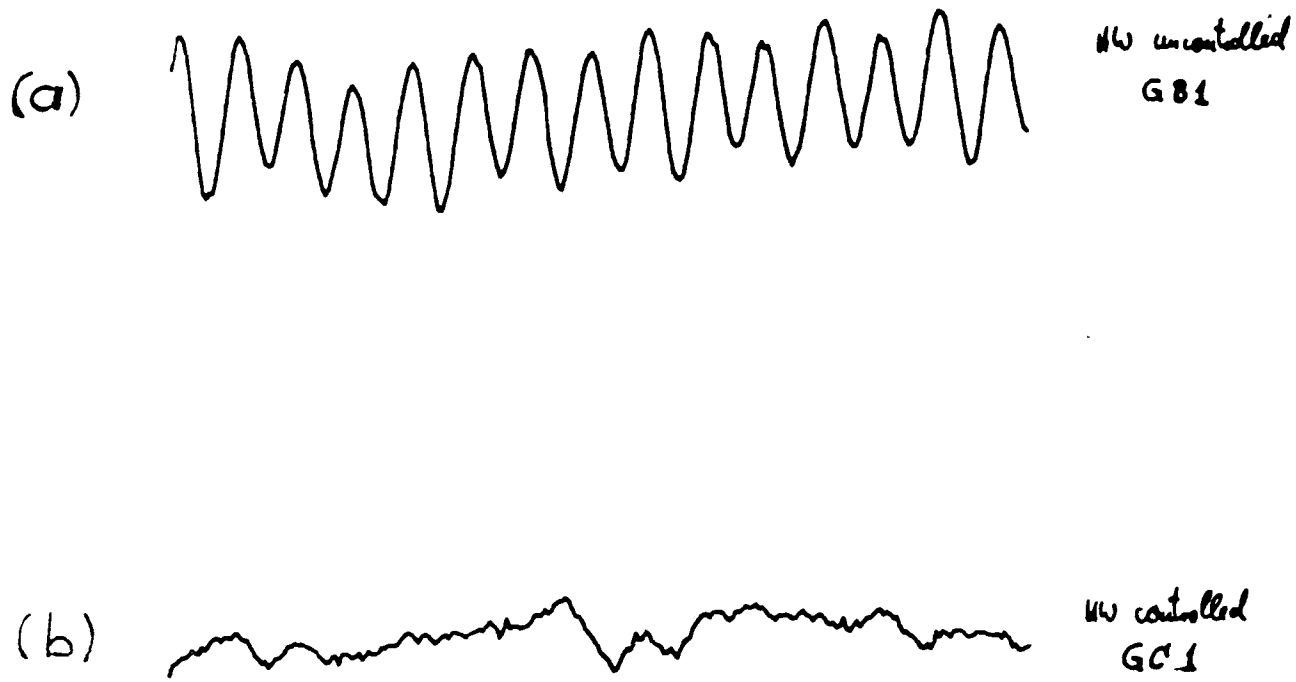

Fig. 16 Centre-line hot-wire trace at target location.
Single mode excitation near leading edge.
(a) uncontrolled signal
(b) controlled signal using control loop.

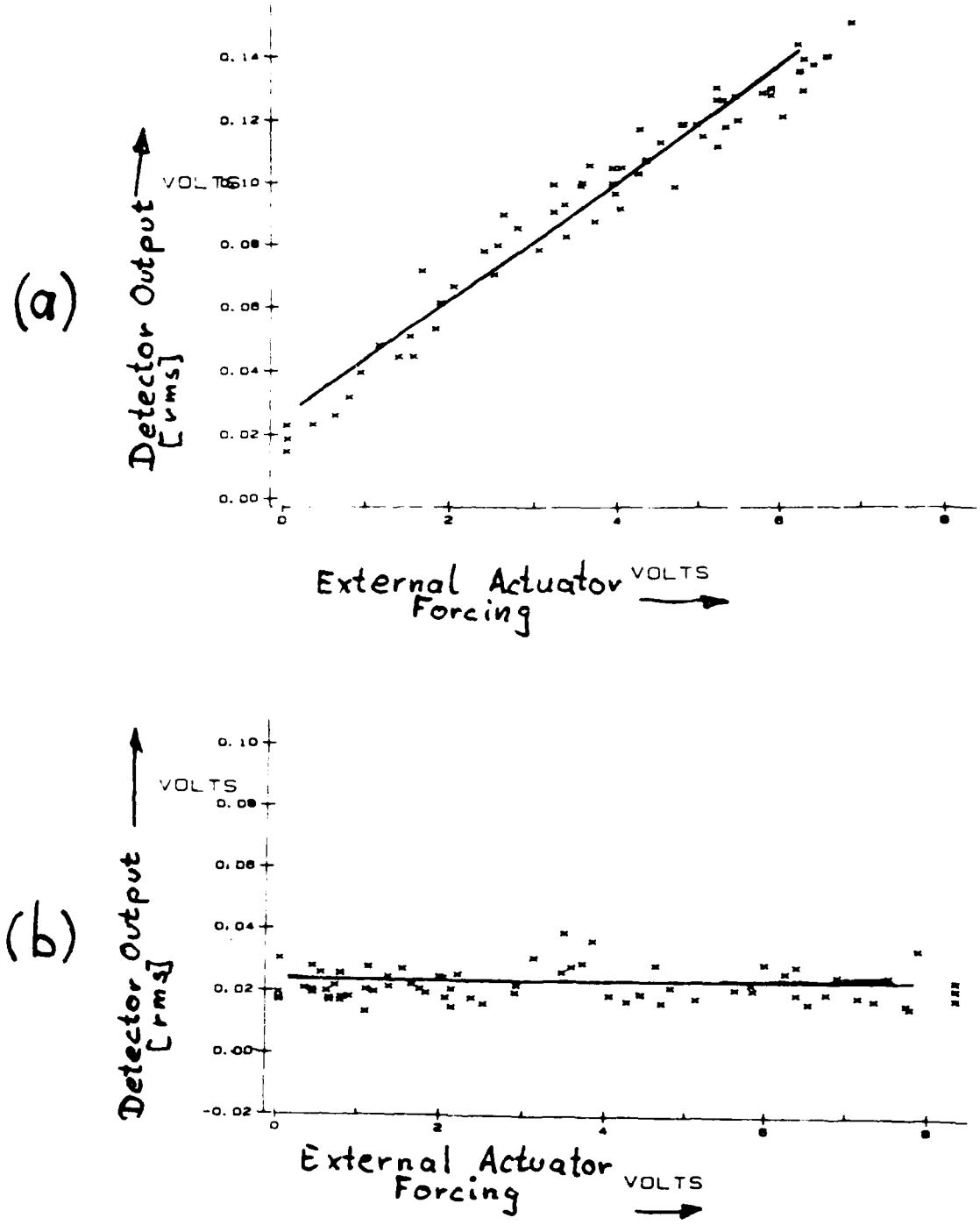

Fig. 17 Actuator/detector cross-talk. Detector output as a function of externally driven actuator forcing level.
(a) two actuators symmetrical to detector microphones, spanwise displaced by 5mm.
(b) two actuators symmetrical to detector microphones, spanwise displaced by 15mm.

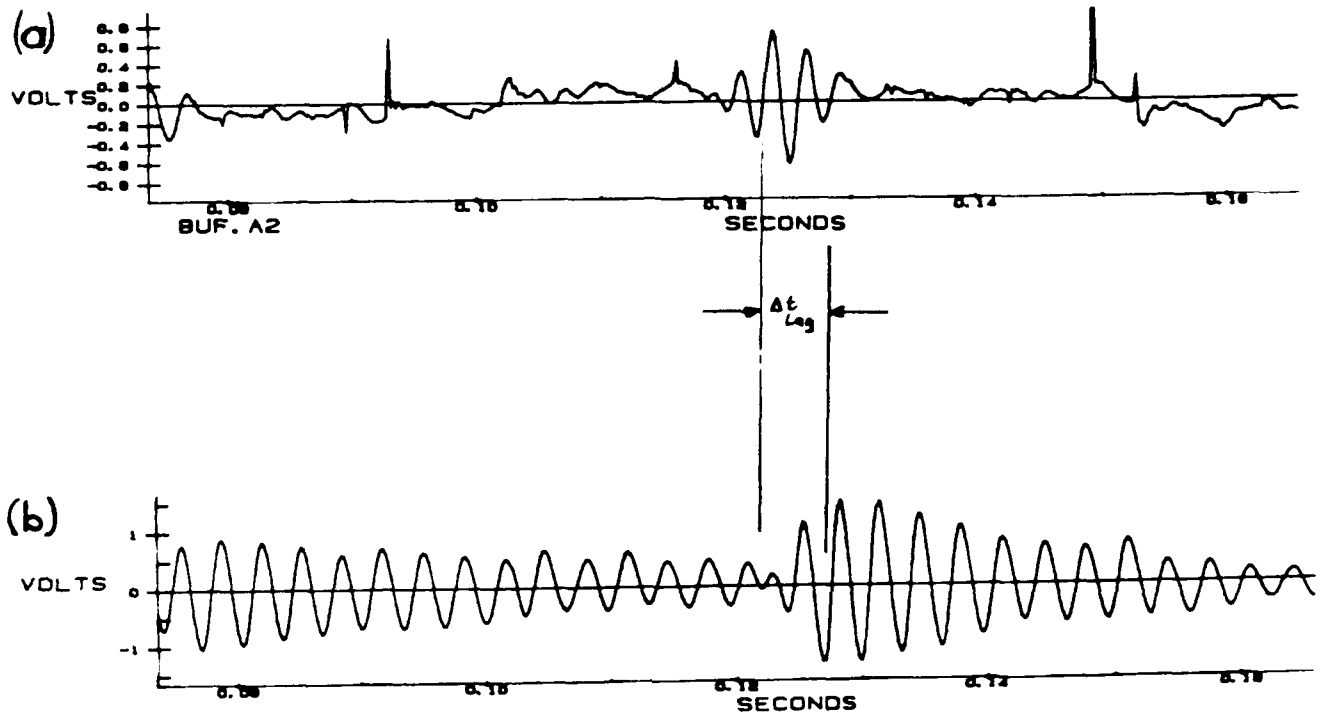

Fig. 18 Settling time of control circuit.
(a) Detector trace showing passing of wave packet. [Spurious spikes in signal are due to floating ground connection in this particular case and should be ignored.]
(b) Synthesized control actuator driving signal showing long settling time.

EXPERIMENTAL SETUP

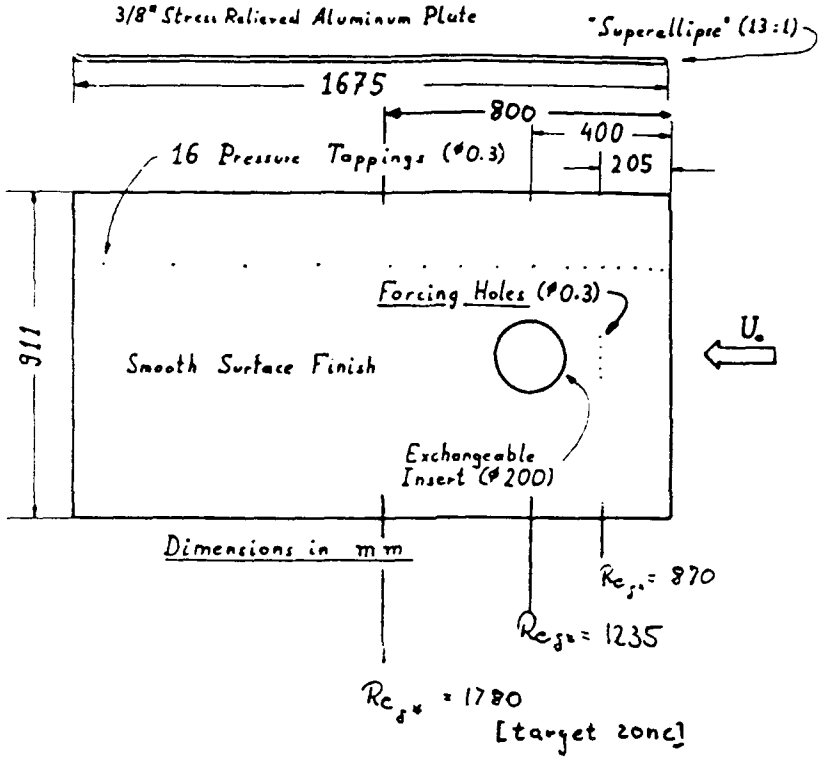

* One and twin source forcing.
* Measuring station at Re_{δ^*} = 1235.
* Control target at Re_{δ^*} = 1780.

Fig. C1 Aluminium test plate for active control experiments.

EXPERIMENTAL FACILITY

- C.U.E.D. low turbulence research tunnel

  (former NPL tunnel).

  * Exchangeable working sections 3ft x 3ft x 6ft.

  * 3-D computer controlled traverse

  * Micro-computer based d.a. system

  * Turbulence Intensity < 0.01%

    (20m/s, 4 Hz to 2000 Hz).

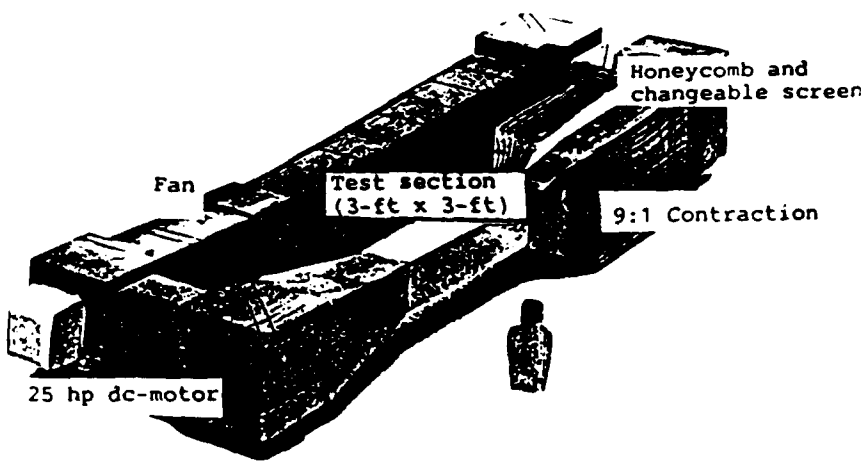

Fig. C2 Cambridge University Low Turbulence Research Tunnel.

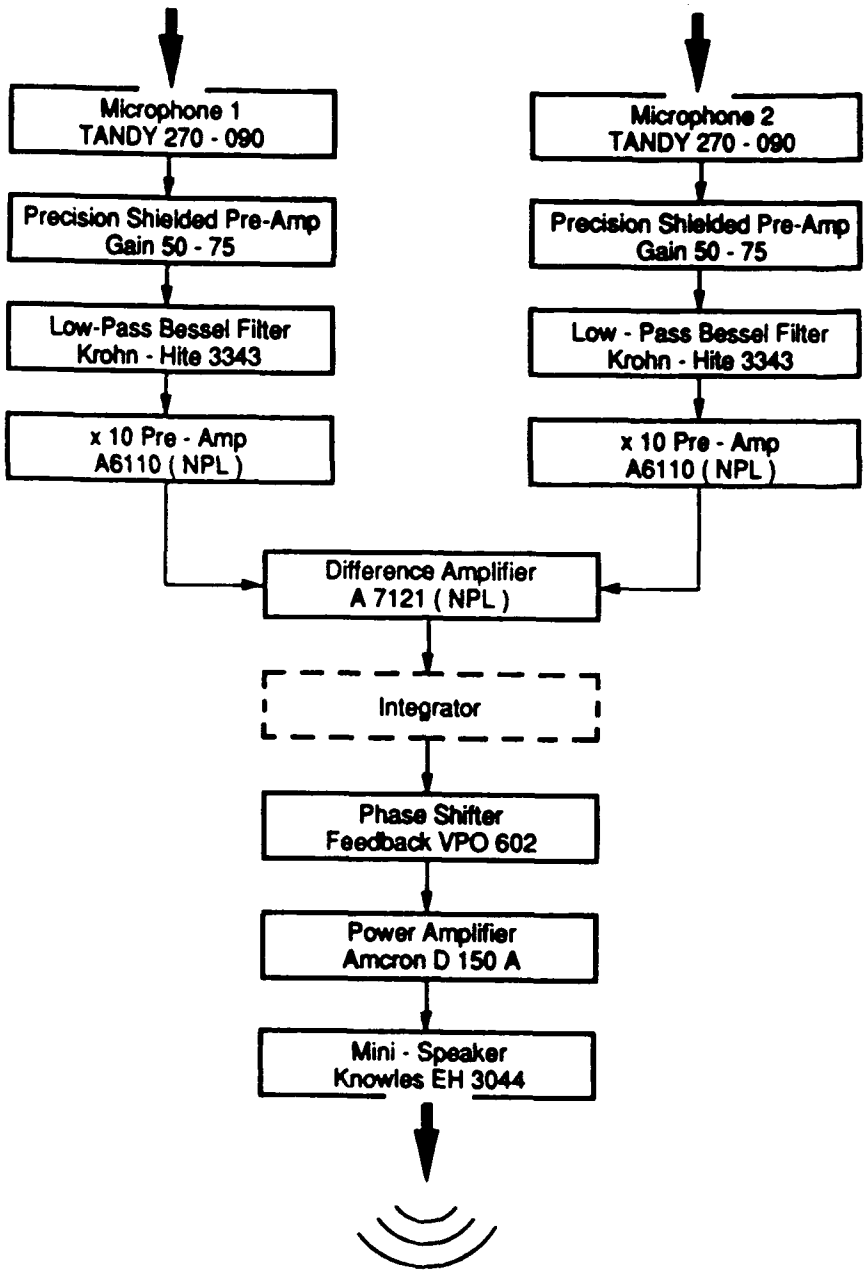

Fig. C3 Electronic hardware for active control experiment.

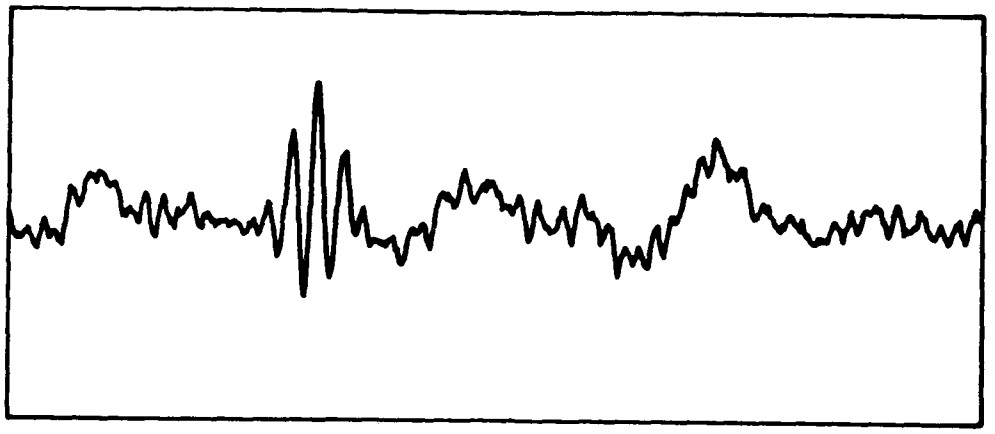

0 (a) 0.13 secs

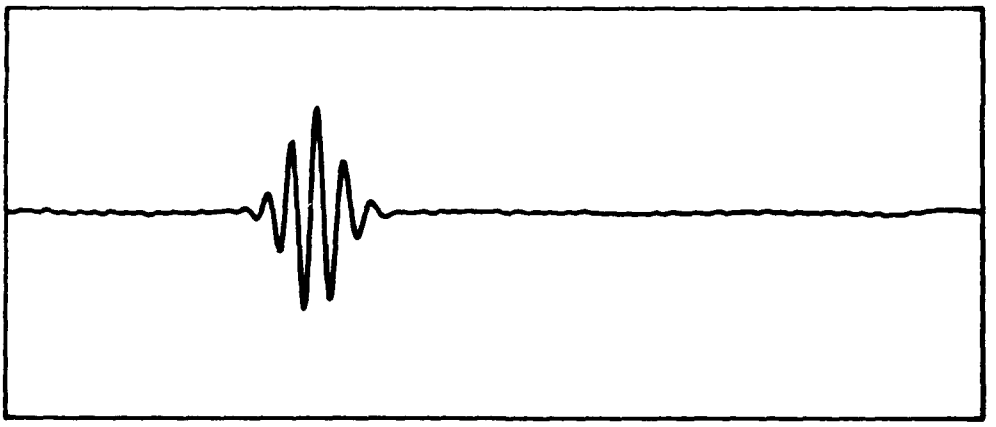

0 0.13 secs

(b)

Fig. D1 Boundary layer response in packet centre-line at Re_{λ}= 1380.
Data analogoue filtered between 20Hz and 2000Hz.
(a) single realization
(b) ensemble average of 189 realizations

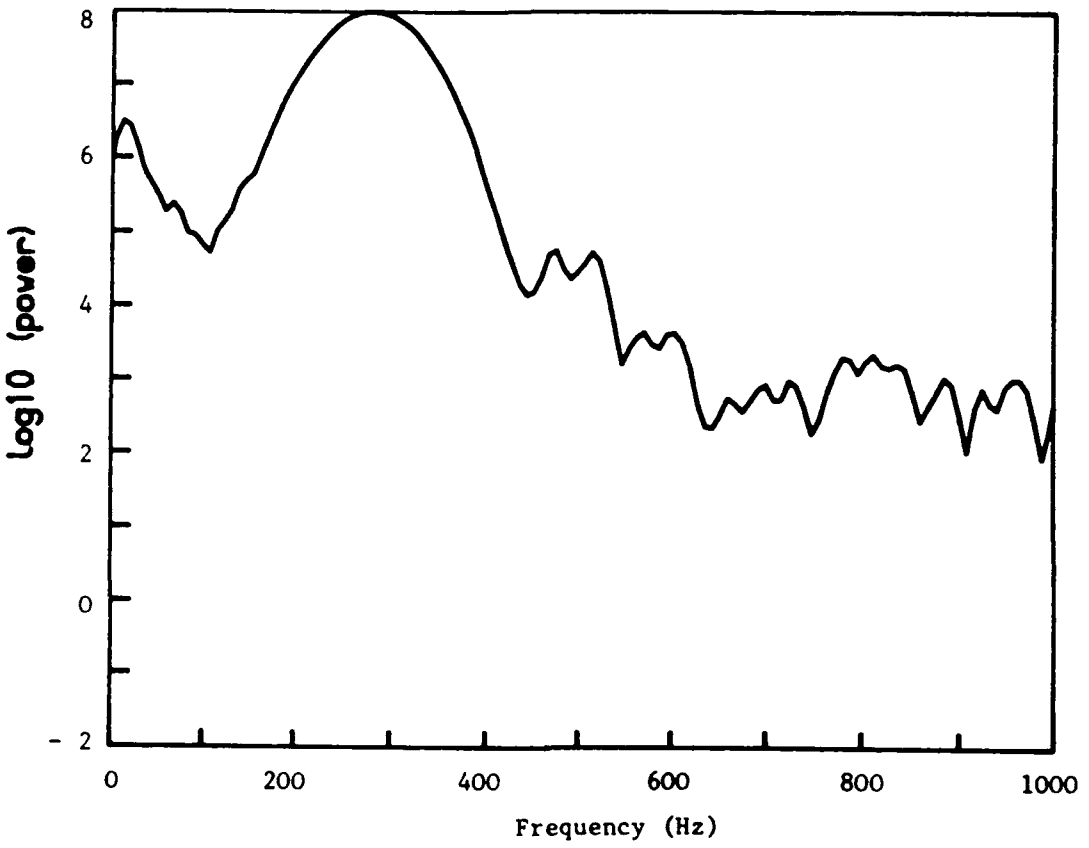

Fig. D2 Power spectral density versus frequency plot of ensemble averaged data shown in Fig. D1b.

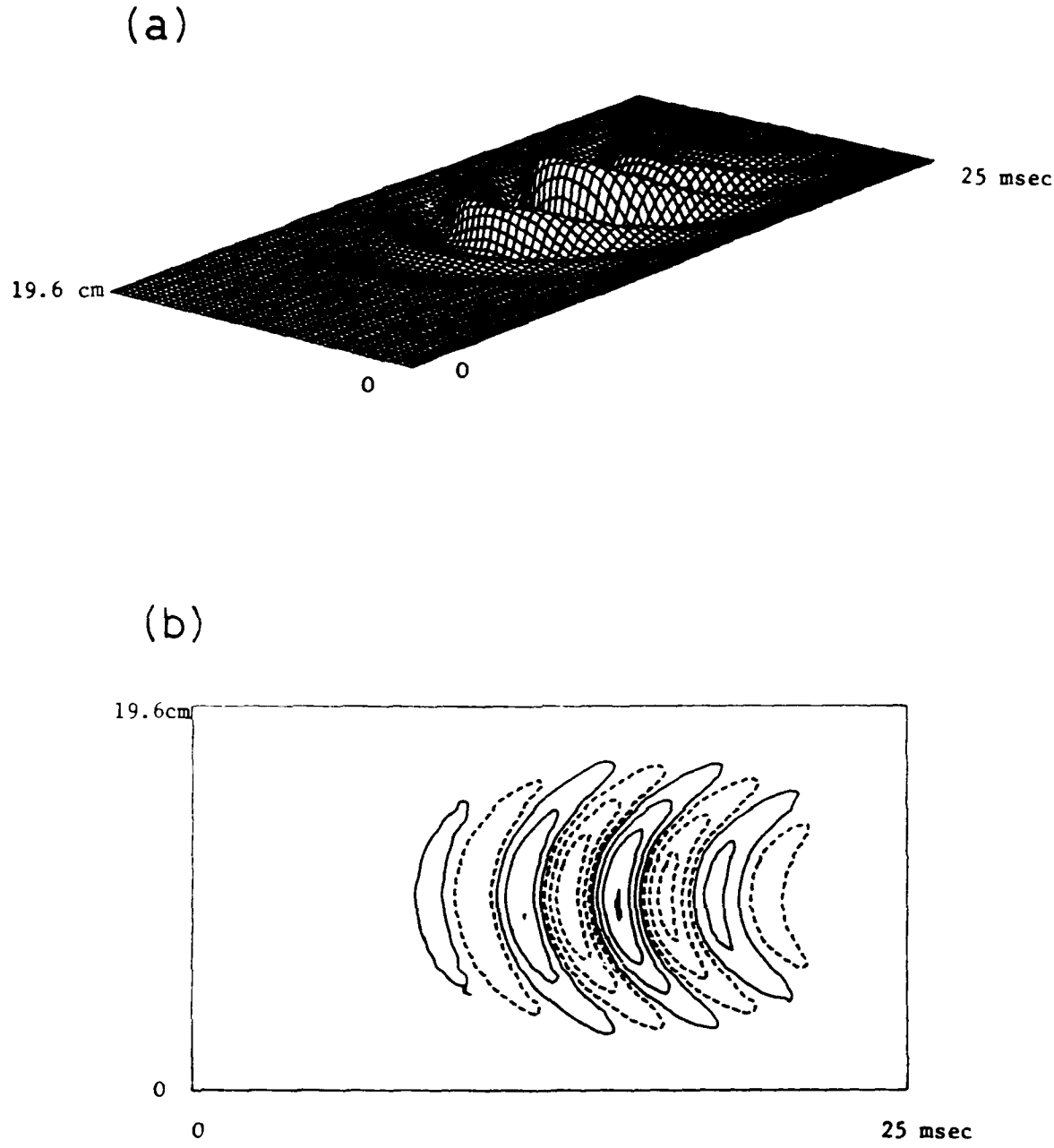

Fig. D3 Measured u-fluctuations at outer boundary layer edge at Re_{x^*} = 1380. Ensemble averaged (189) and digitally filtered between 80Hz and 500Hz.
(a) perspective view
(b) contour plot, negative contours dashed

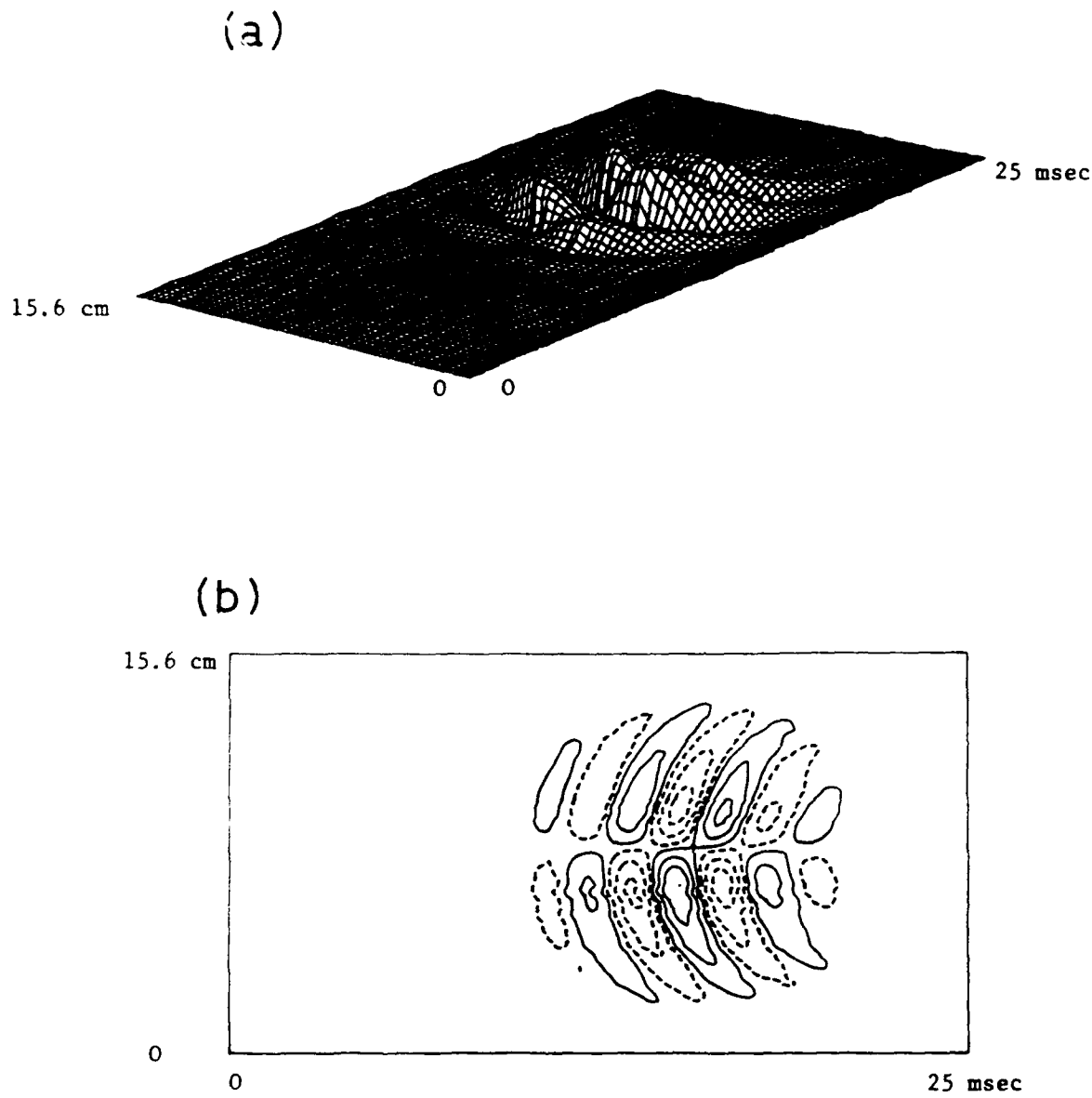

Fig. D4 Measured u-fluctuations in the boundary layer at Re_{δ^*}= 1235 for twin pulse interaction experiment. Two pulses of same strength buth opposite sign excite flow at Re_{δ^*}= 880. Ensemble averaged data digitally filtered between 80Hz and 500Hz.
(a) perspective view
(b) contour plot, negative contours dashed

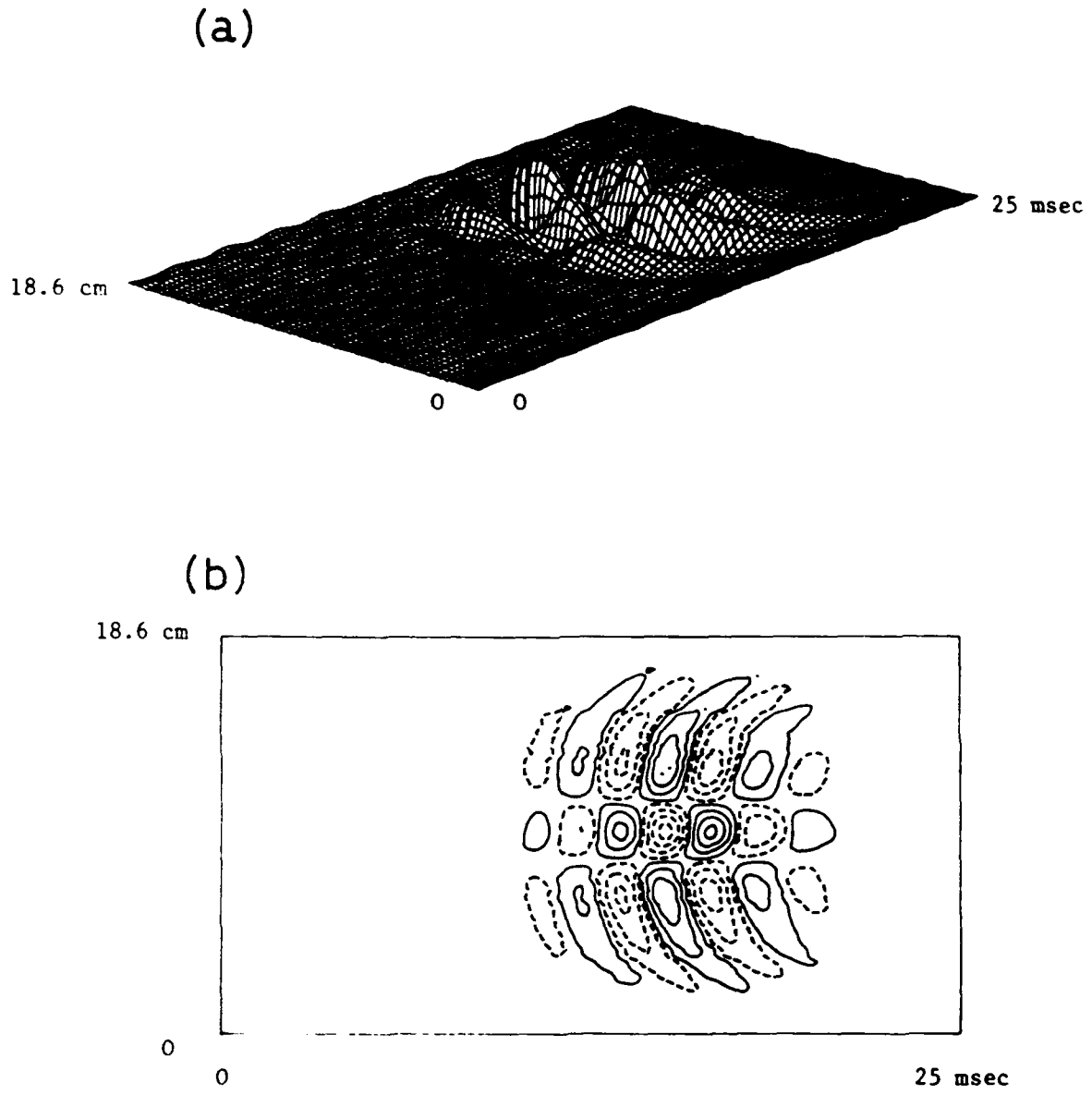

Fig. D5 Measured u-fluctuations in the boundary layer at $Re_\delta^* = 1235$ for triple pulse interaction experiment. Three pulses of same strength (3cm apart spanwise) excite flow at $Re_\delta^* = 880$. Middle pulse of opposite sign. Ensemble averaged data digitally filtered between 80Hz and 500Hz.
(a) perspective view
(b) contour plot, negative contours dashed

Appendix B: Project Plan

Phase One - Preliminaries

- Review of Literature.
- Familiarization (R.H.) with wind tunnel setup, computer controlled data-acquisition system.
- Test plate design.
- Three-dimensional traverse.

Phase Two - Transfer functions

- Selection of method for detection and control.
- Experimental determination of detector and controller transfer function.

Phase Three - Numerical modelling

- Implement and experiment with computer model of various control arrangements using Gaster's (1978) rapid series eigenvalue expansion method.
- Based on above modelling identify the most promising control arrangements.

Phase Four - Active control experiment

- Experimental study of the most promising control arrangements identified in phase three using a small number of detectors and controllers.
- Prepare final report.

Appendix C: Hardware Development

The experiments to be performed require a flat plate which is suited for the testing of several different exciter, detector and controller arrangements. A plate (Fig. C1) which allows for changeable inserts has been designed, build and installed in the Cambridge University Engineering Department (C.U.E.D.) low turbulence wind tunnel (Fig. C2). The plate allows disturbance excitation at five spanwise locations (3cm apart) via embedded loudspeakers 20.5cm downstream of the leading edge.

An important feature of the plate is the provision for exchangeable inserts which allow the testing of various different control arrangements. Inserts can be exchanged while the plate is positioned in the tunnel. Great care was taken that the edge of the insert was flush with the working side of the plate in order to avoid the creation of flow disturbances. The gap between insert and plate was filled and polished in order to achieve the required surface continuity.

Control actuators and disturbance detectors had to be selected according to frequency response characteristic, ease of installation, physical robustness and availability. The "buried loudspeaker" technique had been successfully used in previous work (Gaster and Grant, 1975) for disturbance excitation in a similar setting. It was decided to use the same technique for control actuation. In order to allow close spanwise spacing of the control actuators a physically small speaker was required. Various earphone speakers were tested. The mini-speakers EH3030 of Knowles Electronics Co. (73 Victoria Road, Burgess Hill, West Sussex, RH15 9LP, England) were found to be the most suitable in view of their frequency response characteristics, their relative high power output and their small physical dimensions (7mm x 3mm x 3mm).

Disturbance detection was originally envisaged to be done with either hot-film sensors flush mounted on the plate surface or embedded microphones a la Kendall (1990). The hot-film sensors, however, were eliminated because of mechanical difficulties. It was very time consuming to attach flying leads to the sensor without producing protrusions on the plate working side which cause unacceptable flow interferences. In addition, the electronic requirements, i.e. a bridge circuit for each sensor and possibly drift compensation, is rather complex. Hence, embedded microphone detectors were used. The microphone detector chosen was a 9.5mm diameter, 10mm high model TANDY No.270-090. The detector communicated with the plate working side via a 1mm diameter hole. Voltage output reading was readily available. The output signal level was only about 0.2mV and careful screening was required.

Electronic Hardware

Figure C3 shows diagramatically the electronic control cirucuit employed in the final experiments. Excluding the integrator which was only used during part of the experiment, and the precision shielded op-amps, the components employed were standard of the shelf components. The time constants of the Bessel Filters were to large to respond to a passing wave packet in time and were partially responsible for the failure to achieve wave packet control. The Phase Shifters caused narrow bandwidth filtering around the principle frequency leading to control actuator ringing after the detector signal had ceased to exist.

Appendix D: Preliminary Wave Packet Experiment

Using the newly designed test plate, some preliminary wave packet experiments were carried out. The purpose of these experiments was threefold: (a) to show that wave packets could be generated with the embedded loudspeaker technique, (b) to demonstrate that the background disturbance level in the C.U.E.D. low turbulence facility was indeed low enough to allow easy detection of a single wave packet in the boundary layer and (c) to investigate if loudspeaker excitation was "reversible," i.e., does a sign change in the driving voltage pulse create a wave packet of same amplitude but 180 out of phase? Point (b) is especially important for the implementation of the control system since some filtering will have to be employed to isolate the relevant wave packet features from "noise" present in the boundary layer. In addition to these three main objectives, the experiments were required to test the new plate setup for (near) zero streamwise pressure gradient and to check the three-dimensional traverse gear and data acquisition software.

Two different sets of experiments were performed. The tunnel speed for all experiments was 20m/sec and measurements were taken using a constant temperature boundary layer hot-wire. A "near zero" streamwise pressure gradient was achieved by adjusting a flap extending downstream from the main plate. In order to avoid flow separation at the leading edge a second small trailing edge flap was adjusted to move the stagnation point slightly to the working

side of the plate. Following work by Gaster and Grant (1975), the hot-wire was positioned just outside the boundary layer at 1.2 boundary layer thicknesses from the plate surface, where the Tollmien-Schlichting eigenfunctions show an outer (flat) maximum.

In the first set of experiments, the downstream and spanwise development of a single wave packet was investigated. The exciter location at 20.5cm from the leading edge corresponds to Re = 880 (Reynolds number based on displacement thickness) and the flow responses were measured at Re_δ = 1235 (40.5cm) and 1380 (50.5cm), respectively. Typically 45 spanwise "data-slices" roughly six displacement thicknesses apart were recorded. The exciting pulse was computer generated and could be varied in amplitude and width. For the experiments described in this report a constant pulse width of 0.5msec was used. To allow ensemble averaging of the data, the pulse generation was synchronised with the data acquisition system. The sampling rate was 4kHz and the signal was analogue filtered between 20Hz and 2kHz. Each record contains 512 data points and collection time per record was thus 0.13sec. An ensemble average was formed using 189 individual records.

Figure D1a shows a typical single realization of the boundary layer response at Re_δ = 1380. Figure D1b shows the same data after ensemble averaging. A power spectral density versus frequency plot of the ensemble averaged data is shown in Fig. D2. The quite satisfactory signal-to-noise ratio is apparent. The Tollmien-Schlichting frequency band shows power spectral densities of about

40dB above the background noise level. A perspective view and a contour plot of the excited wave packet at the two different Reynolds numbers are shown in Figs. 4 and D3. In order to emphasize the Tollmien-Schlichting wave response, the ensemble averaged records presented in the last two figures were hanned and digitally filtered between 80Hz and 500Hz. At the higher Reynolds number, the stronger three-dimensional modulation of the signal and the increased packet "length" are apparent.

The first set of experiments established that (a) the embedded loudspeaker technique is suited to the generation of wave packets in laminar boundary layers and (b) the C.U.E.D. low turbulence wind tunnel provides the desired flow quality for this type of experiments.

The second series of experiments involved the interaction of wave packets generated simultaneously at different spanwise locations. Only the signal at Re_{δ_1}= 1235 was recorded. First, two pulses 3cm apart of same amplitude but opposite sign were introduced at the exciter location to disturb the flow. The experiment was then repeated using three spanwise drivers 3cm apart. Again all pulses generated had the same amplitude but the middle pulse was of opposite sign. The data acquisition and data reduction performed was as described above. Here, however, 55 and 63 spanwise "slices" were collected in order to map out the interaction region for the "twin" pulse and "triple" pulse experiments respectively.

Figures D4 and D5 show perspective views and contour plots of the flow response to twin pulse and triple pulse excitation. The quality of the data obtained is not as high as in the first set of experiments reported above. This was especially so in the triple pulse experiment which showed an underlying modulation of about 500Hz. This was traced to vibrations of the hot-wire when placed in a shearflow, a phenomenon traced to lack of wire tension. The contour plots of both experiments show the symmetry of the flow response for "positive" and "negative" pulse excitation. It should be pointed out that the lines represent the same absolute values for positive and negative contours drawn. The contour plots for both experiments show narrow regions of wave cancellation between adjacent wave packets of opposite sign.

The second series of experiments achieved objective (c) formulated above, i.e., sign switching of the driving pulse leads to sign switching of the resulting wave packet.

Appendix E: Programme Listings

```
      Program maincon
c ****************************************************************
c       Control of instability waves
c
c       march 31, 91 modified to allow phase shifting in
c                 order to asses sensitivity to off-timing
c
c      changed to read in unformatted data files to speed up
c      run (march 29, 15:00)
c
c       july 16, 91 maincontr2.f with double loop (110,105)
c                   to map out ampgain, phaseshift space (Hch).
c
c       july 18, 91 maincontr3.f implements one detector driving
c                   several (three) actuators spanwise where the
c                   two sideactuators are driven with amplitude
c                   weight of 0.5 of the middle actuator amplitude (Hch)
c
c       july  25, 91 maincontr4.f implements random forcing in
c                   space and time. Note that FUNCTAION DRAN2 had
c                   to be corrected.(Hch)
c
c       july 26, 91  maincontr5.f speeds up convolution with
c                   known system transfer functions by using
c                   option of reading unformatted Fourier
c                   coefficients of these from data directory
c                   DAT/Fsy....  Hence convol2d is modified
c                   in order to take advantage of this. (Hch)
c                   Furthermore pogram was modulized into
c                   more subroutines and common block
c                   is used to reduced compiled file storage
c                   requirements.
c
c       sept 5, 91  modified just for target field superposition
c                   of whole fields (in scontr.f) (maincontr6.f)
c
c      Subroutines required:
c                     sin      - prepare physical space data field
c                                at location of microphone detectors
c                                written in array Height1
c                     convol2d - 2D fast Fourier transform of 512x128
c                                double precision fields. If both fields
c                                are in physical space (in1 = in2 = 0), Height1
c                                then physical space result is in Height1.
c                                If arrays are in proper fourier form (in1 and/
c                                in2 = 1) then array temp1 and/or temp2 are use
c                                and convolution is speeded up significantly.
c                                Convoluted result is always returned in Height
c                                (physical space).
c
c                     FOURN    - 1D fast Fourier transform
c
c                     scontr   - control of disturbance field and continuation
c                                of controlled field to target location.
c                                Uncontrolled physical space input field in
c                                Height1, controlled ouput field also in
c                                Height1 (Height2 is dummy field -destroyed).
c
c                     sanaly   - Analyze control performance at target location
c                                in certain unspoiled part (wraparound) of
c                                field Height2.
c
c                     sout     - output of resulting field to harddisc director
c                                ./DAT/<filename>
c
c      Data files from directory ./DAT:
c                     FsystrI  - file with Fourier space representation
c                                of system transfer function I (unformatted
c                                double precision).
c
```

```
c                     FsystrII - file with Fourier space representation
c                                of system transfer function II (double precisi
c                                unformatted)
c
c         Roland Heinrich          Cambridge ,March 27, 1991
c
c  ****************************************************************
c
        implicit real(a-b,d-h,o-y),complex(c,z),integer(i-n)
        Character*16 fname
        Character*1 A
c        parameter(inmx=10,iampmx=22)
        parameter(inmx=1,iampmx=2)
        parameter(ndim = 2,itmax=512,kzmax=128,ivec=itmax*kzmax*2)
        double precision psen,ampgain,pi,fact1,fact2,fact3,fscale,help,
     +           ampdel
        dimension psvec(1:iampmx,-inmx:inmx)
c
        double precision temp1,temp2,Height1,Height2
        common/fld/temp1(ivec),temp2(ivec),
     +       Height1(itmax,kzmax),Height2(itmax,kzmax)
c
        pi         = 4.d0*datan(1.d0)
        print*,'pi = ',pi
        idum       = -1
        fname(1:4) ='DAT/'
c
c ***** set phys. space disturbance field at Detector location
c
c 1      call sinf
c
c ***** control by setting selective spanwise values to zero
c       centerline is at 1,use 1 < ncontrol < 64
c
 1          print*,' What control amplifier gain ? '
           read(*,*)ampgain
           print*,' Timeshift nshift*.25msecs, nshift = ?'
           read(*,*)nshift
c
            print*,'- ------------------------------'
            print*,'ampgain ',ampgain
            nshift = 1s
            print*,'nshift ',nshift
           call scont(ampgain,nshift)
           goto 555
c
c ***** Pull whole field forward by npull such that noncorrupted field
c       (by wraparound) starts at ntime =1 to ntime = 420.
c       Note also that in spanwise direction noncorrupted
c       field lies between iz=35 and iz=93. Important for power
c       calculation.
c
 333     npul    = 360
         do ik   = 1,kzmax
           ii    = 0
           do it = npul,itmax
            ii   = ii + 1
            Height2(ii,ik) = Height1(it,ik)
           end do
         end do
c
        do ik    = 1,kzmax
           ii    = itmax-npul+1
           do it = 1,npul-1
            ii   = ii+1
            Height2(ii,ik)  = Height1(it,ik)
           end do
         end do
c
c ***** analyse control performance at target location
```

```
c       in un-spoiled area of field Height2
c
cc        itl  = 1
cc        ith  = 420
cc        izl  = 35
cc        izh  = 93
 555    itl  = 1
        ith  = 512
        izl  = 1
        izh  = 128
          do ik = 1,kzmax
           do it = 1,itmax
            Height2(it,ik) = Height1(it,ik)
           end do
          end do
c
        call sanaly(itl,ith,izl,izh)
c
c ***** write out result
c
        call sout(Height2)
c
         pause 'new control configuration?'
         goto 1
 900     print*,'Error in reading ',fname,' start over ?'
         pause
         goto 1
 910     print*,'End reached in reading ',fname,' start over?'
         pause
         goto1
 999     end
       Subroutine sinf
c ******************************************************************
c
c     prepares Height1(itmax,kzmax) to correspond to the uncontrolled
c     disturbance field at the location of the detector (and
c     perharps controller array).
c     Output              :  Height1(itmax,kzmax)
c
c     Subroutines required:   convol2d
c                             Fourn
c
c      Roland Heinrich                      Cambridge, July 31, 91
c ******************************************************************
        Character*16 fname
        Character*1 A
        parameter(itmax=512,kzmax=128,ivec=itmax*kzmax*2)
        double precision temp1,temp2,Height1,Height2
        common/fld/temp1(ivec),temp2(ivec),
     +        Height1(itmax,kzmax),Height2(itmax,kzmax)
c
        fname(1:4) = 'DAT/'

 1      print*,' Do you have double precision phys. space '
        print*,' input file corresponding to disturbance '
        print*,' flow field at control location (1) or do '
        print*,' you have Fourier space input data (2) at '
        print*,' exciter location (all product of ranfield'
        print*,' input 1 or 2 : ?'
        read(*,*) infld
        if(infld.eq.1) then
        print*,' Phys. dist. field at control location (doubl.prec.)? '
        read(*,*) fname(5:16)
        print*,fname
        open(1,file=fname,form="unformatted")
        read(1,ERR=900,END=910) Height1
        close(1)
        goto 10
 900    print*,'Error in reading ',fname,' try again '
        pause
```

```
        goto 1
 910    print*,'End of file encountered in ',fname,' try again'
        pause
        goto 1
        else if (infld.eq.2) then
        open(1,file="DAT/FsystrIun",form="unformatted")
        read(1,ERR=900,END=910)  temp2
        close(1)
c
c  ****  Read in fourier transform of input field (512x128)
c        which was generated with ranfield.f
c
        print*,' Fourier space field of disturbance input ? '
        read(*,*) fname(5:16)
        open(1,file=fname,form="unformatted")
        read(1) temp1
        close(1)
c
c  ***** convolute random field with systrI
c
        in1=1
        in2=1
        call convol2d(in1,in2)
        else
        pause 'Wrong infield integer, try again'
        goto 1
        endif
 10     print*,'Phys. dist. field at detector location'
        print*,'(Height1) set.'
c
        return
        end


         subroutine convol2d(in1,in2)
c  ****************************************************************
c
c    Use 2-d Fast Fourier transform (FOURN) to convolute arrays
c    of itmax t-points * kzmax z-point of data.
c
c    July 26, 1991 modified to allow convolution and backtransform
c                  if fields are passed down as appropriate fourier
c                  coefficients in vector temp1 and/or temp2 as
c                  indicated by controllparameter in1 and in2.
c                   in1 = 0 : data in datin1 need transform
c                   in1 = 1 : fourier tranformed data in temp1
c                             are ready for multiplication.
c                   in2 = 0 and in2 = 1 as above for in1. (Hch)
c
c                   temp1,datin1 : holding convoluted  result
c                                  upon return
c                   temp2,datin2 : unaltered by subroutine
c
c    Roland Heinrich                          Cambridge, march 26,91
c ***************************************************
c
      implicit real  (a-h,o-y)
      double precision pi,helpr,helpi
      character*12 fname
      parameter(ndim = 2,itmax =512,kzmax=128,ivec=itmax*kzmax*2)
      dimension nvec(ndim)
c
      double precision temp1,temp2,datin1,datin2
      common/fld/temp1(ivec),temp2(ivec),
     +        datin1(itmax,kzmax),datin2(itmax,kzmax)
c
      nvec(1) = itmax
      nvec(2) = kzmax
c
      pi4 = datan(-1.d0)
```

```
      pi  = 4.d0* pi4
c
c *** prepare  c o m p l e x data vectors for subroutine FOURN
c     if necessary as indicated  by dummy argument in1,in2
c
      If(in1.eq.0) then
      jj = 1
      do 10 ik = 1,kzmax
        do 15 it = 1,itmax
           temp1(jj)  = datin1(it,ik)
           temp1(jj+1)= 0.d0
           jj         = jj + 2
  15     continue
  10  continue
c
c* check max dimension
         if((jj-1).ne.ivec)  stop 'convol2d jj n.e. ivec '
c
c *** transform into fourier
         call FOURN(temp1,nvec,ndim,+1)
        end if
c
      If(in2.eq.0) then
      jj = 1
      do 11 ik = 1,kzmax
        do 17 it = 1,itmax
           temp2(jj)  = datin2(it,ik)
           temp2(jj+1)= 0.d0
           jj         = jj + 2
  17     continue
  11  continue
c
c* check max dimension
         if((jj-1).ne.ivec)  stop 'convol2d jj n.e. ivec '
c
c *** transform into fourier
         call FOURN(temp2,nvec,ndim,+1)
        end if
c
c *** convolute data in fourier space, temp1(jj) holds convolution
c     this is start point if in1 and in2 .ne. 0 indicating that
c     temp1,temp2 hold allready fourier coefficients in proper form
c
        do 16 jj = 1,ivec,2
         helpr = temp1(jj)*temp2(jj) - temp1(jj+1)*temp2(jj+1)
         helpi = temp1(jj)*temp2(jj+1) + temp2(jj)*temp1(jj+1)
         temp1(jj)   = helpr
         temp1(jj+1) = helpi
c         print*,'convoluted,j,j+1,', jj,temp1(jj),temp1(jj+1)
  16     continue
c
c *** backtransform into physical space
c
       call FOURN(temp1,nvec,ndim,-1)
       fact     = 1.d0/dfloat(nvec(1)*nvec(2))
c
c ***** rearrange data vector in (time,space) array
c       (see arrangement convention 'Num. Recipes' pg 451)
c       Note that the imaginary part of convoluted sum in
c       physical space should be identical zero. Check!
c
       jj = 1
       dsumim = 0.d0
       do 20 ik = 1,kzmax
         do 25 it = 1,itmax
          datin1(it,ik) = fact*temp1(jj)
          dsumim        = dsumim + dabs(temp1(jj+1))
          jj            = jj + 2
  25    continue
  20   continue
```

```
c
       print*,' sum of imag. part should be zero ',dsumim
      return
       end

      Subroutine FOURN(data,nn,ndim,isign)
c**********************************************************
c
c     Replaces DATA by its NDIM-dimensional discrete Fourier
c     transform if ISIGN is input as 1. NN is an integer
c     array of length NDIM,containing the lengths of each dimension
c     (number of complex values), which MUST all be powers of 2.
c     DATA is a real array of length twice the product of these
c     lengths, in which the data are stored as in a multidimen-
c     sional complex FORTRAN array. I ISIGN is input as -1, DATA
c     is replaced by its inverse transform times the product of
c     the lengths of all dimension.
c
c     from Press, Flannery, Teukolsky, and Vetterling,
c      "Numerical Recipes", Cambridge University Press, !986,
c       pg. 451.
c
c     Converted to overall double precision (R.Heinrich)
c
c     Roland Heinrich                    Cambridge, Febr. 8, 1991
c**********************************************************
c
       Implicit real (a,b,d-h,o-y), complex(c,z),
     +   integer(i-n)
       Double Precision wr,wi,wpr,wpi,wtemp,theta,tempr,tempi,
     +   data
       Dimension nn(ndim),data(*)
c
c *** Compute total number of complex values.
c
       ntot  = 1
       do 11 Idim = 1,ndim
          ntot = ntot*nn(idim)
  11   continue
       print*,'fourn ntot,ndim ',ntot,ndim
c
c       do 500 i = 1,ntot*2
c         print*,'fourn-i,data ',i,data(i)
c  500  continue
c
c *** Main loop over the dimensions.
c
       nprev = 1
       do 18 idim = 1,ndim
          n   = nn(idim)
          nrem= ntot/(n*nprev)
          ip1 = 2*nprev
          ip2 = ip1*n
          ip3 = ip2*nrem
c
c *** This is the bit reversal section of the routine
c
          i2rev = 1
          do 14 i2=1,ip2,ip1
            if(i2.lt.i2rev) then
               do 13 i1=i2,i2+ip1-2,2
                 do 12 i3=i1,ip3,ip2
                   i3rev         = i2rev+i3-i2
                   tempr         = data(i3)
                   tempi         = data(i3+1)
                   data(i3)      = data(i3rev)
                   data(i3+1)    = data(i3rev+1)
                   data(i3rev)   = tempr
                   data(i3rev+1) = tempi
  12             continue
```

```
 13          continue
           endif
c
           ibit = ip2/2
  1        if ((ibit.ge.ip1).and.(i2rev.gt.ibit)) then
              i2rev = i2rev-ibit
              ibit  = ibit/2
           goto 1
           endif
           i2rev = i2rev + ibit
 14        continue
c
c *** Here begins the Danielson-Lanczos section of
c     the routine.
c
           ifp1 = ip1
  2        if(ifp1.lt.ip2) then
             ifp2 = 2 * ifp1
c
c *** Initialize for trig recurrence
c
            theta = isign * 6.28318530717959d0/(ifp2/ip1)
            wpr   = -2.d0*dsin(0.5d0*theta)**2
            wpi   = dsin(theta)
            wr    = 1.d0
            wi    = 0.d0
c
            do 17 i3 = 1,ifp1,ip1
              do 16 i1 = i3,i3+ip1-2,2
                do 15 i2 = i1,ip3,ifp2
                  k1         = i2
                  k2         = k1 + ifp1
                  tempr      = wr*data(k2)-wi*data(k2+1)
                  tempi      = wr*data(k2+1)+wi*data(k2)
                  data(k2)   = data(k1)-tempr
                  data(k2+1) = data(k1+1) - tempi
                  data(k1)   = data(k1) + tempr
                  data(k1+1) = data(k1+1) + tempi
 15             continue
 16             continue
c
c *** trigonometric recurrence.
c
              wtemp = wr
              wr    = wr*wpr - wi*wpi + wr
              wi    = wi*wpr + wtemp*wpi + wi
 17         continue
c
            ifp1 = ifp2
            goto 2
           endif
           nprev = n*nprev
 18      continue
         return
        end

      Subroutine scontr(ampgain,ni)
c  ********************************************************************
c     Controls field according to user interaction with regard to
c     control inputs and control amplitude and possible phase shift
c             field1 = uncontrolled input field
c                      holds controlled field upon return
c             field2 = dummy field which is destroyed in routine
c
c     Roland Heinrich                              Cambridge, july 29, 1991
c ********************************************************************
c
      character*16 fname
      double precision ampgain,help
      parameter(ndim = 2,itmax=512,kzmax=128,ivec itmax*kzmax*2)
```

```
c
      double precision temp1,temp2,Field1,Field2
      common/fld/temp1(ivec),temp2(ivec),
     +      Field1(itmax,kzmax),Field2(itmax,kzmax)
c
c ***** Preset Field2 with 0.d0
c
      do ik = 1,kzmax
        do it = 1,itmax
        Field2(it,ik) = 0.d0
        end do
      end do
c
c ***** control by setting selective spanwise values to zero
c     centerline is at 64,use 1 < ncontrol < 128
c     Control actuator input is 2*3mm to either side
c     of detector line with weight 0.5
c
      print*,'Control phase - : Set selected microphone position'
      print*,'                  Actuate at position +/- 6mm.'
 90   print*,'Enter micontrol > 1000 if  you'
      print*,'have set all control points. 3 <= ncontrol <=126.'
      print*,'Enter mic-control =? '
      read*,ncontrol
      if (ncontrol.eq.0) then
c ***** no control
      do ik= 1,kzmax
        do it = 1,itmax
        Field2(it,ik) = Field1(it,ik)
        end do
      end do
      end if
c
      if (ncontrol.GT.1000) goto 95
c
      do it = 1,itmax
      help                    = Field1(it,ncontrol)
      Field2(it,ncontrol-2)   = Field2(it,ncontrol-2) - 0.5d0*help
      Field2(it,ncontrol+2)   = Field2(it,ncontrol+2) - 0.5d0*help
      end do
c
      goto 90
c
c     convolute controlled Field2 with SystrII (Field1)
c
 95   open(3,file="DAT/FsystrIIun",form="unformatted")
      read(3) temp1
      close(3)
c
      in1 = 1
      in2 = 0
      call convol2d(in1,in2)
c
c ***** amplifier gain and off-timing of control signal
c      in ni*0.25 msec
c
      if(ni.gt.0) then
       do it = 1,itmax-ni
          do ik = 1,kzmax
            Field2(it,ik) = Field1(it+ni,ik)
          end do
       end do
       do it = 1,ni
          do ik = 1,kzmax
            Field2(itmax-ni+it,ik) = Field1(it,ik)
          end do
       end do
c
       elseif (ni.lt.0) then
c
```

```
         do it = 1,-ni
            do ik = 1,kzmax
             Field2(it,ik) = Field1(itmax+ni+it,ik)
            end do
         end do
c
         do it =-ni+1,itmax
           do ik = 1,kzmax
            Field2(it,ik) = Field1(ni+it,ik)
           end do
         end do
c
       else
c
       do it = 1,itmax
         do ik = 1,kzmax
           Field2(it,ik) = Field1(it,ik)
         end do
       end do
c
      end if
c
c ***** now read in uncontrolled field which is to be
c       superposed with controll output
c
 200    fname='DAT/ptargran'
        open(3,file=fname,form="unformatted")
        read(3,ERR=900,END=910) Field1
        close(3)
c
 196    do ik = 1,kzmax
          do it = 1,itmax
          Field1(it,ik) = ampgain*Field2(it,ik)
     1                    + Field1(it,ik)
          end do
        end do
        return
 900    print*,'ERRor reading',fname,' try again'
        pause
        goto 200
 910    print*,'END of file ',fname,' try again ?'
        pause
        goto 200
        end

       Subroutine sanaly(itl,ith,izl,izh)
c  ********************************************************************
c     Analyze data in in subset itl-ith,izl-izh  of field2 itmax x kzmax
c       ( pseudopower per point )
c        field2 = controlled input field
c
c      Roland Heinrich                                  Cambridge, july 30, 1991
c ********************************************************************
c
       double precision psen,rpsen
       parameter(ndim = 2,itmax=512,kzmax=128,ivec=itmax*kzmax*2)
c
        double precision temp1,temp2,Field1,Field2
        common/fld/temp1(ivec),temp2(ivec),
     +        Field1(itmax,kzmax),Field2(itmax,kzmax)
c
c
c  *** find pseudo disturbance energy in field
c
         psen   = 0.d0
         icount = 0
         do ik  = izl,izh
            do it = itl,ith
             icount = icount+1
             psen     psen + 1.d0*Field2(it,ik)*Field2(it,ik)
```

```
          end do
         end do
         psen = dsqrt(psen)
c
c ***** calculate residual power per point
c
            rpsen = psen/dfloat(icount)
        Print*,' Power in controlled subfield  ',psen
        Print*,' Power per pcint in contr.field', rpsen
c
cc         print*,' psvec(iamp,ni) ',psvec(iamp,ni)
c
ctest        go to 101
cl 110      continue
cl 105      continue
cll         print*, ' Enter filename for Power vector psvec(iamp,in) '
c
cl          fname(1:4)='DAT/'
cl          read(*,107) fname(5:16)
 107      format(A12)
cl          open (2,file=fname,form='formatted')
cl          write(2,*) ((iamp,in,psvec(iamp,in),
cl     1           in=-inmx,inmx),iamp=1,iampmx)
  102   close(2)
c
        return
        end
         Subroutine sout(Height1)
c  ************************************************************
c       Write out data fields for possible post-processing
c       via graphics routines. Hence change field data
c       to single precision for countourplotting contsim*.f
c
c       Roland Heinrich          Cambridge ,March 31 1991
c
c  ************************************************************
c
        implicit real(a-b,d-h,o-y),complex(c,z),integer(i-n)
        Character*16 fname
        Character*1 A
        parameter(ndim = 2,itmax=512,kzmax=128,ivec=itmax*kzmax*2)
        double precision psen,psvec,Height1
        dimension Height1(itmax,kzmax)
        dimension sHeight(itmax,kzmax)
c
c ***** convert Height2 to single precision for later use in contour
c       plot routine
c
         do ik = 1,kzmax
          do it = 1,itmax
           sHeight(it,ik) = sngl(Height1(it,ik))
          end do
         end do
c
 100     print*,' Do you want to store field single precision (1), '
         print*,' double precision (2) or both (3)? Enter 1,2 or 3: '
         read(*,*) istore
         if (istore.eq.1) then
         print*,' filename to write controlled result (sngl.prec.)'
         print*,' at target location =  (in subdir DAT)'
         print*,' (unformatted store) '
         fname(1:4) = 'DAT/'
         read*,fname(5:16)
         open(4,file=fname,ERR=900,form="unformatted")
         write(4,ERR=900) sHeight
         write(4,ERR=900) psen
         close(4)
         else if(istore.eq.2) then
         print*,' filename to write controlled result (double prec.)'
         print*,' at target location =  (in subdir DAT)
```

```
      print*,' (unformatted store) '
      fname(1:4) = 'DAT/'
      read*,fname(5:16)
      open(4,file=fname,ERR=900,form="unformatted")
      write(4,ERR=900) Height1
      write(4,ERR=900) psen
      close(4)
      else if (istore.eq.3) then
      print*,' filename to write controlled result (sngl.prec.)'
      print*,' at target location =  (in subdir DAT)'
      print*,' (unformatted store) '
      fname(1:4) = 'DAT/'
      read*,fname(5:16)
      open(4,file=fname,ERR=900,form="unformatted")
      write(4,ERR=900) sHeight
      write(4,ERR=900) psen
      close(4)
      print*,' filename to write controlled result (double prec.)'
      print*,' at target location =  (in subdir DAT)'
      print*,' (unformatted store) '
      fname(1:4) = 'DAT/'
      read*,fname(5:16)
      open(4,file=fname,ERR=900,form="unformatted")
      write(4,ERR=900) Height1
      write(4,ERR=900) psen
      close(4)
      else
      pause ' error in storage integer istore '
      goto 100
      end if
C
      return
 900  print*,'Error in write operation file ',fname
      print*,' Try again ? '
      pause
      goto 100
      end
```

```
      program ranfld
c  ****************************************************************
c
c       Programm to set the input data field (itmax*kzmax)
c       used as input for control modelling (maincontr5.f).
c       Output is written out either as physical space field
c       at detector location (this requires convolution) with
c       systrI or as field Fourier component at exciter
c       location. In either case is the resulting file
c       written as unformatted double precision.
c
c       August 2, 1991 random field is set in Fourier space
c                 with random phase and unit amplitude of
c                 fourier coefficients. (Hch)
c
c            irand =  starting integer for random number gen.
c
c       Subroutines required : FOURN
c                              sranfld
c                              dran2
c                              convol2d
c
c        Roland Heinrich          Cambridge ,July 27 1991
c
c  ****************************************************************
c
      implicit real(a-b,d-h,o-y),complex(c,z),integer(i-n)
      Character*16 fname
      Character*1 A
      parameter(ndim=2,itmax=512,kzmax=128,ivec=itmax*kzmax*2)
      double precision temp1,temp2,datin1,datin2
      common/fld/temp1(ivec),temp2(ivec),
     +       datin1(itmax,kzmax),datin2(itmax,kzmax)
c
      dimension nvec(ndim)
c
      nvec(1)   = itmax
      nvec(2)   = kzmax
      irand      = -1
      fname(1:4)='DAT/'
c
      call sranfld(irand,temp1)
c
 1    print*,' Enter 1 to store Fourier coefficients of field'
      print*,' at exciter location or 2 to calculate phys. field'
      print*,' at detector location downstream '
      read(*,*) ifield
c
      if (ifield.eq.1) then
c
      print*,'*UN*formatted file for Fourier coef.'
      print*,' of random field (double prec. )in DAT ?'
      read*, fname(5:16)
      print*,fname
      open(1,file=fname,form="unformatted")
      write(1) temp1
      close(1)
c
      else if (ifield.eq.2) then
c
      open(1,file="DAT/FsystrIun",form="unformatted")
      read(1)  temp2
      close(1)
c
      in1 = 1
      in2 = 1
      call convol2d(in1,in2)
      print*,'*UN*formatted file for phys. field at '
      print*,' detector location downstream (doubl. prec.) in DAT?'
      read*, fname(5:16)
```

```
        print*,fname
        open(1,file=fname,form="unformatted")
        write(1) datin1
        close(1)
        else
        pause ' wrong integer in ifield, try again '
        goto 1
        end if
c
999       end
         Subroutine sranfld(idum,temp)
c*************************************************************
c       Preset Fourier vector temp with random phase and
c       unity amplitude coefficients.
c
c       Roland Heinrich                    Cambridge, July 24, 1991
c*************************************************************
c
        Double complex chelp,cim
        Double Precision temp,rand,pi
        parameter(ndim = 2,itmax =512,kzmax=128,ivec=itmax*kzmax*2)
        Dimension temp(ivec)
c
        pi  = 4.d0*datan(1.d0)
        cim =(0.d0,1.d0)
c
        do ii=1,ivec,2
           rand       = dran2(idum)
           chelp      = zexp(cim*rand*2.d0*pi)
           temp(ii)   = dble(chelp)
           temp(ii+1) = dimag(chelp)
          end do
c
        return
        end

        Double Precision Function dRAN2(idum)
c*************************************************************
c
c       Random Function generator, see Numerical Recipes, Press et al.
c       page 192. (Made double precision by Roland Heinrich)
c       Returns a uniform random deviate between 0.0 and 1.0. Set
c       "idum" to any negative value to initialize or reinitialize
c       the sequence.
c
c        Roland Heinrich                    Cambridge, Feb 5, 1991
c*************************************************************
c
        Dimension  ir(97)
        double precision rm
        Parameter(m=714025, ia = 1366, ic=150889,rm=1.d0/M)
        Data iff /0/
c
        if(idum.lt.0.or.iff.eq.0) then
            iff  =1
            idum  = mod(ic-idum,m)
            do 11 j=1,97
             idum  = mod(ia*idum+ic,m)
             ir(j) = idum
 11          continue
            idum   = mod(ia*idum+ic,m)
            iy     = idum
        endif
        j = 1 + (97*iy)/m
        if(j.gt.97.or.j.lt.1) pause
         iy = ir(j)
         dran2 = iy*rm
         idum = mod(ia*idum+ic,m)
         ir(j)= idum
c
```

```
return
end
```

```
      PROGRAM dstwpD
C     ***************************************************************
C
C     Stability program for parallel three-dimensional Blasius boundary
C     layer (spatial stability).  This program is based on Mike Gasters
C     rapid series expansion eigenvalue calculation using Shanks
C     transformation to accelerate the convergence process (qqsum).
C
C     This program calls the following subroutines
C        qnewt  ------  multi-dimensional newton raphson root finder
C        ludcmp ------  l.u. decomposition for qnewt
C        lubksb ------  used with ludcmp to solve linear system of eqts.
C        userfun------  provides function and derivatives for qnewt
C        qfsub  ------  rapid series eigenvalue expansion
C
C        The error-integer "ierr" should be zero for normal performance.
C        It is given the value 1000 if the iteration iter in this main
C        program part fails to converge within tolerance tol.
C        For each call to the newton subroutine qnewt which leads
C        to non-convergence within the subroutine in ntrial attempts,
C        ierr is incremented by 1.
C
C        The first three subroutines are adapted from "Numerical Recipes"
C        William H. Press, Brian P. Flannery, Saul A. Teukolsky,
C        William T. Vetterling, Cambridge University Press, 1986.
C
C       October 9, 1990 modified to double precision and use of
C                  qfsub  (Roland Heinrich)
C       October 17, 1990 modified for "B" version,i.e. outer loop is
C                  eliminated and dfuserb is used (hch).
C       October 18, 1990 this program dst_wpB is modified dstab3dB
C                  to allow mapping of Re, spanwise wavenumber br
C                  space. The physical experimental parameters are
C                  set in DATA statement. Make tolerances of convergence
C                  test value-dependent (atol,omegatol)
C
C       November 6, 1990  extrapolate guess for alpha from previous
C                   calculated values (Hch).
C
C       November 10, 1990 preset all eigenvalues "ca" to (1.0,1.0)
C                  and calculate only up to frequncy ( in frequency
C                  loop iomega) where tolerance criterium is missed for
C                  the first time. Also "taper off" the last (in omega)
C                  value s.t. a smooth frequency window is used --> avoids
C                  ringing. At same time set ierr to -99 as flag.
C                  Read runparameter from file HeadwpD. (Hch)
C
C     ROLAND HEINRICH                                  CAMBRIDGE, MAY 29,1990
C     ***************************************************************************
C
      parameter (np=2)
C
      implicit real*8 (a-h,o-y)
      double precision rel(32,32), img(32,32),eta,delta,dnu
      double precision arcenr,arceni,arrad,ascenr,asceni,asrad
      double precision pomst,pomdel,pbdel
      double complex cim,ca,castrt,castrt1,chlp,chlp1,can,cam1
     1 ,castrt1m1,castrtm1
      double complex ccalp(9,20,55)
      dimension rRe(9,20,55),rbr(9,20,55),romr(9,20,55)
      dimension ierarr(9,20,55)
C
      dimension  x(np)
C
      common /inp2/ Rehat,Reihat,omsetr,omseti,br
      common /head04/ eta,delta,eps0,eps1,arcenr,arceni,
     1  arrad,ascenr,asceni,asrad,m,im,istep
      common /coef04/ rel,img
C
C ****** The following data statement contains parameters for experiment
```

```
c        performed aug14, 90, U0 = 20 m/s, nu = 1.57e-5 m*m/s. Variables starting
c        sith P are Physical varialbes which have to be nondimensionalized
c        for run using this program.
c
      DATA U0,dnu /20.d0,1.57d-5/
      DATA Restart,Redel,Pbstart,castrt/1260.d0,65.d0,
     1   0.d0,(.15d0,.005d0)/
c
c ****** read in run-parameters
c
      open(5,file='HeadwpD',form='formatted')
      read(5,950) Pomst
      read(5,950) Pomdel
      read(5,950) Pbdel
      read(5,960) iomax
      read(5,960) ibmax
      read(5,960) itermax
      close(5)
 950  format(10X,D10.4)
 960  format(10X,I5)
c
      print*,'Pomst = ',Pomst,' Pomdel = ',Pomdel,' Pbdel =',Pbdel,
     1 ' iomax = ', iomax,' ibmax = ',ibmax,' itermax = ',itermax
c
      cim      = (0.d0,1.d0)
      dum      = dnu/U0/U0
      PRe      = Restart
      castrt1  = castrt
      Pomr     = Pomst
 1    tolfac   = 1.d-4
      iRemax   = 9
      ierr     = 0
c
c**** Preset all eigenvalues with (1.,1.0)
c
        do i = 1,iRemax
          do ii = 1,ibmax
           do iii = 1, iomax
             ccalp(i,ii,iii)   = (1.d0,1.d0)
             ierarr(i,ii,iii)  = -99
           end do
          end do
        end do
c
c *** write Header in eigmap
c
      open (10,file = 'Head04',form ='formatted')
      read (10,*) m,eta,im
      read (10,*) delta,eps0,eps1,istep
      read (10,*) arcenr,arceni,arrad
      read (10,*) ascenr,asceni,asrad
      close(10)
c
      open (10,file = 'fcoef',form = 'formatted')
      read (10,15) ((rel(i,j),i=1,im),j=1,im),
     1        ((img(i,j),i=1,im),j=1,im)
      close(10)
  15  format(2X,E24.16E3)
c
       open(13,file = 'eigmap2',form = 'formatted')
c
       write(13,300) Restart,Redel,Pomst,Pomdel,Pbstart,Pbdel
 300   format(2X,'restart =  ',f6.0,2X,' delre = ',F6.0,/,2X
     2 ,' Pomstart = '
     1 ,f8.3,2X,' Pdelomr = ',f6.3,/,2X,' Pbstart = ',F6.3,
     3  2X,' Pbdel = ',f8.3,/ )
c
c *********** OUTER loop 490 in Re 'iren '*****************
c
           do 490  iren = 1,iRemax
```

```
              Rehat   = Pre
              Reihat  = 0.d0
              castrt  = castrt1
              chlp1   = castrt1
c
c             Program parameter Re dependent

              bst     = Pre * Pb * dum*U0
              bdel    = Pre * Pbdel * dum*U0
              omrdel  = Pre * Pomdel* dum
              omstrt  = Pre * Pomr  *dum
c
c             keep loop starting value
              br      = bst
c
c ************loop 550 in spanwise wavenumber 'ib'  ********
c
            do 550 ib = 1,ibmax
             ca   = castrt
             cam1 = castrt
             chlp = castrt
             atol = zabs(castrt)*tolfac
c
c           keep loop starting value
            omr   = omstrt
c
c ************ inner frequency loop 'iomega' ******************
c
            do 551 iomeg = 1,iomax
             omsetr  = omr
             omseti  = 0.d0
             omtol   = omsetr*tolfac
c
c  ****** start Newton-Raphson* with 3-D paramters*****
c
          ierr    = 0
          can     = 2.d0*ca - cam1
          x(1)    = dble(can)
          x(2)    = dimag(can)
c
        call dqnewt(itermax,x,2,atol,omtol,ierr)
c
          cam1   = ca
          ca     = dcmplx(x(1),x(2))
c
          write(13,900) PRe,omr,test4
          write(13,910) ca,ierr
c
          ccalp(iren,ib,iomeg) = ca
          rbr(iren,ib,iomeg)   = br
          romr(iren,ib,iomeg)  = omr
          RRe(iren,ib,iomeg)   = PRe
          ierarr(iren,ib,iomeg)= ierr
c
           if (iomeg.eq.1) then
             castrtm1 = chlp
             chlp     = ca
             castrt   =  2.d0*chlp - castrtm1
             if (ib.eq.1) then
               castrt1m1 = chlp1
               chlp1     = ca
               castrt1 = 2.d0*ca - castrt1m1
             end if
           end if
c
c    ***** if ierr = 1, end omega loop and jump to next "b" value
c          since series is starting to have convergence problems.
c          remember the higher omega values lead to stronger decaying
c          eigenvalues alpha (provided I am above stability "banana" as
c          has to be the case for this exit procedure to sbe sencsible).
```

```
c
        if (ierr.eq.1) then
          iomfin = iomega
          goto 552
        end if
c


c
c   ***** Update omega
c
           omr   = omr + omrdel
 551   continue
c
       iomfin  = iomax
c
c   *** Window off eigenvalues smoothly with cos(45,90,135).
c
 552       ccalp(iren,ib,iomfin-2) = .85355339d0*ccalp(iren,ib,iomfin-2)
           ccalp(iren,ib,iomfin-1) = .5d0*ccalp(iren,ib,iomfin-1)
           ccalp(iren,ib,iomfin)   = .14644660d0*ccalp(iren,ib,iomfin)
c
c  ***** update spanwise wavenumber
c
           br    = br + bdel
c
         write(13,*) '************** br = ',br,'*******'
 550   continue
c
c  ***** update physical Reynoldsnumber
c
           PRe   = PRe + Redel
         write(13,*) '########### PRe = ',PRe,'######'
490   continue
c
       open(1,file="eigwp",form="unformatted")
       write(1) ccalp
       write(1) romr
       write(1) rbr
       write(1) RRe
       write(1) ierarr
       close(1)
c
 900   format(3x,F6.0,3X,F6.3,3X,E12.3)
 910   format(3x,2F9.6,3X,I6)
       close(13)
c
      END
c
       SUBROUTINE dqNEWT(NTRIAL,X,N,TOLX,TOLF,ierr)
C     ************************************************************************
C     Given an initial guess X for a root in N dimension, take NTRIAL Newton-
C     Rahpson steps to improve the root. Stop if the root converges in either sum
C     variable increments TOLX or summed function values TOLF.
C
C     INPUT :     A(i,j) = del(fi)/del(xj)
C                 B(i)   = - fi
C    Ref: Numerical Recipes, W.H. Press et al. pg. 273
C
c    version for eigenvalue calculation gaster series
c     ierr is error indicator. Should be zero for normal run. Each time the
c     tolerance criterium is not met for ntrial attempts, ierr is incremented
c     by one.
C
c     September 24,1990  modified for double precision (Hch)
c
C     Roland Heinrich                                Cambridge, May 29, 1990
C     ************************************************************************
C
       PARAMETER (NP = 2)
```

```
      implicit real*8 (a-h,o-z)
      DIMENSION X(NP), ALPHA(NP,NP), BETA(NP), INDX(NP),xinit(NP)
C
      common /inp2/ Rehat,Reihat,omsetr,omseti,br
C
c  ***** keep initial guess for error message
c
      do 2 i = 1,np
        xinit(i) = x(i)
 2    continue
c
      DO 13 K = 1,NTRIAL
         CALL dUSERFU(X,ALPHA,BETA)
         ERRF = 0.d0
         DO 11 I=1,N
            ERRF = ERRF+ABS(BETA(I))
  11     CONTINUE
         IF (ERRF.LE.TOLF) RETURN
C
         CALL dLUDCMP(ALPHA,N,NP,INDX,D)
         CALL dLUBKSB(ALPHA,N,NP,INDX,BETA)
         ERRX = 0.d0
C
         DO 12 I = 1,N
           ERRX  = ERRX + ABS(BETA(I))
           X(I)  = X(I) + BETA(I)
  12     CONTINUE
         IF (ERRX.LE.TOLX) RETURN
  13  CONTINUE
C
c  ****** write message if tolerance criteria not met ***
C
      print*, '        Tolerance criteria in qnewt not'
      print*, '         met within NTRIAL attempts for case'
      print*, '     Rehat = ',rehat,' omsetr = ',omsetr,' br = ',br
      print*, '         ntrial = ', ntrial
      print*, '         errf   = ',errf,'  tolf = ',tolf
      print*, '         errx   = ',errx,'  tolx = ',tolx
      print*,' The initial guess for ca was ',xinit(1),xinit(2)
      print*, ' The failed ca value = ',x(1),x(2)
      print*,'ca value reset to initial guess before return'
      do 800 i = 1,np
        x(i)  = xinit(i)
 800  continue
      ierr     =  ierr + 1
C
      RETURN
      END
C
      SUBROUTINE dUSERFU(X,ALPHA,BETA)
C     ********************************************************************************
C     User supplied function and derivative for multiple dimensional
C     newton-rahpson according to NUMERICAL RECIPES by W.H. Press p. 271.
C
c     this program is used for eigenvalue calculation Gaster series
c
c     September 22,1990  modified to double precision (Hch)
c     October 9, 1990    modified to use dqfsum (Hch)
c  $$$$$   October 16, 1990   modified to take variation of Re(2-d) into
c  $$$$$                       acount when calculation domega/dx. Here
c  $$$$$                       X is 3d wavenumber "a" and ALPHA
c  $$$$$                       contains derivatives domega/da (Hch)
c
C     Roland Heinrich                              Cambridge, May 29, 1990
C     ********************************************************************************
C
      PARAMETER (NP=2)
C
      implicit real*8 (a-h,o-z)
      double precision dxr,dxi,drer,drei,
```

```
     1             delxr
      complex*16 ca,ca1,com,com1,calp,calp1,cRe,cRe1
c
      DIMENSION X(NP), ALPHA(NP,NP), BETA(NP)
c
      common /inp2/ Rehat,Reihat,omsetr,omseti,br
c
      delxr = .0005d0
c
      DO 20 J = 1,NP
      DO 10 I = 1,NP
       ALPHA(I,J) = 0.
  10  CONTINUE
       BETA(J)    = 0.
  20  CONTINUE
c
c ****** calculate corresponding 2-d parameters
c        according to parallel flow Squire's transform
c
      ca     = dcmplx(x(1),x(2))
      calp   = cdsqrt(ca*ca + br*br)
      cre    = Rehat*ca/calp
c
cc      print*,' 2d-parameters cre,cbet,calp '
cc      print*, 'cre = ',cre
cc      print*, 'cbet= ',cbet
cc      print*, 'calp= ',calp
c
      drer   =  dble(cre)
      drei   =  dimag(cre)
      dxr    =  dble(calp)
      dxi    =  dimag(calp)
c
c **** note IQ has to be 14,18,22,..... for subroutine
c      dqfsum which uses full shanks
c
      IQ  = 22
      call dqfsum(dxr,dxi,drer,drei,IQ,1,dbetr,dbeti)
c
c ****  calculate 3-d omega
c
      com    = ca/calp*dcmplx(dbetr,dbeti)
c
      BETA(1) = -( dble(com) - omsetr )
      BETA(2) = -( dimag(com) - omseti )
c
      ca1     = dcmplx(x(1)+delxr,x(2))
      calp1   = cdsqrt(ca1*ca1 + br*br)
      cRe1    = Rehat*ca1/calp1
c
      dRer1   =  dble(cRe1)
      dRei1   =  dimag(cRe1)
      dxr1    =  dble(calp1)
      dxi1    =  dimag(calp1)

c
      call dqfsum(dxr1,dxi1,dRer1,dRei1,IQ,1,dbetr1,dbeti1)
c
c ****  calculate 3-d omega
c
      com1   = ca1/calp1*dcmplx(dbetr1,dbeti1)
c
      fprr  = (dble(com1 - com)) /delxr
      fpri  = (dble(com1 - com)) /delxr
c
cc        afprr  = dabs(fprr)
cc        afpri  = dabs(fpri)
cc       if((afprr.lt.1.d-8).or.(afpri.lt.1.d-8)) then
cc        print*,'pause in duserfun.f, slope small '
cc        print*,' fprr = ',fprr,'  fpri= ',fpri
```

```
cc          pause
cc         else if ((afprr.gt.1.d5).or.(afpri.gt.1.d5)) then
cc          print*,'pause in duserfun.f, slope large '
cc          print*,' fprr = ',fprr,'  fpri= ',fpri
cc          pause
cc         end if
c
        ALPHA(1,1) =  fprr
        alpha(1,2) = -fpri
        alpha(2,1) = -alpha(1,2)
        alpha(2,2) =  alpha(1,1)
C
        RETURN
        END
c
C ***************************************************************************
C       Program QFSum
C ***************************************************************************
C
C  Fast version of series program   Feb 1990
c  uses Quick summation but Full matrix shanks
C
        SUBROUTINE DQFSUM (ALPHAR,ALPHAI,REYR,REYI,IQ,INUM,OMEGaR,OMEGaI)
C
        implicit real*8 (a-h,o-z)
        Double Precision Real(32,32), Imag(32,32), Cr(32), Ci(32)
        Double Precision Omegar, Omegai, Realsum, Imagsum
        Double Precision Eta, Delta, Br, Bi
        Double Precision ARcenr, ARceni, ARrad
        Double Precision AScenr, ASceni, ASrad
        Double Precision Alphar, Alphai, Reyr, Reyi
        Double Precision Ur, Ui, Vr, Vi, Zr, Zi, Temp
        Double Precision Clr, Cli, Ctr, Cti, Clmag, CCr, CCi
c
        common /head04/ eta,delta,eps0,eps1,arcenr,arceni,
     1    arrad,ascenr,asceni,asrad,m,im,istep
        common /coef04/ real,imag
C
        Integer R
C
        Tol=1.d-10
C
        IR=IQ+1
C
        Do 100 In=1,Inum
        Ur=Alphar*Alphar-Alphai*Alphai-AScenr
        Ui=2.0D0*Alphar*Alphai-ASceni
        Vr=Alphar*Reyr-Alphai*Reyi-ARcenr
        Vi=Alphar*Reyi+Alphai*Reyr-ARceni
        Ur=Ur/ASrad
        Ui=Ui/ASrad
        Vr=Vr/ARrad
        Vi=Vi/ARrad
C
        Temp=Ur*Ur+Ui*Ui
        Br=Ur/Temp
        Bi=-Ui/Temp
C
        Temp=Vr*Vr+Vi*Vi
        Zr=(Ur*Vr+Ui*Vi)/Temp
        Zi=(-Ur*Vi+Ui*Vr)/Temp

C
C    Diagonal summation of series
C
        CCr=0.0D0
        CCi=0.0D0
C
        Do 20 R=1,IR
C
```

```
      Temp=Br*Vr-Bi*Vi
      Bi=Br*Vi+Bi*Vr
      Br=Temp
C
      Realsum=0.0D0
      Imagsum=0.0D0
C
      Do 10 J=R,1,-1
      I=R-J+1
C
      Realsum=Realsum+Real(I,J)
      Imagsum=Imagsum+Imag(I,J)
C
      Temp=Realsum*Zr-Imagsum*Zi
      Imagsum=Realsum*Zi+Imagsum*Zr
      Realsum=Temp
C
10    Continue
C
      CCr=CCr+Br*Realsum-Bi*Imagsum
      CCi=CCi+Br*Imagsum+Bi*Realsum
C
C     Write (*,*) R, CCr, CCi
      Cr(R)=CCr
      Ci(R)=CCi
C
20    Continue
C
C   Shanks Transformation -- Full Matrix
C
      L = 0
      M = IQ
c
 40   Do 50 J=2,M
      Jmn=J-1
      Jpl =J+1
      Clr=Cr(Jmn)+Cr(Jpl)-Cr(J)-Cr(J)
      Cli=Ci(Jmn)+Ci(Jpl)-Ci(J)-Ci(J)
      Clmag=Clr*Clr+Cli*Cli
      If (Clmag .Lt. Tol) Then
      Cr(Jmn)=Cr(J)
      Ci(Jmn)=Ci(J)
      Else
      Ctr=Cr(Jmn)*Cr(Jpl)-Ci(Jmn)*Ci(Jpl)-Cr(J)*Cr(J)+Ci(J)*Ci(J)
      Cti=Cr(Jmn)*Ci(Jpl)+Ci(Jmn)*Cr(Jpl)-2.0D0*Cr(J)*Ci(J)
      Cr(Jmn)=(Ctr*Clr+Cti*Cli)/Clmag
      Ci(Jmn)=(-Ctr*Cli+Cti*Clr)/Clmag
      End If
50    Continue
C
      M = M-2
      if (M.Ne.0) goto 40
      if (L.eq.1) goto 80
      L=1
c
      M = IQ/2 -1
      IM= M+1
c
      Do 70  J=2,IM
       Cr(J) = Cr(2*J-1)
 70    Ci(J) = Ci(2*J-1)
      Goto 40
c
 80   Omegar = Cr(1)*Alphar - Ci(1)*Alphai
      Omegai = Cr(1)*Alphai + Ci(1)*Alphar
100   Continue
      return
      End
c
      SUBROUTINE dLUBKSB(A,N,NP,INDX,B)
```

```
C     ************************************************************************
C     Solves the set of N linear equations A.X = B. Here A is input, nat as the
C     but rather as its "LU" decomposition, determined by the routine "LUDCMP.
C     is input as the permutation vector returned by LUDCMP. B is input as the r
C     side vector B and returns with the solution vector X. A, N, NP and INDX ar
C     modified by this routine and can be left in place for successive calls wit
C     different right-hand sides B. This routine takes into account the possibli
C     that B will begin with many zero elements, so it is efficient for use in
C     matrix inversion
C     Ref.: Numerical Recipes, W.H. Press et al. pg 37
C
c     September 22, 1990  modified for double precision (Hch)
c
C     Roland Heinrich                                    Cambridge, May 29, 199
C     ************************************************************************
C
      implicit real*8 (a-h,o-z)
      DIMENSION A(NP,NP), INDX(N), B(N)
C
      II = 0
      DO 12  I=1,N
           LL    = INDX(I)
           SUM   = B(LL)
           B(LL) = B(I)
            IF (II.NE.0) THEN
             DO 11 J=II,I-1
                  SUM = SUM - A(I,J)*B(J)
11           CONTINUE
            ELSE IF (SUM.NE.0.) THEN
             II = I
            ENDIF
           B(I) = SUM
12    CONTINUE
      DO 14 I=N,1,-1
           SUM   = B(I)
           IF(I.LT.N) THEN
         DO 13 J=I+1,N
           SUM   = SUM-A(I,J)*B(J)
13       CONTINUE
        ENDIF
           B(I)  = SUM/A(I,I)
14    CONTINUE
C
      RETURN
      END
C
       SUBROUTINE dLUDCMP(A,N,NP,INDX,D)
C     ************************************************************************
C     Given an N xN matrix A, with physical dimension NP, this routine replaces
C     "LU" decomposition of a rowwise permutation of itself. A and N are input.
C     , arranged as in equation (2.3.14) of "Numerical Recepices " W. H. Press e
C     pg. 35.; INDX is an output vector which records the row permutation effect
C     the partial pivoting; D is output as +/- 1 depending on whether the number
C     interchanges was even or odd, respectively. This routine is used in combin
C     with LUBKSB to solve linear equations or invert a matrix.
C
c     September 22, 1990 modified for double pecision (Hch)
c
C     Roland Heinrich                                  Cambridge, May 29, 1990
C     ************************************************************************

      PARAMETER (NMAX=100, TINY=1.0d-20)
      implicit real*8 (a-h,o-z)
      DIMENSION A(NP,NP),INDX(N),VV(NMAX)
      D = 1.
      DO 12 I = 1,N
           AAMAX=0.d0
          DO 11 J = 1,N
           IF (ABS(A(I,J)).GT.AAMAX) AAMAX=ABS(A(I,J))
11        CONTINUE
```

```
            IF (AAMAX.EQ.0.) then
                 PAUSE 'SINGULAR MATRIX. '
            end if
            VV(I) = 1./(AAMAX)
 12     CONTINUE
C
        DO 19 J=1,N
            DO 14 I=1,J-1
              SUM=A(I,J)
              DO 13 K=1,I-1
                SUM = SUM - A(I,K)*A(K,J)
 13           CONTINUE
              A(I,J) = SUM
 14         CONTINUE
            AAMAX = 0.
            DO 16 I=J,N
              SUM      = A(I,J)
              DO 15 K=1,J-1
                 SUM   = SUM-A(I,K)*A(K,J)
 15           CONTINUE
              A(I,J)   = SUM
              DUM      = VV(I)*ABS(SUM)
              IF (DUM.GT.AAMAX) THEN
                 IMAX  = I
                 AAMAX = DUM
              ENDIF
 16         CONTINUE
            IF (J.NE.IMAX)THEN
              DO 17 K=1,N
                DUM=A(IMAX,K)
                A(IMAX,K) = A(J,K)
                A(J,K) = DUM
 17           CONTINUE
              D= -D
              VV(IMAX) = VV(J)
            ENDIF
            INDX(J)=IMAX
            IF(A(J,J).EQ.0.) THEN
C             A(J,J) = TINY
              PRINT *, 'A(J,J) SINGULAR (SET TINY) FOR J,J' ,J
            ENDIF
C
            IF(J.NE.N) THEN
             DUM= 1./A(J,J)
              DO 18 I=J+1,N
                A(I,J)=A(I,J)*DUM
 18           CONTINUE
            ENDIF
 19     CONTINUE
        RETURN
C
        END
```

```
1000, 10.0D0, 32
0.000000001, 1.E-20, 1.E-5,1
460.0D0, 0.0D0, 255.0D0
0.063d0, 0.0D0, 0.04275D0
0.1D0, -0.0D0
Pomst  =   500.d0
Pomdel =    28.d0
Pbdel  =    20.d0
iomax  =    55
ibmax  =    10
itermax=    300
```

Head04

HeadwpD

File fcoef

Complex Fourier coefficients,
for wave packet eigenvalue calculation

i	j	real part	imag. part
1	1	0.3223253786563900E+000	0.1613119803369000E-001
2	1	-0.2418700978159900E-001	-0.4377522855065800E-003
3	1	0.7942718453705302E-002	-0.3595384769141701E-002
4	1	-0.3036302514374300E-002	0.2014757832512300E-002
5	1	0.1272812020033600E-002	-0.1098888693377400E-002
6	1	-0.5578315467573702E-003	0.5821559461765000E-003
7	1	0.2523936855141101E-003	-0.3075402346439700E-003
8	1	-0.1167238078778600E-003	0.1623029093025300E-003
9	1	0.5490734838531397E-004	-0.8574187813792403E-004
10	1	-0.2618405960674900E-004	0.4535679545369902E-004
11	1	0.1263278954866101E-004	-0.2402895006525799E-004
12	1	-0.6158098585729002E-005	0.1274826263397699E-004
13	1	0.3030638026757502E-005	-0.6772615961381200E-005
14	1	-0.1505099589849100E-005	0.3602559672799500E-005
15	1	0.7541312925241098E-006	-0.1918572706927101E-005
16	1	-0.3811991859947701E-006	0.1022883452606000E-005
17	1	0.1943971028595100E-006	-0.5459203293867201E-006
18	1	-0.1000188092348300E-006	0.2916541177455700E-006
19	1	0.5192057628278201E-007	-0.1559655800065200E-006
20	1	-0.2719245806304099E-007	0.8348379054723402E-007
21	1	0.1436661190013000E-007	-0.4472842363156799E-007
22	1	-0.7655186706756501E-008	0.2398678411452701E-007
23	1	0.4112458817928700E-008	-0.1287566142593700E-007
24	1	-0.2226347994849200E-008	0.6918002615208295E-008
25	1	0.1213921518861101E-008	-0.3720592500755500E-008
26	1	-0.6662281837321902E-009	0.2002958021662899E-008
27	1	0.3677884663488800E-009	-0.1079366596101700E-008
28	1	-0.2040865254571101E-009	0.5822549664635800E-009
29	1	0.1137550123542200E-009	-0.3144229876461701E-009
30	1	-0.6364654636659097E-010	0.1699737572913299E-009
31	1	0.3572324380751702E-010	-0.9198661971021599E-010
32	1	-0.2010223064397000E-010	0.4983688461912500E-010
1	2	0.3764735534787199E-001	-0.1096595078706700E-001
2	2	-0.2053064294159401E-002	-0.6840560119599102E-002
3	2	0.7804390043020202E-003	0.6861797883175301E-003
4	2	-0.3220866783522100E-003	-0.3602366778068200E-003
5	2	0.1607301092008100E-003	0.1076236585504400E-003
6	2	-0.7966860721353399E-004	-0.4196212466922601E-004
7	2	0.4099830402992700E-004	0.1427129063813499E-004
8	2	-0.2122368641721600E-004	-0.4537243057711700E-005
9	2	0.1107928710553100E-004	0.9904952094075302E-006
10	2	-0.5798076472274296E-005	0.1295994422889600E-006
11	2	0.3037801661776000E-005	-0.3866861106871501E-006
12	2	-0.1590507167748001E-005	0.3618830533014299E-006
13	2	0.8312615591421498E-006	-0.2705580470774300E-006
14	2	-0.4332437129051000E-006	0.1832859766182100E-006
15	2	0.2249863797487699E-006	-0.1174688293303900E-006
16	2	-0.1163220559874400E-006	0.7264628720804501E-007
17	2	0.5982752071531598E-007	-0.4381351459414899E-007
18	2	-0.3058424624669001E-007	0.2593211156920500E-007
19	2	0.1552484896194500E-007	-0.1512300151773600E-007
20	2	-0.7816018943174198E-008	0.8712952137557302E-008
21	2	0.3897175915312800E-008	-0.4968416345008102E-008
22	2	-0.1920981373970701E-008	0.2807754917455401E-008
23	2	0.9337800532804902E-009	-0.1573949193201000E-008
24	2	-0.4461136460243198E-009	0.8757866098996203E-009
25	2	0.2084456218742800E-009	-0.4839281197987999E-009
26	2	-0.9453641341972098E-010	0.2656248832000299E-009
27	2	0.4109439871724497E-010	-0.1448558217820300E-009
28	2	-0.1672276032926900E-010	0.7848858368797504E-010
29	2	0.6043600949551296E-011	-0.4225309685468299E-010
30	2	-0.1641670523480600E-011	0.2259558859463200E-010
31	2	0.1104174362348800E-013	-0.1200011097435300E-010
32	2	0.4636372665997600E-012	0.6326588992272598E-011
1	3	-0.1283412706106900E-001	-0.3782355459407000E-002
2	3	0.1200836704811100E-003	0.5877360235899697E-003
3	3	-0.2647271030582500E-003	-0.4775901034008699E-003

4	3	0.1119829903473100E-003	0.3470053343335201E-004
5	3	-0.5917461021454098E-004	-0.3356829256517800E-004
6	3	0.3102428308920901E-004	0.3799055093622900E-005
7	3	-0.1607303784112400E-004	-0.2979282101023299E-006
8	3	0.8396067642024706E-005	-0.1470806296310900E-005
9	3	-0.4340464784036202E-005	0.1396764560013300E-005
10	3	0.2234226940345300E-005	-0.1073991143130100E-005
11	3	-0.1138868356065400E-005	0.7305732196982700E-006
12	3	0.5746144324803002E-006	-0.4695613426974901E-006
13	3	-0.2861150107946701E-006	0.2903555014199800E-006
14	3	0.1401979403681300E-006	-0.1748854998595600E-006
15	3	-0.6731085733235897E-007	0.1032482970231301E-006
16	3	0.3146558213984501E-007	-0.5999518037924600E-007
17	3	-0.1417664385883200E-007	0.3440246132413398E-007
18	3	0.6046207534637898E-008	-0.1950165895436798E-007
19	3	-0.2352392503013301E-008	0.1094153656566700E-007
20	3	0.7568264348556397E-009	-0.6080690617693597E-008
21	3	-0.1219838396959700E-009	0.3348950894377400E-008
22	3	-0.9300516606858306E-010	-0.1828337037323999E-008
23	3	0.1375995567487500E-009	0.9895023689310294E-009
24	3	-0.1219906259342100E-009	-0.5307969064283201E-009
25	3	0.9169635883932202E-010	0.2821261002594601E-009
26	3	-0.6338354147095203E-010	-0.1484972145249200E-009
27	3	0.4161035752070500E-010	0.7733847590119001E-010
28	3	-0.2636401340294598E-010	-0.3980798329861202E-010
29	3	0.1626985351999000E-010	0.2021798180262800E-010
30	3	-0.9835244597911100E-011	-0.1010899176867600E-010
31	3	0.5845742726689998E-011	0.4959730542930503E-011
32	3	-0.3424968208348700E-011	-0.2376124470793201E-011
1	4	0.4891649819910500E-002	0.2312668832019000E-002
2	4	-0.3271847672294800E-003	-0.4290250362828401E-003
3	4	0.6939046579645904E-004	0.4648862159228900E-004
4	4	-0.7333208486670597E-004	-0.5076560773886701E-004
5	4	0.2879907333408499E-004	-0.4128159616811900E-005
6	4	-0.1663749571889600E-004	-0.6333055466711800E-006
7	4	0.8228060323745002E-005	-0.2947733946712102E-005
8	4	-0.4225125849188798E-005	0.1953499804585600E-005
9	4	0.2113396703862200E-005	-0.1497659582128100E-005
10	4	-0.1042418261931700E-005	0.9631414741306800E-006
11	4	0.5031774321651000E-006	-0.6073055942579197E-006
12	4	-0.2359472262014601E-006	0.3674449828849902E-006
13	4	0.1063605097328900E-006	-0.2177288394023000E-006
14	4	-0.4514414797540701E-007	0.1264929636590800E-006
15	4	0.1729144294415600E-007	-0.7236617705075298E-007
16	4	-0.5291003191132403E-008	0.4083128501974900E-007
17	4	0.5702917027505801E-009	-0.2275248611738300E-007
18	4	0.9721010663099603E-009	0.1252931269846200E-007
19	4	-0.1234565671914800E-008	-0.6820601861079501E-008
20	4	0.1056303933211200E-008	0.3670184822723902E-008
21	4	-0.7822532066548095E-009	-0.1951415029566300E-008
22	4	0.5364329536128300E-009	0.1024401896643200E-008
23	4	-0.3503781986768901E-009	-0.5302916439298099E-009
24	4	0.2211493349557600E-009	0.2701995294174300E-009
25	4	-0.1360155460483600E-009	-0.1351464634646901E-009
26	4	0.8194346590162397E-010	0.6608751740300203E-010
27	4	-0.4852399732024900E-010	-0.3139848797628600E-010
28	4	0.2830941731035701E-010	0.1434489072665900E-010
29	4	-0.1629807053205000E-010	-0.6186053405632403E-011
30	4	0.9269355248642295E-011	0.2422101798640899E-011
31	4	-0.5211722112902198E-011	-0.7745524057203900E-012
32	4	0.2898038579946000E-011	0.1121861054032500E-012
1	5	-0.2287265611812500E-002	-0.1310433610342400E-002
2	5	0.1306006306549500E-003	0.1825430226745100E-003
3	5	-0.8714091381989403E-004	-0.4431783600011800E-004
4	5	0.2536410647735500E-004	0.4078320898770499E-006
5	5	-0.2143877645721700E-004	-0.2647962219270999E-005
6	5	0.8161139703588599E-005	-0.4275434093870000E-005
7	5	-0.4792507297679500E-005	0.1974598490051000E-005
8	5	0.2188780854339700E-005	-0.1893456555990300E-005
9	5	-0.1083624397324500E-005	0.1127553787228000E-005

10	5	0.4949774847773396E-006	-0.7346052939283297E-006
11	5	-0.2194350372519700E-006	0.4371982242901100E-006
12	5	0.8922443583969692E-007	-0.2590394956314400E-006
13	5	-0.3135414772259498E-007	0.1491320773539000E-006
14	5	0.7247473288174399E-008	-0.8461537959192398E-007
15	5	0.1572662555737699E-008	0.4720060076124400E-007
16	5	-0.3923178226727900E-008	-0.2595072423616801E-007
17	5	0.3820721072855799E-008	0.1405801075549100E-007
18	5	-0.2994703152126000E-008	-0.7503086152382801E-008
19	5	0.2120774666991600E-008	0.3941698967224700E-008
20	5	-0.1414045547321101E-008	-0.2035103641162600E-008
21	5	0.9051071558907603E-009	0.1030052487749300E-008
22	5	-0.5621230148023002E-009	-0.5091184140937299E-009
23	5	0.3409129367693000E-009	0.2442306912264800E-009
24	5	-0.2027285977979100E-009	-0.1125578172334100E-009
25	5	0.1185277570536800E-009	0.4892324045879800E-010
26	5	-0.6825583154235203E-010	-0.1929320245230799E-010
27	5	0.3875965520760998E-010	0.6211164395308904E-011
28	5	-0.2171888190127800E-010	-0.9076183814932206E-012
29	5	0.1201252899235600E-010	-0.9129518972403297E-012
30	5	-0.6557434283072102E-011	0.1287445085436400E-011
31	5	0.3531309142670900E-011	-0.1139585171020000E-011
32	5	-0.1874333370802100E-011	0.8609545910399905E-012
1	6	0.1155133359134200E-002	0.7439779583364700E-003
2	6	-0.9139500616583998E-004	-0.8856764179654403E-004
3	6	0.3818675759248399E-004	0.1806862383091401E-004
4	6	-0.2513972867745900E-004	-0.1255855750059700E-005
5	6	0.8408450412389399E-005	-0.3267402917117600E-005
6	6	-0.6177950126584600E-005	0.2013199491557299E-005
7	6	0.2259152779515699E-005	-0.2245070618300801E-005
8	6	-0.1286934548261299E-005	0.1237397327713600E-005
9	6	0.5174964599064003E-006	-0.8772461228545597E-006
10	6	-0.2316054832363101E-006	0.5051157359048400E-006
11	6	0.8239690174605098E-007	-0.3057180038012999E-006
12	6	-0.2304902579908199E-007	0.1740267379091200E-006
13	6	-0.5660225066428401E-009	-0.9868082884168004E-007
14	6	0.7497948040224899E-008	0.5451589046856498E-007
15	6	-0.8083861580132602E-008	-0.2967082757265899E-007
16	6	0.6574810473836099E-008	0.1583533659754699E-007
17	6	-0.4747379822589401E-008	-0.8293946862636401E-008
18	6	0.3201551912468400E-008	0.4250661156390799E-008
19	6	-0.2063437865018600E-008	-0.2124663112113002E-008
20	6	0.1286505457720500E-008	0.1029524687723400E-008
21	6	-0.7814862645893996E-009	-0.4788375806974400E-009
22	6	0.4645714923867700E-009	0.2099045104397800E-009
23	6	-0.2710475732747899E-009	-0.8347423446908298E-010
24	6	0.1554856521313000E-009	0.2714403528336600E-010
25	6	-0.8779227345101502E-010	-0.4096140527459802E-011
26	6	0.4881573270609802E-010	-0.3905728605119201E-011
27	6	-0.2672962372274299E-010	0.5599025149766200E-011
28	6	0.1440528512447500E-010	-0.4985926168460402E-011
29	6	-0.7632294102277701E-011	0.3780572209455300E-011
30	6	0.3968000407417202E-011	-0.2636468300620799E-011
31	6	-0.2018274653306499E-011	0.1744281043387900E-011
32	6	0.9996856857943898E-012	-0.1111991358368500E-011
1	7	-0.6207895348779901E-003	-0.4275549435988097E-003
2	7	0.5494606011780000E-004	0.4716699913842600E-004
3	7	-0.2697741729207300E-004	-0.6423236300179300E-005
4	7	0.1194484048028200E-004	-0.5254572101875999E-006
5	7	-0.7283873856067700E-005	0.2545557663324900E-005
6	7	0.2561361270636600E-005	-0.2133742100340900E-005
7	7	-0.1669170615059600E-005	0.1412515075571700E-005
8	7	0.5511540734914898E-006	-0.1007123501040001E-005
9	7	-0.2873398727842899E-006	0.5764466095570198E-006
10	7	0.8222573200100701E-007	-0.3603877303248699E-006
11	7	-0.2191170089815800E-007	0.2020414768821900E-006
12	7	-0.6580677780476696E-008	-0.1158003541945600E-006
13	7	0.1250482206671700E-007	0.6329359791834602E-007
14	7	-0.1206880551052300E-007	-0.3429713757441299E-007
15	7	0.9336679873683801E-008	0.1805568494717100E-007

16	7	-0.6573134481158095E-008	-0.9305259673908497E-008
17	7	0.4352224802772800E-008	0.4654383989333200E-008
18	7	-0.2765316198249899E-008	-0.2249430197665000E-008
19	7	0.1702247676149700E-008	0.1036899788253700E-008
20	7	-0.1021468798434500E-008	-0.4458946822882799E-009
21	7	0.5997095597898300E-009	0.1699291957146800E-009
22	7	-0.3452798880143599E-009	-0.4889092602988798E-010
23	7	0.1951993011672900E-009	0.1015267514156700E-011
24	7	-0.1084157416619800E-009	0.1419989473228100E-010
25	7	0.5914846390453501E-010	-0.1608915084494500E-010
26	7	-0.3167016648930598E-010	0.1341851716546398E-010
27	7	0.1661336866687301E-010	-0.9860862126842601E-011
28	7	-0.8513327195980301E-011	0.6746944582885996E-011
29	7	0.4241604897176100E-011	-0.4403598145852301E-011
30	7	-0.2038861484157700E-011	0.2776854050520701E-011
31	7	0.9328320451154600E-012	-0.1704399859095400E-011
32	7	-0.3956927559049800E-012	0.1022998743008300E-011
1	8	0.3472458338365001E-003	0.2501737326383600E-003
2	8	-0.3471606760285799E-004	-0.2471319749020000E-004
3	8	0.1636026354390200E-004	0.2916585117418400E-005
4	8	-0.8201192031265197E-005	0.1808303068173700E-005
5	8	0.3631588015196000E-005	-0.1799942310754001E-005
6	8	-0.2006310069191400E-005	0.1660673888181900E-005
7	8	0.6803346082051601E-006	-0.1052026163961300E-005
8	8	-0.3849222878216101E-006	0.6777846692784799E-006
9	8	0.8976159193707606E-007	-0.4142605121160202E-006
10	8	-0.3217852295733800E-007	0.2360507380672100E-006
11	8	-0.1114683900738100E-007	-0.1363840311796600E-006
12	8	0.1587726572438400E-007	0.7404410240496904E-007
13	8	-0.1592112042203600E-007	-0.4020103361312998E-007
14	8	0.1206583011281700E-007	0.2090616568750600E-007
15	8	-0.8507067938978700E-008	-0.1065861177096400E-007
16	8	0.5597772911869496E-008	0.5213318221564098E-008
17	8	-0.3542820481428101E-008	-0.2442081870057700E-008
18	8	0.2168131674196199E-008	0.1067627652950900E-008
19	8	-0.1292546403242100E-008	-0.4174064427431300E-009
20	8	0.7527677925445200E-009	0.1271772409605599E-009
21	8	-0.4292299016217500E-009	-0.9771023400106898E-011
22	8	0.2398201359721200E-009	-0.2930330283978900E-010
23	8	-0.1312963765487400E-009	0.3571273138325298E-010
24	8	0.7036791982439903E-010	-0.3051425084832401E-010
25	8	-0.3684356639222002E-010	0.2270308940843800E-010
26	8	0.1877829662599900E-010	-0.1564800025666300E-010
27	8	-0.9260928829357701E-011	0.1025860126013800E-010
28	8	0.4374123459272001E-011	-0.6484702098213902E-011
29	8	-0.1941330559848700E-011	0.3983525748846300E-011
30	8	0.7774267883099699E-012	-0.2389480106834699E-011
31	8	-0.2507459300957201E-012	0.1403785182714500E-011
32	8	0.3249711358842800E-013	-0.8091772152503397E-012
1	9	-0.2000474341912200E-003	-0.1484198874095500E-003
2	9	0.2205145938205500E-004	0.1340333346888700E-004
3	9	-0.1035634977597500E-004	-0.6799712082283800E-006
4	9	0.4981268375558998E-005	-0.1406387696079000E-005
5	9	-0.2382498905717501E-005	0.1628367613193400E-005
6	9	0.1006377033263600E-005	-0.1084664631889600E-005
7	9	-0.4820353751711101E-006	0.7932791277198704E-006
8	9	0.1305336354562300E-006	-0.4573246599193199E-006
9	9	-0.5246430845318200E-007	0.2819498376993601E-006
10	9	-0.1253537362799800E-007	-0.1585158457828600E-006
11	9	0.1658314019437100E-007	0.8800819273346900E-007
12	9	-0.1960625617414300E-007	-0.4754302196374701E-007
13	9	0.1456331055749200E-007	0.2465320037003900E-007
14	9	-0.1056949905375900E-007	-0.1248735159720100E-007
15	9	0.6934862462060201E-008	0.6003608721272300E-008
16	9	-0.4414659304785600E-008	-0.2744624527650799E-008
17	9	0.2696528556000999E-008	0.1142032246548300E-008
18	9	-0.1604856136872000E-008	-0.4032469080872400E-009
19	9	0.9302206227523900E-009	0.8577775295615098E-010
20	9	-0.5269673031271800E-009	0.3235147566504899E-010
21	9	0.2917187880147099E-009	-0.6345059200274500E-010

22	9	-0.1577604158420300E-009	0.6051427414721601E-010
23	9	0.8317818656067299E-010	-0.4737206460436700E-010
24	9	-0.4260441652248502E-010	0.3363663167443901E-010
25	9	0.2106681669389299E-010	-0.2248764369161500E-010
26	9	-0.9946135928751207E-011	0.1441058210260900E-010
27	9	0.4390772034151800E-011	-0.8939269463548204E-011
28	9	-0.1730865667806700E-011	0.5399284318252703E-011
29	9	0.5311599684393300E-012	-0.3186597036589100E-011
30	9	-0.3949113917280600E-013	0.1841580490533099E-011
31	9	-0.1267406183258100E-012	-0.1043242098611200E-011
32	9	0.1552918221531900E-012	0.5794199213309001E-012
1	10	0.1178528691525600E-003	0.8912580960895898E-004
2	10	-0.1409151263942500E-004	-0.7268514764291501E-005
3	10	0.6588044470845498E-005	-0.8478147606183498E-007
4	10	-0.3104950337729000E-005	0.1268378468921600E-005
5	10	0.1429191115676100E-005	-0.1119605371968600E-005
6	10	-0.6154281209092000E-006	0.8484583418066904E-006
7	10	0.2246797379257300E-006	-0.5100789621792501E-006
8	10	-0.7614639940811702E-007	0.3330213758090399E-006
9	10	-0.3496972711403098E-008	-0.1818749950643900E-006
10	10	0.1505470414997500E-007	0.1065717682990901E-006
11	10	-0.2234129503619900E-007	-0.5610659670196599E-007
12	10	0.1661547699427500E-007	0.2977644264490199E-007
13	10	-0.1273098693133099E-007	-0.1488175804809100E-007
14	10	0.8326819234127900E-008	0.7142134439419600E-008
15	10	-0.5396890490061399E-008	-0.3206127585642100E-008
16	10	0.3294507555651200E-008	0.1289190865172400E-008
17	10	-0.1969056251383000E-008	-0.4172084344666898E-009
18	10	0.1138652061527500E-008	0.5202129352288600E-010
19	10	-0.6431644661297796E-009	0.7491031406292603E-010
20	10	0.3536657355862600E-009	-0.1006242103529500E-009
21	10	-0.1894326639995100E-009	0.8851087918149105E-010
22	10	0.9846345266906198E-010	-0.6681574737932299E-010
23	10	-0.4941250186796300E-010	0.4641212761336001E-010
24	10	0.2370184257194400E-010	-0.3054238112420999E-010
25	10	-0.1066802722549100E-010	0.1931929963228099E-010
26	10	0.4329387976592702E-011	-0.1184318615399200E-010
27	10	-0.1417504893845600E-011	0.7070248900231702E-011
28	10	0.1929139899041499E-012	-0.4122193905664600E-011
29	10	0.2425030391339101E-012	0.2350656778601898E-011
30	10	-0.3360367539784202E-012	-0.1311579534216100E-011
31	10	0.3002503844509698E-012	0.7155951720939901E-012
32	10	-0.2295990275073099E-012	-0.3811127032449900E-012
1	11	-0.7064790406730001E-004	-0.5405758565757399E-004
2	11	0.9063448487722797E-005	0.3950290647480897E-005
3	11	-0.4191812422504901E-005	0.3897607427916200E-006
4	11	0.1952019601958499E-005	-0.9773674491953004E-006
5	11	-0.8586345074945701E-006	0.8403079618801701E-006
6	11	0.3528353147430602E-006	-0.5705877583750400E-006
7	11	-0.1168280192587200E-006	0.3737888789601100E-006
8	11	0.2024697209890300E-007	-0.2122570208484800E-006
9	11	0.1179747677326800E-007	0.1277956158674000E-006
10	11	-0.2215465322308300E-007	-0.6646775574381502E-007
11	11	0.1832565210690999E-007	0.3665818582021501E-007
12	11	-0.1472674604485700E-007	-0.1791263848360800E-007
13	11	0.9747264329007496E-008	0.8805108642206999E-008
14	11	-0.6484711878584903E-008	-0.3872870024679299E-008
15	11	0.3963841255227900E-008	0.1554559925232000E-008
16	11	-0.2395671661048500E-008	-0.4765663419448201E-009
17	11	0.1384297565465400E-008	0.3587579192054803E-010
18	11	-0.7832773318838803E-009	0.1139337166278199E-009
19	11	0.4288659705142800E-009	-0.1392518184095699E-009
20	11	-0.2283471467468000E-009	0.1193051352155201E-009
21	11	0.1173495467465800E-009	-0.8888973584975098E-010
22	11	-0.5788050247423899E-010	0.6120230017225802E-010
23	11	0.2699034919173600E-010	-0.3998649328318400E-010
24	11	-0.1157052578748500E-010	0.2512008136224000E-010
25	11	0.4249752025980999E-011	-0.1528941903639100E-010
26	11	-0.1021050973805400E-011	0.9055233993193706E-011
27	11	-0.2347132633650400E-012	-0.5231132801236702E-011

28	11	0.5987897894535500E-012	0.2950539985946400E-011
29	11	-0.6001473189937199E-012	-0.1624454802444400E-011
30	11	0.4828321444917702E-012	0.8716531728174301E-012
31	11	-0.3498658882137400E-012	-0.4543944430793200E-012
32	11	0.2378934180723200E-012	0.2288131164575300E-012
1	12	0.4294487007428000E-004	0.3306431244709500E-004
2	12	-0.5852113645232699E-005	-0.2133177758878400E-005
3	12	0.2681706519069800E-005	-0.4485429769829401E-006
4	12	-0.1218072725350799E-005	0.7408037276945799E-006
5	12	0.5225575137046698E-006	-0.5961035753898600E-006
6	12	-0.1937998632684000E-006	0.4054677731346601E-006
7	12	0.5562138483128400E-007	-0.2482009620052799E-006
8	12	0.2134326049230100E-008	0.1488043750441599E-006
9	12	-0.1806420968364400E-007	-0.8035085841129298E-007
10	12	0.1950074768330999E-007	0.4488891391929402E-007
11	12	-0.1605021182626799E-007	-0.2193697845598300E-007
12	12	0.1122311932277900E-007	0.1112204817133000E-007
13	12	-0.760677121292020lE-008	-0.4812036547008298E-008
14	12	0.4712336743040202E-008	0.2000631660337100E-008
15	12	-0.2888564054615000E-008	-0.6017977227656999E-009
16	12	0.1673570504401301E-008	0.5325922342036502E-010
17	12	-0.9531624378666894E-009	0.1439208197062700E-009
18	12	0.5209517817128502E-009	-0.1764246110314000E-009
19	12	-0.2770225715487100E-009	0.1520572001645300E-009
20	12	0.1412482630858100E-009	-0.1134121477286400E-009
21	12	-0.6882379388617499E-010	0.7811852553718499E-010
22	12	0.3135179962865399E-010	-0.5098621524979299E-010
23	12	-0.1286192159721800E-010	0.3196159656382298E-010
24	12	0.4244201778219600E-011	-0.1938723660777100E-010
25	12	-0.5770965844954798E-012	0.1142672935439100E-010
26	12	-0.7423999566144603E-012	-0.6558126004058098E-011
27	12	0.1030569509938300E-011	0.3667120426764598E-011
28	12	-0.9234337470034902E-012	-0.1996035932025402E-011
29	12	0.7075040423312804E-012	0.1054845013420700E-011
30	12	-0.4981844472541603E-012	-0.5385411084094002E-012
31	12	0.3320583554216500E-012	0.2632701728063499E-012
32	12	-0.2126457782644999E-012	-0.1212047091381600E-012
1	13	-0.2640332604642000E-004	-0.2036796468019000E-004
2	13	0.3792021971094100E-005	0.1136193645834300E-005
3	13	-0.1717481723062500E-005	0.4107886297788400E-006
4	13	0.7632903020748900E-006	-0.5461235446091502E-006
5	13	-0.3112309627795201E-006	0.4221874405629898E-006
6	13	0.1072503721388800E-006	-0.2792595239498000E-006
7	13	-0.1939406324424900E-007	0.1706263930145699E-006
8	13	-0.1025900608908600E-007	-0.9733778938425498E-007
9	13	0.1861464049568400E-007	0.5412844572560997E-007
10	13	-0.1646660763299200E-007	-0.2751072614160001E-007
11	13	0.1262774773636000E-007	0.1405894778372400E-007
12	13	-0.8647132787586997E-008	-0.6184465384251299E-008
13	13	0.5552272863695896E-008	0.2677312593846199E-008
14	13	-0.3434945439195800E-008	-0.8271599516440599E-009
15	13	0.2015563937973800E-008	0.1253626091823900E-009
16	13	-0.1157144602359500E-008	0.1570395896655100E-009
17	13	0.6343018332799498E-009	-0.2072257920815401E-009
18	13	-0.3383485713825999E-009	0.1853372316729099E-009
19	13	0.1719178965853299E-009	-0.1397791743462702E-009
20	13	-0.8330157397207200E-010	0.9716096677214697E-010
21	13	0.3734886358519601E-010	-0.6366212418340600E-010
22	13	-0.1483763632792500E-010	0.3999573588986399E-010
23	13	0.4450672469458199E-011	-0.2425834186303701E-010
24	13	-0.1448841453711600E-012	0.1427120487756900E-010
25	13	-0.1310029450370100E-011	-0.8158772268895799E-011
26	13	0.1534513401763000E-011	0.4533897562941600E-011
27	13	-0.1308890062307100E-011	-0.2445308712462100E-011
28	13	0.9785987124810699E-012	0.1275257677235700E-011
29	13	-0.6784527909094200E-012	-0.6386074394987297E-012
30	13	0.4469665197855099E-012	0.3031017548494501E-012
31	13	-0.2833820417907900E-012	-0.1328734756771100E-012
32	13	0.1741639466109799E-012	0.5058225634679002E-013
1	14	0.1638705180084800E-004	0.1262303885596300E-004

2	14	-0.2463790679030399E-005	-0.5909419087402100E-006
3	14	0.1101841007766800E-005	-0.3412975217997899E-006
4	14	-0.4767710208852800E-006	0.3957044611979701E-006
5	14	0.1850483357657100E-006	-0.2961461404993302E-006
6	14	-0.5500875843722498E-007	0.1919908925174200E-006
7	14	0.3397639281033100E-008	-0.1150274044903200E-006
8	14	0.1404683391825800E-007	0.6495723425814503E-007
9	14	-0.1584285058697801E-007	-0.3460288411361000E-007
10	14	0.1349087597191101E-007	0.1768253632406000E-007
11	14	-0.9554999458316599E-008	-0.8184015243273304E-008
12	14	0.6438491517712899E-008	0.3610229226680400E-008
13	14	-0.4015797028245101E-008	-0.1216705958206900E-008
14	14	0.2418229172462799E-008	0.2717330527257601E-009
15	14	-0.1396218696214600E-008	0.1392766457719600E-009
16	14	0.7744992980285303E-009	-0.2249960218136900E-009
17	14	-0.4151173571553800E-009	0.2166216372945199E-009
18	14	0.2116139069530099E-009	-0.1667657539838900E-009
19	14	-0.1026044665897200E-009	0.1181377357051300E-009
20	14	0.4573150885755998E-010	-0.7802773011045304E-010
21	14	-0.1790214330943400E-010	0.4936192080085000E-010
22	14	0.5068988631618003E-011	-0.3002706416843598E-010
23	14	0.1828675557334600E-012	0.1768803679913500E-010
24	14	-0.1901285335767500E-011	-0.1009984283706400E-010
25	14	0.2099941965108500E-011	0.5593101069095699E-011
26	14	-0.1756670980554400E-011	-0.2997024286730000E-011
27	14	0.1299769211531001E-011	0.1546678150138300E-011
28	14	-0.8946796211870000E-012	-0.7617015742103501E-012
29	14	0.5858534686022098E-012	0.3517360827511701E-012
30	14	-0.3692926498453899E-012	-0.1466418403806699E-012
31	14	0.2255699289464500E-012	0.4975745970846697E-013
32	14	-0.1340296146637400E-012	-0.7774724840434100E-014
1	15	-0.1025148230837700E-004	-0.7863885912229300E-005
2	15	0.1604346152817000E-005	0.2952956492663400E-006
3	15	-0.7074324344102900E-006	0.2686438733690001E-006
4	15	0.2972803372358600E-006	-0.2833561438819700E-006
5	15	-0.1082541984942500E-006	0.2061035360156900E-006
6	15	0.2648460473153599E-007	-0.1313433131144800E-006
7	15	0.4785201568324702E-008	0.7721969552676498E-007
8	15	-0.1332110688423400E-007	-0.4276899545629897E-007
9	15	0.1332756571770200E-007	0.2228449247354501E-007
10	15	-0.1024890750045400E-007	-0.1085792256105800E-007
11	15	0.7237874743992700E-008	0.4875885917243700E-008
12	15	-0.4625900551502601E-008	-0.1841304220207000E-008
13	15	0.2871239468405000E-008	0.5126457036652702E-009
14	15	-0.1671589977547700E-008	0.6712218975080100E-010
15	15	0.9465259687147007E-009	-0.2225421791290900E-009
16	15	-0.5098541588921500E-009	0.2410154575915900E-009
17	15	0.2631602713520898E-009	-0.1925673231983899E-009
18	15	-0.1281796474517100E-009	0.1404435873153500E-009
19	15	0.5750378298530200E-010	-0.9393102268218101E-010
20	15	-0.2257947821771000E-010	0.6015364595324300E-010
21	15	0.6384160127631501E-011	-0.3680377877457500E-010
22	15	0.2692297339929000E-012	0.2178581100242800E-010
23	15	-0.2456095439876100E-011	-0.1245785072323500E-010
24	15	0.2704798624658700E-011	0.6896458664556995E-011
25	15	-0.2262090905216799E-011	-0.3682633625129400E-011
26	15	0.1672899666016500E-011	0.1887258144900300E-011
27	15	-0.1150529216169299E-011	-0.9176446495035005E-012
28	15	0.7522229367173896E-012	0.4141156818501798E-012
29	15	-0.4730413651933601E-012	-0.1648108461770700E-012
30	15	0.2879805768851701E-012	0.4921381363412801E-013
31	15	-0.1703311021958700E-012	-0.8539410303347500E-015
32	15	0.9805222904229700E-013	-0.1556691211210901E-013
1	16	0.6456580649683000E-005	0.4921098025079099E-005
2	16	-0.1046573288476800E-005	-0.1375764924205200E-006
3	16	0.4543790907973699E-006	-0.2045064064759599E-006
4	16	-0.1847416655209600E-006	0.2009523853985201E-006
5	16	0.6227188720231400E-007	-0.1427096378847600E-006
6	16	-0.1077415490158300E-007	0.8929894335096799E-007
7	16	-0.7602661611372199E-008	-0.5165844285670600E-007

8	16	0.1172819708017400E-007	0.2793693631986099E-007
9	16	-0.1041852915051300E-007	-0.1418291439847499E-007
10	16	0.7811565616577800E-008	0.6610802127937598E-008
11	16	-0.5236368227912200E-008	-0.2740605964390900E-008
12	16	0.3342482957080501E-008	0.8896791636736598E-009
13	16	-0.1987186193375100E-008	-0.8545299190476598E-010
14	16	0.1150350592560300E-008	-0.1899453649922800E-009
15	16	-0.6258705775863404E-009	0.2505754770343299E-009
16	16	0.3293272599069800E-009	-0.2148512062705199E-009
17	16	-0.1616963091200000E-009	0.1626580259372900E-009
18	16	0.7394041628971904E-010	-0.1110427097494900E-009
19	16	-0.2952051103566300E-010	0.7233674770290603E-010
20	16	0.8795337722022898E-011	-0.4466894562571399E-010
21	16	-0.7683601883001401E-013	0.2667129191114001E-010
22	16	-0.2880199334240300E-011	-0.1531591693748600E-010
23	16	0.3310955459454000E-011	0.8505190475516194E-011
24	16	-0.2812616892861100E-011	-0.4540663851859700E-011
25	16	0.2096741833976201E-011	0.2320488419471602E-011
26	16	-0.1448731109035498E-011	-0.1119559414793100E-011
27	16	0.9494515633770604E-012	0.4972042200700199E-012
28	16	-0.5975381864656297E-012	-0.1907599376854299E-012
29	16	0.3635044468122002E-012	0.5040403383842401E-013
30	16	-0.2145288341501999E-012	0.6762687757472296E-014
31	16	0.1230100819381999E-012	-0.2480917828486802E-013
32	16	-0.6851042357123402E-013	0.2615320442579200E-013
1	17	-0.4090125912625800E-005	-0.3091610551564401E-005
2	17	0.6837071850895901E-006	0.5564831795368297E-007
3	17	-0.2918388588568599E-006	0.1521769235068900E-006
4	17	0.1143148082860500E-006	-0.1414734498439401E-006
5	17	-0.3494712785823101E-007	0.9830413461031601E-007
6	17	0.2640863527858500E-008	-0.6049208423064600E-007
7	17	0.8024024111819003E-008	0.3432646877854500E-007
8	17	-0.9606901052450198E-008	-0.1817182493368800E-007
9	17	0.8011403984653500E-008	0.8893675129684199E-008
10	17	-0.5746380260518402E-008	-0.3950887172976500E-008
11	17	0.3797091974178102E-008	0.1462875931501600E-008
12	17	-0.2336870474906000E-008	-0.3401705306327299E-009
13	17	0.1381055714233500E-008	-0.1089859244518500E-009
14	17	-0.7671443480461394E-009	0.2360901474318701E-009
15	17	0.4118017871146400E-009	-0.2297239343196400E-009
16	17	-0.2053466702234299E-009	0.1823919765220300E-009
17	17	0.9641554915562596E-010	-0.1287723955245601E-009
18	17	-0.3956120847581302E-010	0.8562829612035504E-010
19	17	0.1282635629651400E-010	-0.5366081190505403E-010
20	17	-0.1114593768843100E-011	0.3242314750018200E-010
21	17	-0.3032660277416100E-011	-0.1876040295334401E-010
22	17	0.3858531983508300E-011	0.1048732108099900E-010
23	17	-0.3383504847825899E-011	-0.5617036349936402E-011
24	17	0.2565013739602700E-011	0.2875732854970598E-011
25	17	-0.1789897223492001E-011	-0.1384461338974100E-011
26	17	0.1180468591800700E-011	0.6104758625696800E-012
27	17	-0.7457874920922801E-012	-0.2293167283666499E-012
28	17	0.4545429516719001E-012	0.5563179921613303E-013
29	17	-0.2682943114635399E-012	0.1414642346000301E-013
30	17	0.1535775358881700E-012	-0.3517831167966701E-013
31	17	-0.8522251914583295E-013	0.3560646650571301E-013
32	17	0.4570806285005497E-013	-0.2896847936225202E-013
1	18	0.2604076371426300E-005	0.1948915041794000E-005
2	18	-0.4471756085422401E-006	-0.1491993018021300E-007
3	18	0.1873689967624200E-006	-0.1114031533688800E-006
4	18	-0.7035510662944901E-007	0.9899879671593201E-007
5	18	0.1892336065623099E-007	-0.6743648839346903E-007
6	18	0.1256484027933900E-008	0.4079569748682799E-007
7	18	-0.7295889670189101E-008	-0.2271554855326499E-007
8	18	0.7581873795459202E-008	0.1170854257992500E-007
9	18	-0.6004502228762503E-008	-0.5526327839788800E-008
10	18	0.4188367874746700E-008	0.2280535316145901E-008
11	18	-0.2692500444823099E-008	-0.7240589794399497E-009
12	18	0.1632774915272301E-008	0.4512591689209700E-010
13	18	-0.9342989715222000E-009	0.1877684813189600E-009

14	18	0.5114796919336600E-009	-0.2301946966376502E-009
15	18	-0.2616213912176600E-009	0.1966439927558700E-009
16	18	0.1262053933581700E-009	-0.1458643900109601E-009
17	18	-0.5381348491817501E-010	0.9945277240630496E-010
18	18	0.1909195891658399E-010	-0.6372223582129497E-010
19	18	-0.3202638891933201E-011	0.3905768417022899E-010
20	18	-0.2718556282865800E-011	-0.2287527632593999E-010
21	18	0.4257223913672900E-011	0.1291068727621300E-010
22	18	-0.3932705289894102E-011	-0.6964972435602499E-011
23	18	0.3063766688266002E-011	0.3588116349179098E-011
24	18	-0.2170987781907599E-011	-0.1733949030365000E-011
25	18	0.1446980989888700E-011	0.7664343877437898E-012
26	18	-0.9205034737919100E-012	-0.2871745538850900E-012
27	18	0.5636297635211500E-012	0.6825832623734102E-013
28	18	-0.3335330330065500E-012	0.1980334909186699E-013
29	18	0.1910574563140900E-012	-0.4611789127125501E-013
30	18	-0.1058666975156500E-012	0.4631986458346200E-013
31	18	0.5657082332959098E-013	-0.3756590443446500E-013
32	18	-0.2895937206400300E-013	0.2741861235668400E-013
1	19	-0.1665242734816300E-005	-0.1232271756634900E-005
2	19	0.2927462219304301E-006	-0.3818398042199100E-008
3	19	-0.1202092079211100E-006	0.8056045430748796E-007
4	19	0.4300697398207395E-007	-0.6893008475117300E-007
5	19	-0.9695581226765203E-008	0.4608617487633599E-007
6	19	-0.2847598157274000E-008	-0.2740828008995800E-007
7	19	0.6146634756731797E-008	0.1494983870031800E-007
8	19	-0.5821526816163198E-008	-0.7491088638289503E-008
9	19	0.4427766153725100E-008	0.3372078394292500E-008
10	19	-0.3008659765768602E-008	-0.1273625094278000E-008
11	19	0.1893861512058899E-008	0.2965322987158499E-009
12	19	-0.1121623238731200E-008	0.9194463940209697E-010
13	19	0.6291392962154399E-009	-0.2067251092530099E-009
14	19	-0.3321348196472200E-009	0.2015959621459698E-009
15	19	0.1646415087597200E-009	-0.1599562843290800E-009
16	19	-0.7357072590030702E-010	0.1129767945862200E-009
17	19	0.2828085161887800E-010	-0.7455692313529400E-010
18	19	-0.6830428583848303E-011	0.4651383792020300E-010
19	19	-0.1689485899271400E-011	-0.2771964255354800E-010
20	19	0.4372076051889501E-011	0.1583437027330400E-010
21	19	-0.4396569913689397E-011	-0.8643414109443802E-011
22	19	0.3567278850785699E-011	0.4497325688940199E-011
23	19	-0.2583279944123901E-011	-0.2194758264018000E-011
24	19	0.1748493060407800E-011	0.9809205314334504E-012
25	19	-0.1123648808547300E-011	-0.3732985600322898E-012
26	19	0.6932483558562401E-012	0.9298632149641307E-013
27	19	-0.4123146865164101E-012	0.2144880715366502E-013
28	19	0.2369411633042201E-012	-0.5665280256635798E-013
29	19	-0.1314502570378200E-012	0.5797878859957100E-013
30	19	0.7016944263051704E-013	-0.4738926400816102E-013
31	19	-0.3578055549329600E-013	0.3475439201835701E-013
32	19	0.1718956296476798E-013	-0.2381136161454200E-013
1	20	0.1069000632014601E-005	0.7812175226717997E-006
2	20	-0.1917887715308100E-006	0.1115814374230700E-007
3	20	0.7704101534500296E-007	-0.5770498034962700E-007
4	20	-0.2606804549998300E-007	0.4778972950703099E-007
5	20	0.4509010054221100E-008	-0.3138794468782201E-007
6	20	0.3236466666221599E-008	0.1834421681223800E-007
7	20	-0.4945126086397496E-008	-0.9788228005902502E-008
8	20	0.4377858076054500E-008	0.4747720883102602E-008
9	20	-0.3222177857864500E-008	-0.2020841494143600E-008
10	20	0.2137416243996900E-008	0.6679954922539400E-009
11	20	-0.1317847275750199E-008	-0.6987165707128497E-010
12	20	0.7634629040076401E-009	-0.1487068940209100E-009
13	20	-0.4168951295291400E-009	0.1914650382683900E-009
14	20	0.2131870652233300E-009	-0.1676847133369500E-009
15	20	-0.9999547717631801E-010	0.1249230024980000E-009
16	20	0.4122465563360898E-010	-0.8549625590825702E-010
17	20	-0.1259308976542299E-010	0.5463899124813500E-010
18	20	0.3672404448682602E-012	-0.3328030559468499E-010
19	20	0.4010790831399102E-011	0.1930373916270200E-010

20	20	-0.4685853267905001E-011	-0.1070943420750101E-010
21	20	0.4032102776663200E-011	0.5646071717796398E-011
22	20	-0.3010285163501699E-011	-0.2798655404645499E-011
23	20	0.2080630372852700E-011	0.1273324002661100E-011
24	20	-0.1355666121895200E-011	-0.4994330144759999E-012
25	20	0.8454957112040404E-012	0.1361879359285100E-012
26	20	-0.5067386397647502E-012	0.1580355787097900E-013
27	20	0.2929251079978501E-012	-0.6526293990904300E-013
28	20	-0.1631322301635201E-012	0.6996603952669600E-013
29	20	0.8726899140398105E-013	-0.5827106917648304E-013
30	20	-0.4448702419900703E-013	0.4317038263326700E-013
31	20	0.2129047467296599E-013	-0.2978060099955200E-013
32	20	-0.9252012133850698E-014	0.1951867148268999E-013
1	21	-0.6885908874210100E-006	-0.4964289246345301E-006
2	21	0.1257185004988100E-006	-0.1286580175730001E-007
3	21	-0.4930735642005901E-007	0.4102103190462002E-007
4	21	0.1563355134237600E-007	-0.3301054007920400E-007
5	21	-0.1695700246884300E-008	0.2131003462579900E-007
6	21	-0.3049519747833101E-008	-0.1223212997558700E-007
7	21	0.3854779162537598E-008	0.6373102046097800E-008
8	21	-0.3241001023113200E-008	-0.2978435942324599E-008
9	21	0.2317770197990400E-008	0.1180663011801600E-008
10	21	-0.1504570135146801E-008	-0.3172173912435698E-009
11	21	0.9080115548343301E-009	-0.4411823337213702E-010
12	21	-0.5143304671051400E-009	0.1581772490766300E-009
13	21	0.2727303938243600E-009	-0.1648709224699700E-009
14	21	-0.1339577893055799E-009	0.1331617593969300E-009
15	21	0.5889875392961502E-010	-0.9549426527311105E-010
16	21	-0.2112155242373101E-010	0.6309621575217903E-010
17	21	0.3859537689443497E-011	-0.3943051440913301E-010
18	21	0.2926236293207500E-011	0.2333907719864699E-010
19	21	-0.4676475786474800E-011	-0.1320400386251000E-010
20	21	0.4391511893714299E-011	0.7078963717294100E-011
21	21	-0.3424927008666097E-011	-0.3580538426514701E-011
22	21	0.2432752567102501E-011	0.1666729905133699E-011
23	21	-0.1614617836133400E-011	-0.6803554030918002E-012
24	21	0.1021465030615100E-011	0.2061866844795000E-012
25	21	-0.6186817551323596E-012	-0.1695028123936700E-014
26	21	0.3607594908569498E-012	-0.6970146709155498E-013
27	21	-0.2022439561742001E-012	0.8128490014327303E-013
28	21	0.1087582104995600E-012	-0.6983800202638895E-013
29	21	-0.5564386774156500E-013	0.5262553698479202E-013
30	21	0.2667556795029800E-013	-0.3668024678481602E-013
31	21	-0.1158980273948200E-013	0.2421438836117500E-013
32	21	0.4167498238730698E-014	-0.1531865353153201E-013
1	22	0.4449006780760100E-006	0.3161164556786401E-006
2	22	-0.8244310834015797E-007	0.1201823707219800E-007
3	22	0.3150394789486200E-007	-0.2898052642308400E-007
4	22	-0.9249449206549800E-008	0.2272755494914200E-007
5	22	0.2510442131953300E-009	-0.1442504249382600E-007
6	22	0.2627291717516300E-008	0.8126295192312201E-008
7	22	-0.2937244891754200E-008	-0.4124850239151101E-008
8	22	0.2368595986013101E-008	0.1846066854938000E-008
9	22	-0.1651529579760300E-008	-0.6667474350408000E-009
10	22	0.1049622500026699E-008	0.1205866240194800E-009
11	22	-0.6203756397482600E-009	0.9222711483403103E-010
12	22	0.3426315897670000E-009	-0.1461854387541100E-009
13	22	-0.1759919293631300E-009	0.1345544092812300E-009
14	22	0.8219799146891299E-010	-0.1030890442455000E-009
15	22	-0.3305871201786398E-010	0.7121760819961402E-010
16	22	0.9291577056369499E-011	-0.4591290195254899E-010
17	22	0.8257345003072306E-012	0.2789778130729599E-010
18	22	-0.4195587887528801E-011	-0.1613939364097900E-010
19	22	0.4553371135002100E-011	0.8837497574021302E-011
20	22	-0.3784683504093300E-011	-0.4574710835841802E-011
21	22	0.2785616138797899E-011	0.2187910226256200E-011
22	22	-0.1894832814958200E-011	-0.9336701333947897E-012
23	22	0.1220405937765700E-011	0.3136194103893502E-012
24	22	-0.7495323806061496E-012	-0.3716535271810298E-013
25	22	0.4421284031160702E-012	-0.6682146697946401E-013

26	22	-0.2501929598827001E-012	0.9038939301903000E-013
27	22	0.1356701209709301E-012	-0.8145690881793801E-013
28	22	-0.6091159902510999E-013	0.6288447139315300E-013
29	22	0.3375463903071197E-013	-0.4449877424005100E-013
30	22	-0.1476593404026300E-013	0.2967875714610600E-013
31	22	0.5360124016596496E-014	-0.1891320386166299E-013
32	22	-0.1072778027367600E-014	0.1160716437380200E-013
1	23	-0.2882322576169799E-006	-0.2016701898810399E-006
2	23	0.5407931524814600E-007	-0.1020586015698700E-007
3	23	-0.2008781940787699E-007	0.2036865609511600E-007
4	23	0.5376358469533200E-008	-0.1560207252282500E-007
5	23	0.4232876826826298E-009	0.9736958794803698E-008
6	23	-0.2147401589880400E-008	-0.5378291145774503E-008
7	23	0.2199533888358500E-008	0.2652476682740700E-008
8	23	-0.1712784247764900E-008	-0.1127679505330500E-008
9	23	0.1166811869346400E-008	0.3581871188540502E-009
10	23	-0.7265587576021904E-009	-0.1645409503092700E-010
11	23	0.4200602365944699E-009	-0.1049611786374500E-008
12	23	-0.2259012699123999E-009	0.1250703984823101E-009
13	23	0.1116505360387900E-009	-0.1062082366498600E-009
14	23	-0.4904103165226402E-010	0.7792479855828204E-010
15	23	0.1720282249984000E-010	-0.5229519595140200E-010
16	23	-0.2633370735014001E-011	0.3282219288025501E-010
17	23	-0.3017729295617900E-011	-0.1948898854797799E-010
18	23	0.4397768607611299E-011	0.1094665070394700E-010
19	23	-0.4025244113720100E-011	-0.5811473698103002E-011
20	23	0.3109438271101101E-011	0.2865852954253599E-011
21	23	-0.2184627045237500E-011	-0.1279126435847800E-011
22	23	0.1438747341750400E-011	0.4717088265132597E-012
23	23	-0.8995635182931798E-012	-0.9839122518031498E-013
24	23	0.5382808998880002E-012	-0.5231465895249102E-013
25	23	-0.3084131799772900E-012	0.9505516220063207E-013
26	23	0.1691498503764199E-012	-0.9209602210621302E-013
27	23	-0.8811950735071500E-013	0.7356097610385106E-013
28	23	0.4304113218178002E-013	-0.5314620474933798E-013
29	23	-0.1909483991280699E-013	0.3594033978846601E-013
30	23	0.7108247977315401E-014	-0.2314388271144601E-013
31	23	-0.1579501406139800E-014	0.1430441119829200E-013
32	23	-0.6493446159088901E-015	-0.8524313423370399E-014
1	24	0.1871882204795800E-006	0.1288702264901100E-006
2	24	-0.3547956950455998E-007	0.8209105395451401E-008
3	24	0.1277775218966300E-007	-0.1425336382254700E-007
4	24	-0.3051385144559001E-008	0.1068212807098200E-007
5	24	-0.6790498718878302E-009	-0.6554577325346102E-008
6	24	0.1695131701673300E-008	0.3545779669877902E-008
7	24	-0.1624620438178700E-008	-0.1693442164274500E-008
8	24	0.1227405399539800E-008	0.6765377147388596E-009
9	24	-0.8181731403489298E-009	-0.1772932495258700E-009
10	24	0.4991507762675001E-009	-0.3372538012746999E-010
11	24	-0.2820302325012799E-009	0.9988054133769403E-010
12	24	0.1471712474110400E-009	-0.1020271922502800E-009
13	24	-0.6955509779249500E-010	0.8170060461498700E-010
14	24	0.2809083000932000E-010	-0.5787577014859701E-010
15	24	-0.7842198244956100E-011	0.3780202539882500E-010
16	24	-0.8770521743757500E-012	-0.2316338787444699E-010
17	24	0.3770331269414799E-011	0.1339699011448900E-010
18	24	-0.4057162591997198E-011	-0.7312816151239200E-011
19	24	0.3361040178812000E-011	0.3727490972133002E-011
20	24	-0.2463686589807001E-011	-0.1738000477043100E-011
21	24	0.1669034810532200E-011	0.6959853158204599E-012
22	24	-0.1067108315773400E-011	-0.1948739157238800E-012
23	24	0.6497773239605400E-012	-0.2044902367283400E-013
24	24	-0.3781721030077200E-012	0.9224617733083806E-013
25	24	0.2103391923526399E-012	-0.1002575098136600E-012
26	24	-0.1111392607718700E-012	0.8396351647808899E-013
27	24	0.5513771473360398E-013	-0.6235888406125000E-013
28	24	-0.2497261668017301E-013	0.4295095027795202E-013
29	24	0.9646056096078194E-014	-0.2802804070377199E-013
30	24	-0.2445232076309100E-014	0.1750338358952902E-013
31	24	-0.5469981013481796E-015	-0.1051098261434300E-013

32	24	0.1497702481511400E-014	0.6091162577987897E-014
1	25	-0.1218332101871100E-006	-0.8247104688052801E-007
2	25	0.2327819004221999E-007	-0.6376626338067100E-008
3	25	-0.8104988680201998E-008	0.9936583111880298E-008
4	25	0.1674391625350300E-008	-0.7295777759708201E-008
5	25	0.7193800555249696E-009	0.4400560804640500E-008
6	25	-0.1305358821035400E-008	-0.2328217840741300E-008
7	25	0.1186600373515000E-008	0.1072424926640300E-008
8	25	-0.8727025768706696E-009	-0.3965258121851901E-009
9	25	0.5697650129476999E-009	0.7466701562597297E-010
10	25	-0.3404752590974200E-009	0.5358001542443701E-010
11	25	0.1876941241318900E-009	-0.8702761428169797E-010
12	25	-0.9468035383486397E-010	0.8053778477456998E-010
13	25	0.4233081593585402E-010	-0.6160118248832404E-010
14	25	-0.1519682123196600E-010	0.4234017303428300E-010
15	25	0.2516799052151900E-011	-0.2696941107938099E-010
16	25	0.2478780418771500E-011	0.1612854294563701E-010
17	25	-0.3765919433934600E-011	-0.9082344251676302E-011
18	25	0.3479556920371602E-011	0.4792129800618202E-011
19	25	-0.2700893328433401E-011	-0.2331700370977701E-011
20	25	0.1898302695591002E-011	0.1003267998192500E-011
21	25	-0.1247420027515600E-011	-0.3379570386562199E-012
22	25	0.7759768847447100E-012	0.3590780355889598E-013
23	25	-0.4602146029715502E-012	0.7791804582189103E-013
24	25	0.2603005430559100E-012	-0.1037282578082200E-012
25	25	-0.1399135934063500E-012	0.9306699291430897E-013
26	25	0.7073162178574197E-013	-0.7171769688535401E-013
27	25	-0.3284121564105200E-013	0.5057249175097400E-013
28	25	0.1325090719388100E-013	-0.3356178318115001E-013
29	25	-0.3816422563851598E-014	0.2123000837899301E-013
30	25	-0.2212519541399700E-015	-0.1288562423537800E-013
31	25	0.1610732463817100E-014	0.7522605483683797E-014
32	25	-0.1805917653984699E-014	-0.4223359214569102E-014
1	26	0.7945334346004498E-007	0.5284679360784104E-007
2	26	-0.1527217996510899E-007	0.4834644684592600E-008
3	26	0.5124197954842201E-008	-0.6904478322411503E-008
4	26	-0.8730123290945400E-009	0.4971612010962200E-008
5	26	-0.6587686507408799E-009	-0.2946635824230301E-008
6	26	0.9866780725786800E-009	0.1522241221962900E-008
7	26	-0.8585901434266006E-009	-0.6728404500222500E-009
8	26	0.6162106380713800E-009	0.2251736019864800E-009
9	26	-0.3942460524708501E-009	-0.1913207960113601E-010
10	26	0.2306178303879101E-009	-0.5723575086102903E-010
11	26	-0.1237790286934300E-009	0.7192484108298204E-010
12	26	0.6003645497409897E-010	-0.6203230984436202E-010
13	26	-0.2501605346483200E-010	0.4570325715103101E-010
14	26	0.7457392342535797E-011	-0.3056894667952098E-010
15	26	0.3025937790265799E-012	0.1901126651937501E-010
16	26	-0.3012544640829101E-011	-0.1108893272344600E-010
17	26	0.3383068131190798E-011	0.6065298003426999E-011
18	26	-0.2852674476847001E-011	-0.3078151015328801E-011
19	26	0.2105818340883400E-011	0.1410118549705100E-011
20	26	-0.1431619146147200E-011	-0.5404780355905397E-012
21	26	0.9142257263727899E-012	0.1252949567015500E-012
22	26	-0.5543682375132298E-012	0.4693884237999701E-013
23	26	0.3198217244423200E-012	-0.9962945860019300E-013
24	26	-0.1753738484728400E-012	0.9937437971032498E-013
25	26	0.9056990044338499E-013	-0.8050792020888899E-013
26	26	-0.4325202644498697E-013	0.5852618872393203E-013
27	26	0.1824831349125501E-013	-0.3968030873498203E-013
28	26	-0.5922209998196801E-014	0.2550544953190698E-013
29	26	0.4406335801230600E-015	-0.1568212892172599E-013
30	26	0.1592960442034300E-014	0.9252800721524595E-014
31	26	-0.2016388824234899E-014	-0.5243855192058699E-014
32	26	0.1787891098801200E-014	0.2836471512448199E-014
1	27	-0.5190837626400901E-007	-0.3390324465612998E-007
2	27	0.1001829819102800E-007	-0.3601061893121498E-008
3	27	-0.3227327738386499E-008	0.4783725859880398E-008
4	27	0.4174865175787801E-009	-0.3380596469426699E-008
5	27	0.5595331975527502E-009	0.1967891627430199E-008

6	27	-0.7350358099955699E-009	-0.9907529241459709E-009
7	27	0.6162981236457200E-009	0.4175420564855897E-009
8	27	-0.432391261684370 1E-009	-0.1221327899925100E-009
9	27	0.2711535995736400E-009	-0.8710312852933098E-011
10	27	-0.1551181127990000E-009	0.5297520755398500E-010
11	27	0.8083839153627498E-010	-0.5735599148404303E-010
12	27	-0.3743126295030502E-010	0.4687797372504603E-010
13	27	0.1419602282948198E-010	-0.3344601678945098E-010
14	27	-0.2984660695676300E-011	0.2181699092218500E-010
15	27	-0.1636605781452100E-011	-0.1324856890860800E-010
16	27	0.2968988336432600E-011	0.7529879497703000E-011
17	27	-0.2861111738153300E-011	-0.3985944387052699E-011
18	27	0.2260994776820400E-011	0.1930836783861601E-011
19	27	-0.1605465218233700E-011	-0.8157672671052497E-012
20	27	0.1058923239892500E-011	0.2572745890026100E-012
21	27	-0.6590817843744903E-012	-0.7027487620959397E-014
22	27	0.3891366937881800E-012	-0.8417103955016604E-013
23	27	-0.2181900900189900E-012	0.1008449576557700E-012
24	27	0.1153992266328400E-012	-0.8768718173443601E-013
25	27	-0.5677306769234102E-013	0.6634798911447609E-013
26	27	0.2505569875383700E-013	-0.4621248452267198E-013
27	27	-0.9021662370877902E-014	0.3030066567663900E-013
28	27	0.1582292062063600E-014	-0.1892377652691100E-013
29	27	0.1363258553387000E-014	0.1132369717470700E-013
30	27	-0.2153039167307799E-014	-0.6492028120056100E-014
31	27	0.2038712801076300E-014	0.3557093262654299E-014
32	27	-0.1608161295305698E-014	-0.1855450870190699E-014
1	28	0.3396803194277699E-007	0.2177272406811400E-007
2	28	-0.6570380683967900E-008	0.2646201702205500E-008
3	28	0.2023628375980000E-008	-0.3305817175558397E-008
4	28	-0.1670077826032601E-009	0.2294068490726900E-008
5	28	-0.4538229791961600E-009	-0.1310755948225100E-008
6	28	0.5411961989665299E-009	0.6416655540242298E-009
7	28	-0.4393109487299498E-009	-0.2557213329978898E-009
8	28	0.3016770167008100E-009	0.6154783627199098E-010
9	28	-0.1854147529956100E-009	0.2077144185819200E-010
10	28	0.1035973182239600E-009	-0.4547387466580199E-010
11	28	-0.5223537227760902E-010	0.4456634714045099E-010
12	28	0.2286246539307001E-010	-0.3488122984896002E-010
13	28	-0.7580990522837396E-011	0.2418918884639100E-010
14	28	0.5319078510979100E-012	-0.1540539050493000E-010
15	28	0.2118069608592100E-011	0.9133084045986900E-011
16	28	-0.2652723093271602E-011	-0.5047091217180702E-011
17	28	0.2322089569240000E-011	0.2574077236083800E-011
18	28	-0.1747850779040800E-011	-0.1175799041464000E-011
19	28	0.1200405660289900E-011	0.4419520034226000E-012
20	28	-0.7707890315594701E-012	-0.9129380059000004E-013
21	28	0.4674779985856798E-012	-0.5280243134549700E-013
22	28	-0.2687363135842100E-012	0.9473744353024799E-013
23	28	0.1458749977366000E-012	-0.9181826306214901E-013
24	28	-0.7399153311533597E-013	0.7334375619859296E-013
25	28	0.3412667622993700E-013	-0.5283763064665299E-013
26	28	-0.1338275634245101E-013	0.3550337243163697E-013
27	28	0.3410407908497001E-014	-0.2260926092612800E-013
28	28	0.7985020357226899E-015	0.1375147401955501E-013
29	28	-0.2156694537991701E-014	-0.8000084732314701E-014
30	28	0.2239183265076500E-014	0.4445827335967802E-014
31	28	-0.1853099083212699E-014	-0.2343944088234701E-014
32	28	0.1369425059122100E-014	0.1154857743418099E-014
1	29	-0.2226117423731499E-007	-0.1399528315460000E-007
2	29	0.4307793677327299E-008	-0.1923978310003299E-008
3	29	-0.1262293491954800E-008	0.2279183064501900E-008
4	29	0.3600686762639199E-010	-0.1553719930491600E-008
5	29	0.3567606765564300E-009	0.8706974585770402E-009
6	29	-0.3946363236195799E-009	-0.4133434983177899E-009
7	29	0.3112292368268000E-009	0.1540834543289900E-009
8	29	-0.2093651085832700E-009	-0.2698872375583900E-010
9	29	0.1260717641393700E-009	-0.2423460390699200E-010
10	29	-0.6868172697238597E-010	0.3724662939186302E-010
11	29	0.3335245621349800E-010	-0.3394578021453901E-010

12	29	-0.1360244469145200E-010	0.2562069480183099E-010
13	29	0.3647833771158698E-011	-0.1731161915208300E-010
14	29	0.7029904544771101E-012	0.1077082520395400E-010
15	29	-0.2140117943971700E-011	-0.6228109174222196E-011
16	29	0.2235840419057001E-011	0.3337503017009102E-011
17	29	-0.1829450436627300E-011	-0.1628526848963799E-011
18	29	0.1323877097357500E-011	0.6889150708233603E-012
19	29	-0.8830895541732399E-012	-0.2136614046495700E-012
20	29	0.5526235935873801E-012	-0.8594082971370300E-016
21	29	-0.3266848055093200E-012	0.7768477972448101E-013
22	29	0.1823841506423300E-012	-0.9095017626395796E-013
23	29	-0.9547318312449704E-013	0.7848497513788399E-013
24	29	0.4592289412240100E-013	-0.5910196784015803E-013
25	29	-0.1937035770769200E-013	0.4094445119865098E-013
26	29	0.6134841949495495E-014	-0.2668096524423800E-013
27	29	-0.2178814115194999E-015	0.1652654623123900E-013
28	29	-0.1962097823964199E-014	-0.9786799937626899E-014
29	29	0.2374933423884700E-014	0.5526806971605504E-014
30	29	-0.2083660180905899E-014	-0.2961814389191701E-014
31	29	0.1588209116595800E-014	0.1495117336956400E-014
32	29	-0.1120017160715100E-014	-0.6906007320334499E-015
1	30	0.1460879506254300E-007	0.9003284340281002E-008
2	30	-0.2823269840135400E-008	0.1386951331561199E-008
3	30	0.7825795567128996E-009	-0.1568046026356700E-008
4	30	0.2697620425651199E-010	0.1050317055550900E-008
5	30	-0.2741852855869800E-009	-0.5767731292571900E-009
6	30	0.2854245451100500E-009	0.2646775854042699E-009
7	30	-0.2192762915687001E-009	-0.9092500363738804E-010
8	30	0.1445773778474500E-009	0.8115259332586200E-011
9	30	-0.8524345118665597E-010	0.2333611776039701E-010
10	30	0.4518202825765099E-010	-0.2953910727132602E-010
11	30	-0.2100424868756200E-010	0.2544803430481999E-010
12	30	0.7811558691561702E-011	-0.1861026437122201E-010
13	30	-0.1395314744821700E-011	0.1227214337096200E-010
14	30	-0.1228107351057599E-011	-0.7459342171722795E-011
15	30	0.1938437474771600E-011	0.4200941244175700E-011
16	30	-0.1811967134494900E-011	-0.2174392827250502E-011
17	30	0.1408577031056200E-011	0.1005290360504800E-011
18	30	-0.9858681796273695E-012	-0.3816611740190000E-012
19	30	0.6402638293677400E-012	0.7990197994347701E-013
20	30	-0.3907300373008600E-012	0.4563446585133400E-013
21	30	0.2248687618489801E-012	-0.8264472006053202E-013
22	30	-0.1215862940927599E-012	0.8037452268409195E-013
23	30	0.6092182829172899E-013	-0.6427673606042300E-013
24	30	-0.2735581672210599E-013	0.4627731303632300E-013
25	30	0.1001721576917000E-013	-0.3101106204510600E-013
26	30	-0.1856006312045901E-014	0.1965432211512700E-013
27	30	-0.1449069978965601E-014	-0.1185805553277800E-013
28	30	0.2367025947805601E-014	0.6820464721837405E-014
29	30	-0.2261307977417001E-014	-0.3724882442692398E-014
30	30	0.1807540569111699E-014	0.1926686129296600E-014
31	30	-0.1296981295758800E-014	-0.9137470621250596E-015
32	30	0.8766484484034196E-015	0.3882565037362000E-015
1	31	-0.9598852379610898E-008	-0.5795985469347898E-008
2	31	0.1849477682114300E-008	-0.9928169397710501E-009
3	31	-0.4816471665947100E-009	0.1076696731772100E-008
4	31	-0.5248160586668300E-010	-0.7087125331040099E-009
5	31	0.2071349619603400E-009	0.3809701998314100E-009
6	31	-0.2049919262114801E-009	-0.1683463229929000E-009
7	31	0.1537179272759200E-009	0.5217824436409800E-010
8	31	-0.9936483580386099E-010	0.1507452582899501E-011
9	31	0.5731425750665798E-010	-0.2050049713320200E-010
10	31	-0.2947586619228598E-010	0.2287657216437600E-010
11	31	0.1301253636093500E-010	-0.1882869034297600E-010
12	31	-0.4260404529166100E-011	0.1338621054281000E-010
13	31	0.1745970040637300E-012	-0.8623258357376397E-011
14	31	0.1359319991636700E-011	0.5118290773847799E-011
15	31	-0.1648830052526599E-011	-0.2801482136549600E-011
16	31	0.1427101600955100E-011	0.1393082914649700E-011
17	31	-0.1064500050607100E-011	-0.6012819365672197E-012

18	31	0.7234774845182901E-012	0.1930938319395100E-012
19	31	-0.4580869646282599E-012	-0.5860909800287502E-014
20	31	0.2725720040300299E-012	-0.6391182071421897E-013
21	31	-0.1524359116581200E-012	0.7724775815754303E-013
22	31	0.7944979309865195E-013	-0.6739723254316202E-013
23	31	-0.3770769774983502E-013	0.5101806157441602E-013
24	31	0.1535314132501300E-013	-0.3540068493337498E-013
25	31	-0.4325466918778302E-014	0.2304388538982500E-013
26	31	-0.5088486373763600E-015	-0.1421340089624101E-013
27	31	0.2165687275034501E-014	0.8342618079920694E-014
28	31	-0.2359853696324701E-014	-0.4661321835111697E-014
29	31	0.1988282365220900E-014	0.2456589517582400E-014
30	31	-0.1482132427754100E-014	-0.1197136440068200E-014
31	31	0.1033881639155000E-014	0.5194123558384801E-015
32	31	-0.6673197667803704E-015	-0.1900258860160900E-015
1	32	0.6314194056500399E-008	0.3733538811445700E-008
2	32	-0.1210908595616900E-008	0.7065222296098696E-009
3	32	0.2938401744145798E-009	-0.7379830080367398E-009
4	32	0.5832601068789201E-010	0.4773491046883302E-009
5	32	-0.1543805500103801E-009	-0.2508814267443400E-009
6	32	0.1463259513556600E-009	0.1062568921739200E-009
7	32	-0.1072638436405700E-009	-0.2878065494260601E-010
8	32	0.6797894885890400E-010	-0.5830714817217599E-011
9	32	-0.3831553477273700E-010	0.1705713868760401E-010
10	32	0.1905412112812599E-010	-0.1739441750359100E-010
11	32	-0.7899850044956704E-011	0.1377689802517500E-010
12	32	0.2136018141876701E-011	-0.9544204836176004E-011
13	32	0.4291557614919500E-012	0.6008975435289900E-011
14	32	-0.1287842228692201E-011	-0.3479589446436798E-011
15	32	0.1345710001765500E-011	0.1845605699518599E-011
16	32	-0.1099427732013900E-011	-0.8750922078984400E-012
17	32	0.7920364667943201E-012	0.3444273132761200E-012
18	32	-0.5240076493377700E-012	-0.8136578840160402E-013
19	32	0.3236965545865700E-012	-0.3140881855274100E-013
20	32	-0.1876183399179101E-012	0.6691094076374803E-013
21	32	0.1016665592858100E-012	-0.6717495076901201E-013
22	32	-0.5073196433801900E-013	0.5448667165781700E-013
23	32	0.2243195660147700E-013	-0.3950930972359101E-013
24	32	-0.7829283079599697E-014	0.2655803365853699E-013
25	32	0.1014554570760200E-014	-0.1682420885549700E-013
26	32	0.1665305314301101E-014	0.1011622799147300E-013
27	32	-0.2336740496534799E-014	-0.5767667566420798E-014
28	32	0.2133175609420000E-014	0.3114009480912602E-014
29	32	-0.1669140150090600E-014	-0.1564889558404100E-014
30	32	0.1188858387074700E-014	0.7189708829918697E-015
31	32	-0.7916979259365091E-015	-0.2725311037736200E-015
32	32	0.4918224281036002E-015	0.6241396682556799E-016

List of References

Antonatos, P. P. "Laminar Flow Control - Concepts and Applications," *Astronautics and Aeronautics*, pp.32-36, 1966.

Ffowcs Williams, J. E., Roebuck, I. and Ross, C. F. "Anti-phase noise reduction," *physics in Technology*, 1984.

Ffowcs Williams, J. E. "Anti-sound," *Proc. R. Soc. Lond.*, A, 395, pp. 63-88, 1984.

Ffowcs Williams, J. E. "Control of Unsteady Flow," AIAA Paper 89-0990, 1989.

Gaster, M. "The development of three-dimensional wave packets in a boundary layer," *J. Fluid Mech.*, 32, 1968.

Gaster, M. and Grant, I. "An experimental investigation of the formation and development of a wave packet in a laminar boundary layer," *Proc. R. Soc. Lond. A*, 347, pp. 253-269, 1975.

Gaster, M. "A theoretical model of a wave packet in the boundary layer on a flat plate," *Proc. R. Soc. Lond. A*, 347, pp. 271-289, 1975.

Gaster, M. "Series Representation of the Eigenvalues of the Orr-Sommerfeld equation," *J. Comp. Physics*, 28, 1978.

Gaster, M. "Propagation of linear wave packets in laminar boundary layers," *AIAA J.*, 19, 1981.

Gaster, M. "A Non-Linear Transfer Function Description of Wave Growth in a Boundary Layer," in Laminar Turbulent Transition, IUTAM Symposium Novosibirsk, 1984, Springer-Verlag, pp. 107-114, 1985.

Heinrich, R.A.E., Gaster, M. "Wave packet interaction in a laminar boundary layer," *Bulletin of the American Physical Society*, Vol. 35, No. 10, pg. 2291, 1990.

Kendall, J. M. "Boundary layer receptivity to freestream turbulence," AIAA 90-1504, presented at 21st Fluid Dynamics, Plasma Dynamics and Lasers Conference, Seattle, WA, June 18-20, 1990.

Kral, L. "Numerical Investigation of Transition Control of a Flat Plate Boundary Layer," Ph.D.-Dissertation, The University of Arizona, 1988.

Ladd, D. M. "Control of Natural Laminar Instability Waves on an Axissymmetric Body," *AIAA Journal*, Vol. 28, pp. 367-369, 1990.

Ladd, D. M. and Hendricks, E. W. "Active Control of 2-D Instability Waves on an Axissymmetric Body," *Experiments in Fluids*, Vol. 6, pp. 69-70, 1988.

Laurien, E. and Kleiser, L. "Numerical Simulation of Transition

Control in Boundary Layers," *Proc. of the Sixth GAMM Conference on Numerical Methods in Fluid Mechanics*, Goettingen, West Germany, 1985.

Laurien, E. "Numerische Simulation zur Aktiven Beeinflussung des Laminar-Turbulenten Uebergangs in der Plattengrenzschichtstroemung," Dissertation, Universitaet Karlsruhe, West Germany, 1985.

Liepmann, H. W., Brown, G. L. and Nosenchuck, D. M. "Control of Laminar-Instability Waves Using a New Technique," *J. Fluid Mech.*, 118, pp. 187-200, 1982.

Liepmann, H. W. and D. M. Nosenchuck "Active Control of Laminar-Turbulent Transition," *J. Fluid Mech*, 118, pp. 187-200, 1982.

Mack, L. M. "Boundary layer stability theory," Report No. 900-277, Jet Propulsion Laboratory, Pasadena, CA, 1969.

Maestrello, L. "Active Transition Fixing and Control of the Boundary Layer in Air," AIAA Paper 85-0564, 1985.

Milling, R. W "Tollmien-Schlichting Wave Cancellation," *Phys. Fluids*, 24, pp. 979-981, 1981

Nenni, J. P. and Gluyas, G. L. "Aerodynamic Design and Analysis of an LFC Surface," *Astronautics and Aeronautics*, pp. 32-36, 1966.

Pfenninger, W. and Reed, V. D. "Laminar-Flow Research and Experiments", pp. 32 -36, 1966.

Roebuck, I. "The relationship between active noise control and adaptive signal processing," A.U.W.E. publication 65837, 1982.

Ross, C. F. "Signal processing algorithms for active control of periodic noise," *Proc. Inst. of Acoust. Spring Conference*, Edinburgh: Institute of Acoustics, 1982.

Schilz, W. "Experimentelle Untersuchungen zur Akustischen Beeinflussung der Stroemungsgrenzschicht in Luft," *Acustica*, 16, pp 208-223, 1965/66.

Strykowski, P. J. and Sreenivasan, K. R. "The Control of Transitional Flows," AIAA Paper 85-0559, 1985.

Thomas, A. S. W. "The control of Boundary-Layer Transition Using a Wave-Superposition Principle," *J. Fluid Mech*, 137, pp. 233-250, 1983.

Wagner, R. D. and Fischer, M. C. "Developments in the NASA Transport Aircraft Laminar Flow Program," AIAA Paper 83-00900, 1983.

Wehrman, O. H. "Tollmien-Schlichting Waves under the Influence of a Flexible Wall," *Phys. Fluids*, 8, pp. 1389-1390, 1965.

Whites, R. C., Sudderth, R. W. and Wheldon, W. G. "Laminar Flow

Control on the X-21," *Astronautics and Aeronautics*, pp. 32-36, 1966.

Zang, T. A. and Hussaini, M. Y. "Numerical Experiments on Subcritical Transition Mechanisms," AIAA Paper 85-0296, 1985a.

Zang, T. A. and Hussaini, M. Y. "Numerical Experiments on the Stability of Controlled Shear Flows," AIAA Paper 85-1698, 1985b.